ABSTRACT

Title of Dissertation:	GEOTECHNICAL AND ENVIRONMENTAL IMPACTS OF STEEL SLAG IN EMBANKMENTS
	Asli YALCIN DAYIOGLU Doctor of Philosophy, 2016
Dissertation directed by:	Prof Ahmet H. AYDILEK Department of Civil and Environmental Engineering

Steel slag is a byproduct of iron and steel production by the metallurgical industries. Annually, 21 million tons of steel slag is produced in the United States. Most of the slag is landfilled, which represents a significant economic loss and a waste of valuable land space. Steel slag has great potential for the construction of highway embankments; however, its use has been limited due to its high swelling potential and alkalinity. The swelling potential of steel slags may lead to deterioration of the structural stability of highways, and high alkalinity poses an environmental challenge as it affects the leaching behavior of trace metals. This study seeks a methodology that promotes the use of steel slag in highway embankments by minimizing these two main disadvantages.

Accelerated swelling tests were conducted to evaluate the swelling behavior of pure steel slag and water treatment residual (WTR) treated steel slag, where WTR is an

alum-rich by-product of drinking water treatment plants. Sequential batch tests and column leach tests, as well as two different numerical analyses, UMDSurf and WiscLEACH, were carried out to check the environmental suitability of the methods. Tests were conducted to study the effect of a common borrow fill material that encapsulated the slag in the embankment and the effects of two subgrade soils on the chemical properties of slag leachate.

The results indicated that an increase in WTR content in the steel slag-WTR mixtures yields a decrease in pH and most of the leached metal concentrations, except aluminum. The change in the levels of pH, after passing through encapsulation and subgrade, depends on the natural pHs of materials.

GEOTECHNICAL AND ENVIRONMENTAL IMPACTS OF STEEL SLAG IN HIGHWAY EMBANKMENTS

by

Asli YALCIN DAYIOGLU

Dissertation submitted to the Faculty of the Graduate School of the
University of Maryland, College Park, in partial fulfillment
of the requirements for the degree of
Doctor of Philosophy
2016

Advisory Committee:
Professor Ahmet H. AYDILEK, Chair
Professor Mohamed S. AGGOUR
Professor Charles W. SCHWARTZ
Professor Dimitrios GOULIAS
Professor Amr M. BAZ

To my soul mate, my other half, the light of my life, Mustafa DAYIOGLU…

Acknowledgements

Despite the fact that only my name is written on the cover of this dissertation, I would not see the finish line of this marathon without the support, guidance, and assistance of many individuals to whom I offer my deepest and most sincere thanks. I graciously acknowledge those, whose wisdom, support and recommendations enriched my work, and made my dissertation writing and graduate school experience an immensely pleasant one.

I owe the greatest gratitude to Dr. Ahmet H. Aydilek, my academic advisor, mentor and thesis chair who has supported and guided me professionally and academically with his tremendous expertise and knowledge throughout my thesis process. My committee members—Dr. Charles Schwartz, Dr. Sherif Aggour, Dr. Dimitrios Goulias and Dr. Amr Baz—have individually and collectively offered excellent insights and feedback, which tremendously contributed to theoretical, methodological and practical foundations of this dissertation. I also would like to thank Dr. Bruce R. James and Dr Alba Torrents for their extremely valuable help, advice and support as well as their continuous encouragement. I would like to acknowledge Mrs. Marya Orf Anderson who never got tired of my endless questions and was always there when I was stuck in the environmental lab.

Moreover, I would like to express my sincere thanks to Dr. Recep Iyisan, Dr. Turan Durgunoglu and Dr. Berrak Teymur for writing the recommendation letters which admitted me to the University of Maryland as well as to Dr. Derin Ural and Dr. M. Tugrul Ozkan from Istanbul Technical University for all their help, support and

encouragement. I am extremely proud of being a member of ITU and look forward to serve back in my country as a faculty member.

I would like thank to all my special friends in my life, Dr. Bora Cetin, Dr. Omur Cimen, Dr. Mesut Cimen and Dr Atila Sezen for all their academic and moral support. Undergraduate research assistants Ms. Zorana Mijic and Mr Sari Hijazi helped me tremendously with the experimental setups and daily measurements. I also thank Dr. Bedrettin Yazan and Mrs. Betul Kilinc Sunel, Mr. Hakan Dinc and Mr Yavuz Gozubuyuk for always supporting and encouraging me through the toughest times. I also would like to thank Mr. Ethem Balik for convincing my husband to give up his fears and starting this long journey.

At this point, I would like to also thank to Dr Mustafa Hatipoglu, the elder brother I never had, for sharing everything with me. He never hesitated one single second when I asked him for help or advice, even if he was extremely busy.

Most importantly, none of this would have been possible without the unconditional love, support and patience of my family. My parents Gulten Gulbahar, Osman Demir Yalcin, Kamuran Dayioglu and Kadir Dayioglu have been a constant source of love, concern, support and strength during all these years. I am forever indebted to them for everything that made me who I am today.

And last, but not least, I would like to express my deepest and most heartfelt gratitude to my dearest husband Mustafa Dayioglu, aka “Dayi” for being my rock, my serenity, my whole world for the last 8 years. Without you and your enormous academic and moral support, I would never be able to go through those four years here in U.S. You never cease to amaze me. I am the luckiest woman on earth to have you.

Table of Contents

List of Tables

List of Figures

1 INTRODUCTION

The American Society of Civil Engineers estimates that $2.2 trillion is needed over a five-year period to improve the nation's infrastructure. Establishing a long-term development and maintenance plan is a national priority. Part of this long-term plan involves evaluating the large volumes of earthen materials that are used in transportation infrastructure construction. In many cases, these materials can be fully or partially replaced with suitable recycled materials that are normally disposed in landfills. This change could generate millions of dollars in savings to taxpayers. For instance, steel slag is a material that the Maryland State Highway Administration (SHA) has expressed an increasing interest in. Steel slag is produced during the separation of molten steel from impurities in steel-making furnaces and is, by mass, approximately 15% of the original steel output. The slag occurs as a molten liquid and is a complex solution of silicates and oxides that solidifies upon cooling. Approximately 21 million tons of slag are produced annually in the United States, and only 10-15% of this slag is reused. The remainder is either stockpiled or placed in landfills (USGS, 2014). Many contractors have approached SHA requesting the use of S, but SHA currently does not have any specifications available to regulate the use of this recycled material.

Processed steel slag has favorable mechanical properties for aggregate use, including good abrasion resistance and high bearing strength (Geiseler 1996, Rohde et al. 2003, Ahmedzade and Sengoz 2009, Deniz et al. 2009, Yildirim and Prezzi 2009). Although steel slag can be an attractive construction material, there are two main

problems that need to be carefully examined. First, steel slag aggregates generally exhibit a tendency to expand, due to the presence of free lime and magnesium oxides that have not yet reacted with silicate structures. Because of this chemical composition, slag can expand in humid environments, which could cause the heaving of pavements and uneven, rough and cracked pavement surfaces. This could result in millions of dollars in annual repair costs to rehabilitate the structures (Motz and Geiseler 2001, Juckes 2003, Rojas 2004, Deniz et al. 2009). The other key issue is the possible release of pollutants to the environment. Steel slag is mainly composed of environmentally benign oxides like calcium, silicon and iron, but it may also contain low concentrations of potentially toxic elements, including chromium, nickel and vanadium. Additionally, the high pH levels of leachate from steel slag (pH>12) exceeds a maximum pH of 8.5 in water discharges as allowed by the United States Environmental Protection Agency (EPA) and the Maryland Department of the Environment (MDE). The pH conditions and the potential for leaching pollutants will be highly influenced by the intended slag application (embankment fill vis-à-vis base) and the possible use of simple additives to mitigate adverse properties. Understanding these issues and finding ways to reduce geotechnical and environmental risks are necessary to promote the use of steel slag in highway construction in Maryland.

Use of steel slag has several benefits to the State. Some of these include: reducing solid waste disposal costs incurred by industries, reducing landfill requirements, minimizing damage to natural resources caused by excavating earthen materials for construction, conserving production energy, and ultimately providing sustainable construction and economic growth. Furthermore, highway engineers will

be able to utilize local materials and thereby reduce environmental impacts and provide cost-benefits to the State. Moreover, these efforts are parallel with the objectives of Green Highways Partnerships, which SHA is a partner in.

As mentioned above, several studies have been conducted regarding the mechanical properties of steel slag. Leaching of metals from steel slag has also been studied (Fällman et al. 2000, Apul et al. 2005, Gomes and Pinto 2006, Huijgen and Comans 2006, Mayes et al. 2008, De Windt et al. 2011). However, there is a lack of information on the flow of steel slag leachate through natural soils. Mineralogy affects the particle charge and buffering capacity of soils significantly, which may result in lower metal concentrations in the leachate. This study consisted of the following tasks:

1) Determining the mechanical properties of steel slag and evaluating its swelling behavior.
2) Conducting batch (small-scale) water leaching tests for a quick estimate of metal leaching behavior.
3) Conducting long-term sequential column leaching tests to study leaching behavior and controlling mechanisms for the trace metals from pure and treated steel slag, and to study the effects of underlying subgrades on fate and transport of these chemicals in the environment.
4) Determining the evaluation of the impact of effluents from steel slags on surface water and groundwater through two recent numerical models.

Section 2 of this study evaluates the mechanical behavior and the swelling potential of steel slag and compares the two different swell suppression methods. Section 3 evaluates metal leaching from pure or treated steel slag within highway embankments

into surface waters. Section 4 evaluates metal leaching from pure or treated steel slag within highway embankments into groundwater. Section 5 provides a summary of research findings and a list of recommendations for future work.

2 ASSESSMENT AND MITIGATION OF SWELLING BEHAVIOR OF STEEL SLAG

2.1 INTRODUCTION

Steel slag has been used in a variety of applications in the construction industry. In particular, steel slag (S) produced via blast furnace is used in a wide range of highway applications, such as granular base, concrete and hot mix asphalt aggregates and supplementary cementitious materials (Rohde et al. 2003, Tsakiridis et al. 2008, Shen et al. 2009, Suer et al. 2009, Wang et al. 2010). Steel slag was reported as having excellent strength characteristics due to their angular shape and rough surface texture (Deniz et al. 2009). Steel slag also possesses high bulk-specific gravity and exhibits good compaction behavior. However, steel slag obtained from basic oxygen furnaces (BOF) and electric arc furnaces (EAF) is less commonly used in highway applications due to their volumetric instability in the presence of moisture. The expansion of free lime (CaO) and free periclase (MgO), as well as the conversion of dicalciumsilicate (C_2S) and the oxidation of iron and carbonation of CaO and Mg silicates results in the volumetric instability of steel slags (Wang 2010). CaO lime can fully hydrate in a few days when immersed in water. This behavior is not favorable, particularly when steel slag is used in rigid matrices (Deniz et al. 2010).

Several efforts were made to use slag in highway bases/subbases, low volume roads and in soil stabilization. Verhasselt and ChoqSuet (1989) performed a series of accelerated swell tests on steel slag samples and claimed that the critical CaO content for slags used in pavements should be 4.5% with a maximum linear expansion limit of

1%, which was set based on swelling tests. The same study also recommended placing sand layers above and below the steel slag layer due to the fact that voids inside the sand layer could tolerate the swelling of the slag. Geiseler (1996) said there is no need to restrict the volumetric expansion of steel slag in certain applications, such as in the construction of parking lots or in landscaping projects. Geiseler (1996) also proposed that the free lime content of non-aged slag should not exceed 7% and 4%, respectively, for use in unbound layers and bituminous (asphalt) road layers. Deniz et al. (2010) conducted swelling tests on different reclaimed asphalt pavement (RAP) samples, including surface binder RAP materials with 60% S aggregates, surface RAP materials with 92% slag aggregates and virgin slag aggregates, among other samples. Results showed that RAP materials with slag aggregates expand less compared to virgin materials mixed with steel slag. Deniz et al. (2010) claimed that the high absorption characteristics of RAP materials and the high alkalinity of S could be the reason for the observed lower swell. This phenomenon was related to the fact that the surface texture of S was rougher than the natural aggregate, its friction properties were superior and its improved adhesion ability with an asphalt binder. In another study, Yıldırım and Prezzi (2009) showed that the addition of 10% Class C-Fly ash by weight can reduce swelling values of EAF slags, as well as the aged and fresh BOF steel slag, to negligible levels.

Wang (1992) found that voids of a granular material could partially compensate for the swelling of steel slag. Expansion tests under a surcharge of 2.5 kPa were conducted on two different types of steel slag. The volume expansion was assumed to be due to the presence of free lime, and an empirical formula related to the initial free lime (CaO) percentage to porosity and compacted density of steel slag was proposed.

Wang et al. (2010) also pointed out that the void volume in bulk steel slag under an external surcharge could internally absorb a volume expansion equal to 7-8% of the void ratio of steel slag. Wang et al. (2010) developed a usability criterion based on the volume expansion of steel slag and the minimum percentage of the volume that can take the volume expansion of steel slag.

Motz and Geiseler (2001) developed another criteria based on the contents of CaO and MgO, as both can influence the swelling behavior of steel slag. As there is no reliable test method to determine the free MgO content of slag, this study suggested the use of a steam test in which a compacted slag specimen is subjected to a flow of steam from a steam unit at 100°C for 24 hours if the MgO content is less than 5%,and 168 hours otherwise (CEN EN 1744-1).

European Code (TC 154) has classified steel slag aggregates into four main groups, ranging from V_A to V_D. Steel slag aggregates can be used in unbound and asphalt layers only if they meet the criterion for Class V_A. For a steel slag aggregate to be classified as Class V_A, the maximum expansion of the steel slag sample can be no more than 3.5% for bituminous mixes and 5% for unbound mixtures, with a 24-hour steam test for slag with MgO less than 5% and a 168-hour steam test for slag with MgO greater than 5%). Yzenas (2008) has performed autoclave tests and developed a scale to evaluate the suitability of steel slag as construction aggregates. According to this scale, a steel slag sample undergoing up to 11% of volumetric expansion may be classified as a "suitable" material. If the measured volumetric expansion is between 11 and 16%, then the material is called "marginal," and further testing is recommended.

Any other materials with a volumetric expansion greater than 16% are not suitable materials for building and should be rejected.

However, Juckes (2003) evaluated the swelling behavior of several S aggregates both in the laboratory and in situ, and the results of the experiment indicated that the two swelling behaviors could be very different. Accelerated laboratory swelling tests are quick and provide the maximum expansion for a given steel slag sample; however, the field rate of swelling was found to be much lower under atmospheric conditions.

Previous research showed that steel slag can be a good alternative to natural aggregates in highway base/subbase layers (Rohde et al. 2003). However, most of these studies suggested that steel slag should be aged under atmospheric conditions before being used. The objective of the current study was to test the efficacy of an innovative method that decreases the swelling potential of steel slag while still preserving their mechanical properties. In order to meet this objective, steel slag materials were coated with bituminous asphalt material, or mixed with water treatment residual (WTR). These mixtures, along with the virgin steel slag material, were subjected to accelerated swelling tests.

2.2 MATERIALS

Steel slag (S) used in this study was produced via blast oxygen furnaces (BOF). S samples were collected from field stockpiles that include six-month-old (6MS), one-year-old (1YS), and two-year-old (2YS). Debris and foreign material in S were removed by hand before testing. All three steel slag materials were classified as well-graded sand with silt (SW), according to Unified Soil Classification System (USCS),

and A-1-b, according to the American Association of State Highway and Transportation Officials (AASHTO) Classification System. They did not exhibit any plasticity and contained 12%, 10% and 12% silty fines by weight, respectively.

Bituminous coating (BC), water treatment residual (WTR) addition and natural sandy soil amendment methodologies were applied to decrease the swell potential of virgin steel slag. WTR, a byproduct that comes from treating drinking water, is an aluminum-based material and does not contain any surface or groundwater pollutants. It was collected from the Rockville Drainage Drinking Water Treatment Plant and was air-dried and sieved through a U.S. No. 40 sieve before mixing with the slag. WTR contains 76% fines by weight and shows no plasticity. Asphalt binder PG-64-22 was used for BC. The physical properties of the asphalt binder can be found at Irving Oil (2013). The asphalt binder is solid at room temperature and is a viscous fluid at 90°C. The measurements conducted according to EPA Method SW-846 and Method 9045 showed that the pH of S and WTR materials were 12.4 and 6.9, respectively. The steel slag S was mixed with the asphalt binder at a ratio of 4% by weight, while WTR materials were added at a ratio of 10%, 20% and 30% by weight.

Sandy soil (or borrow material) that is commonly used in embankment construction by the Maryland State Highway Administration (SHA) was utilized in preparing the soil and S mixtures. Soil was collected from a pit in Denton, Maryland, and was sieved through U.S. No. 4 sieve (4. 75 mm) upon transporting to the laboratory. The soil was classified as poorly graded sand with silt (SP-SM), according to the Unified Soil Classification System, and A-3 (fine sand), according to the American Association of State Highway and Transportation Officials (AASHTO) Classification

System. The soil showed no plasticity based on consistency limit tests per ASTM D4318. The physical properties of the soil, along with the steel slags and the WTR, are summarized in Table 2.1 .

All mixtures prepared in the current study were compacted at their optimum moisture contents (w_{opt}) and maximum dry unit weights ($\gamma_{dry\text{-}max}$) using the standard Proctor effort (ASTM D698). S was sieved through a U.S. 3/8" (9.5 mm) sieve before it was mixed with the asphalt binder. For preparation of the S-WTR mixtures, it was sieved through a U.S.3/4" (19 mm) sieve. Finer S material was preferred in the S-BC mixtures to prevent coarser aggregates from absorbing large portions of the asphalt binder. This procedure helps to achieve a more uniform coating of the S aggregates.

2.3 METHODS

2.3.1 Bitumen Coating

The S was oven-dried for 24 hours at 105 °C and sieved through U.S. 3/8" (9.5 mm) sieve. The oven-dried sample was weighed and placed into the oven. The required amount of asphalt binder (PG 64-22) was calculated, weighed and put into the oven together with all the metal equipment that was used during hot mixing (like spoons, buckets, etc). The binder, slag and equipment were heated to 170 °C and kept in the oven for 3.5 hours. The heated equipment was placed into the mixer, and S samples were taken out from the oven to be thoroughly mixed for approximately 1-2 minutes (Figure 2.1a). The heated binder was then taken from the oven and poured into the mixer. The bitumen and S were thoroughly mixed until all of the particles were visibly

coated and the mixture was warm. Finally, the bitumen-covered S samples were spread on a flat surface and left overnight to cool completely (Figure 2.1b).

2.3.2 Volumetric Expansion Tests

In accelerated swelling tests, compacted steel slag samples were exposed to hot water or steam in order to accelerate the swelling rate, and the swelling process was monitored for a shorter period of time compared to ASTM D1883 long-term swelling tests. For both tests, steel slag specimens were prepared at optimum water contents in cylindrical molds, lateral movement was prevented and one-dimensional swelling was measured.

Tests were performed in accordance with ASTM D4792. Samples were compacted in standard CBR-molds, which were equipped with dial gauges, and researchers followed the same procedures described in ASTM D1883. Specimens were immersed in hot water (70±3°C). A surcharge load of 2.5 kPa was applied on the specimens. ASTM D4792 recommends a test duration of seven days minimum; however, the accelerated swelling tests were generally continued beyond seven days to ensure a steady-state swelling ratio was reached, i.e., to fully assess both short- and long-term expansion behavior. The test setup is shown in Figure 2.2.

Table 2.1 Physical properties of the steel slag, water treatment residual and sandy soil.

Material	G_s	Gravel Content (%)	Sand Content (%)	Fines Content (%)	I_P (%)	w_n (%)	w_{opt} (%)	$\gamma_{dry\text{-}max}$ pcf (kN/m^3)
Steel Slag (6MS)	3.46	35	53	12	NP	6	10	151.6 (23.9)
Steel Slag (1YS)	3.45	21	69	10	NP	9	11	142.9 (22.5)
Steel Slag (2YS)	3.45	21	67	12	NP	10	13.5	141.2 (22.2)
Water Treatment Residual (WTR)	1.88	0	24	76	NP	385	42	65.3 (10.3)
Sandy Soil (Borrow Material)	2.60	0	89	11	NP	5	11	122.2 (19.2)

Note: I_p: plasticity index, G_s: specific gravity NP: non-plastic, w_n: natural water content, w_{opt}: optimum moisture content, $\gamma_{dry\text{-}max}$: maximum dry unit weight.

(a)

(b)

Figure 2.1 (a) Bitumen coating procedure and **(b)** bitumen coated samples

Figure 2.2 ASTM D4792 Accelerated swell test set-up

2.4 RESULTS

2.4.1 Index Properties and Compaction Characteristics

Grain-size distribution is one of the most important characteristics of granular materials affecting their mechanical properties. Molten slag solidifies in the slag pits and subsequently breaks down into smaller-size particles during the cooling process. During this natural particle breakdown process, S particles of varying dimensions, from boulder to silt size, are generated, resulting in a variable gradation with a wide range of particle sizes.

The S can generally be classified as a coarse-grained material, since it consists of significant percentage of gravel-sized particles (Evans, 2006). Typically, it has a well-graded grain-size distribution, with particle shapes varying from subrounded to angular. In addition, S particles have very rough surfaces, which results in higher friction angles in comparison with natural soils. In previous studies, friction angles between 40° and 50° were reported for S (Lee 1974, Noureldin and McDaniel 1990).

In the current study, gradation of the slag was altered during bituminous coating, as well as during sand and WTR amendment. For all three S mixtures tested, the processing of S results in a relatively coarser aggregate material, likely providing a stronger but more brittle highway base/subbase layer. Figure 2.3 shows that the gradation curves of the bitumen-coated S tend to be more uniform compared to original grain size distributions of S.

As seen in Figure 2.3, all S specimens have fine particle contents between 10 and 12%, consistent with the values reported by Barra et al. (2001) and Rohde et al. (2003). The fine-grained nature of the WTR also increases the total fines content of the

WTR-slag mixtures. A similar trend was observed when slag was mixed with a sandy soil. Sandy soil included a larger amount of sand-sized particles compared with steel slag, which resulted in a finer grain-size distribution as compared to steel slag.

Due to its high specific gravity (G_s>3.0) and well-graded gradation, the reported $\gamma_{dry,max}$ of S is higher than that of a natural aggregate. Rohde et al. (2003) conducted standard Proctor compaction tests on EAF slag samples with different gradations; both regular (single-peak) and irregular compaction curves were observed for different gradations of EAF slags. The optimum moisture content and maximum dry unit weight of EAF slag samples were in the range of 3-6% and 23-26 kN/m^3, respectively. Andreas et al. (2005) presented a standard Proctor compaction curve on a ladle slag and EAF slag mixture that contained 35% EAF slag by weight. A single peak compaction curve, with a $\gamma_{dry,max}$ = 22 kN/m^3 and w_{opt}= 13%, was reported. Pennsylvania Department of Transportation studied the compaction characteristics of granulated blast furnace slags and observed oddly-shaped curves with double peaks (Lee and Suedkamp 1972, Lee 1976). In addition, the fine particle content of S was reported to have a significant influence on the compaction behavior of the slag.

The optimum moisture content (w_{opt}) and maximum dry density ($\gamma_{dry,max}$) of the pure steel slag materials used in this study are provided in Table 2.2. These values are consistent with the compaction characteristics of typical S reported by others (Rohde et al. 2003, Deniz et al. 2010). BC coating results in a 2-3% decrease in w_{opt} of all the S-BC mixtures compared with pure slag, as the optimum moisture content of the coated granular steel slag is influenced by the amount of fine particles (Figure 2.4). Past literature indicates that coarser materials tend to provide higher dry densities (Holtz

and Kovacs, 1981). However, bituminous material (asphalt binder PG 64-22) is a viscous and lightweight material with G_s= 1.1; thus, its addition may have caused a decrease in $\gamma_{dry,max}$ of the S-BC mixtures. Similar trends are also observed for the S-WTR samples. The S specimens prepared with WTR yielded the lowest maximum dry unit weights in all mixtures and the optimum moisture content values were increased from 13.5% to 21% (Table 2.2). WTR contains 76% silty fines and has a specific gravity of 1.88, which is probably the main reason for obtaining lower $\gamma_{dry,max}$ and higher w_{opt} for the S-WTR mixtures.

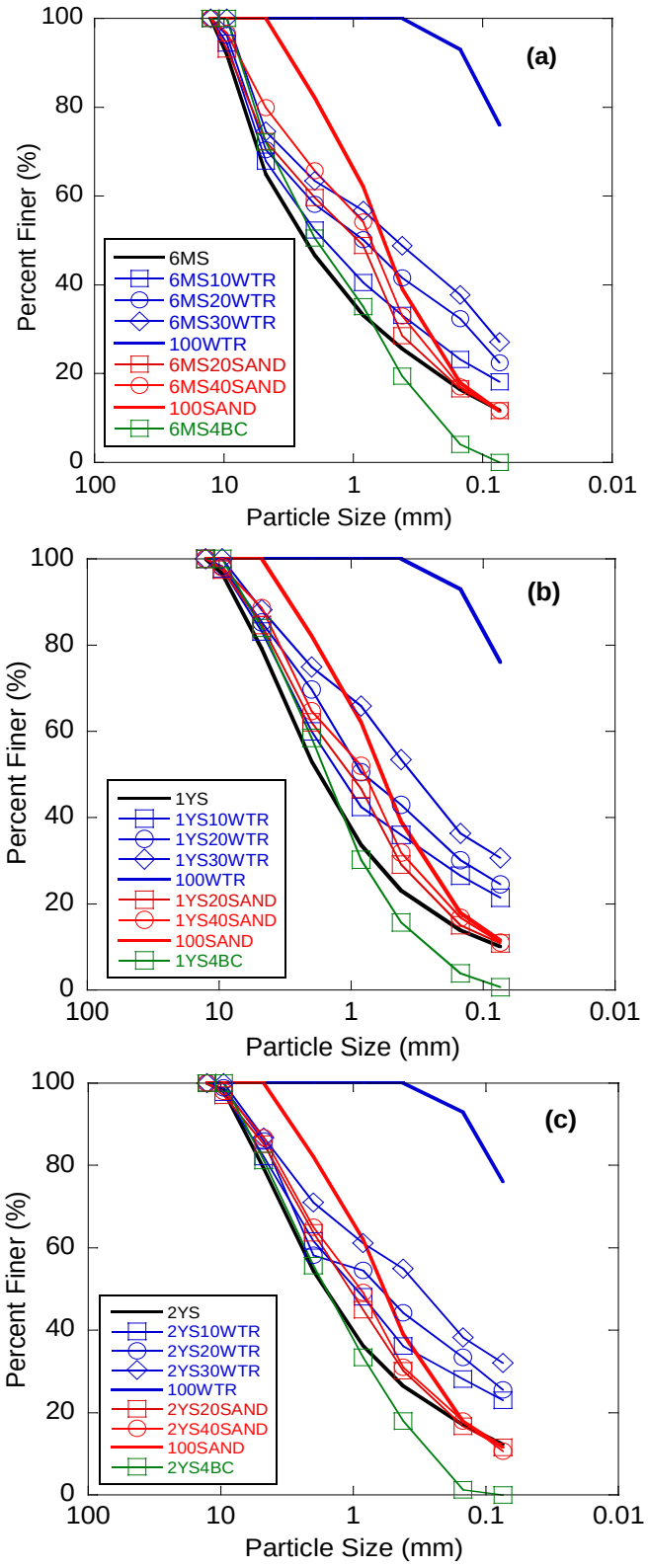

Figure 2.3 Grain size distributions of pure, bitumen-coated, and WTR or sand-amended steel slag aged for (a) 6 months, (b) 1 year, and (c) 2 years.

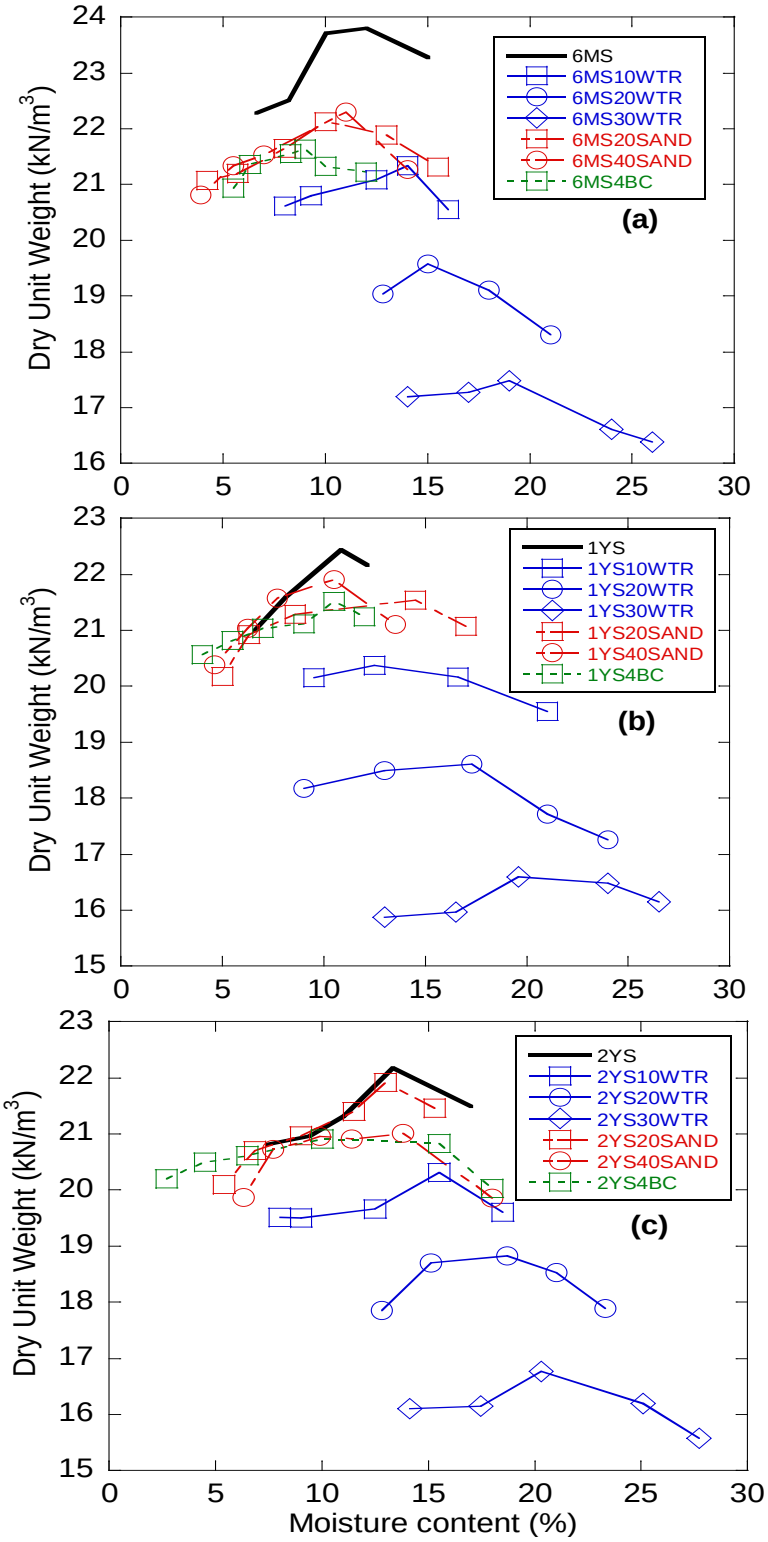

Figure 2.4 Compaction curves of pure, bitumen-coated and WTR or sand-amended steel Slag, aged for (a) 6 months, (b) 1 year and (c) 2 years (Note: S: steel slag, BC:bituminous coating, WTR: water treatment residual).

2.4.2 Strength Characteristics

The results of the direct shear tests are given in Table 2.2. Due to various subrounded to angular particle shapes and a rough surface, S typically yields very high friction angles in comparison to sandy soils. The friction angles and cohesion values obtained for pure S samples align with the existing values in literature. Yildirim and Prezzi (2009) reported a friction angle of ~50° and a cohesion of 50-75 kPa, which is similar to the values of ϕ'=49^0 and ϕ'=50^0 reported by Lee (1974) and Noureldin and McDaniel (1990), respectively. As seen in Table 2.2, a bitumen coating and a WTR addition to S decreases the internal friction angles to ϕ'=45-46^0 and ϕ'=36-44^0, respectively. This can be related to the fact that the addition of bitumen results in rounder particles, and that WTR consists of nonangular fine-grained particles.

2.4.3 Volumetric Expansion Tests

Figure 2.5 shows the volumetric expansion for the pure as well as treated S specimens. The volume of pure S increases with time, and the rate of increase declines after 40 days of testing as the hydration of both free lime (CaO) and magnesia (MgO) minerals contributes to swelling (Sorlini et al. 2012). A continuous increase in the swelling ratio of the steel slag after 40 days might be due to hydration of the magnesia (MgO) minerals in S. The hydration rate of CaO is relatively faster, and it typically takes only a few weeks for CaO minerals to complete their hydration process; for comparison, it takes years for the MgO minerals to complete the hydration process (Emer, 1974, Geiseler 1994, Motz and Geiseler 2001, Juckes 2003, Yildirim and Prezzi 2009).

Table 2.2 Compaction and shear strength parameters of the materials tested

Sample ID	Internal Friction Angle, φ (°)	Cohesion, c kip/ft^2 (kPa)	w_{opt} (%)	$\gamma_{dry\text{-}max}$ pcf (kN/m^3)
6MS	51	0.84 (40)	10	152 (23.9)
1YS	49	0	11	143 (22.5)
2YS	49	0.54 (26)	13.5	141 (22.2)
6 MS4BC	45	0.54 (26)	9	138 (21.6)
1 YS 4BC	46	0.40 (19)	10.5	137 (21.5)
2 YS 4BC	46	0.56 (27)	10	133 (20.9)
6 MS10WTR	44	0.31 (15)	14	136 (21.3)
1 YS10WTR	43	0.25 (12)	13	130 (20.4)
2 YS10WTR	42	0	14	129 (20.3)
6 MS20WTR	41	0.17 (8)	15	125 (19.6)
1 YS 20WTR	39	0	17.5	118 (18.6)
2 YS 20WTR	39	0.29 (14)	18	120 (18.8)
6 MS30WTR	39	0.33 (16)	19	111 (17.5)
1 YS30WTR	37	0.25 (12)	20	106 (16.6)
2 YS30WTR	36	0.25 (12)	20	107 (16.8)
6MS20SAND	46	0.40 (19)	10	141 (22.1)
1YS20SAND	44	0.38 (18)	14	137 (21.5)
2YS20SAND	44	0.40 (19)	13	140 (21.9)
6MS40SAND	42	0.44 (21)	11	142 (22.3)
1YS20SAND	41	0.50 (24)	11	139 (21.9)
2YS20SAND	40	0.42 (20)	13	134 (21.0)

Note: w_n: natural water content, w_{opt}: optimum moisture content, $\gamma_{dry\text{-}max}$: maximum dry unit weight.

The data in Figure 2.5 indicates that the bitumen-coated S specimens exhibited initial settlements during the early stages of the accelerated swelling tests. Deniz et al. (2010) also found that reclaimed asphalt materials (RAP) that contain S aggregates exhibited initial settlements before the onset of expansion, and that the porous nature of the RAP materials with lower densities yielded an elactic strain of 0.2-0.3% as soon as a surcharge load was placed. BC coated steel slags used in the current study have a higher porous structure than pure S and S-WTR mixtures, since fines in the steel slag were replaced with bituminous materials during the coating process.

The relatively higher porosity of the S-BC mixtures, and the fact that the lubricant nature of the bitumen dominates the material behavior, could be responsible for the observed instant high settlement rates. However, even though the ultimate swelling amounts of pure S materials with different aging properties are different, the ultimate swelling ratios of S-BC samples are almost identical. This shows that bitumen coating covers a significant amount of surface area and prevents Ca leaching. The bitumen coating decreases the infiltration rate of water into the steel slag aggregates, which prevents the hydration of free lime (CaO) and magnesia (MgO), and reduced the swelling of the granular S-BC mixture. This finding is consistent with previous research studies (Kandahl and Hoffman 1997, Deniz et al. 2010).

A summary of ultimate swelling ratios for all materials is given in Table 2.3. As expected, increasing the sand amount results in a lower ultimate swelling ratio for all S specimens. Amendment of steel slag with 20- 40% sand by dry weight limits the expansion of all three pure steel slag materials (Figure 2.5). However, this decrease in

the ultimate swelling ratios is not related to any chemical reaction. The sand particles replaced some of the S particles and resulted in lower ultimate swelling.

Aging had mixed effects on the swelling ratios measured in this study. Das et al. (2007) conducted experiments both in the laboratory and situ, which showed that the free lime content decreases to a constant near-zero value after 9 to 12 months of aging. Rohde et al. (2003) performed ASTM D4792 expansion tests on EAF slag and showed that the expansion of a 4 month-aged EAF slag was less than 0.5%, which is the limit value recommended by ASTM D2940. Even though total elemental analysis (TEA) results suggest that the overall chemical compositions and total Ca content of all three S mixtures used in the current study are similar (see Table 3.2 in Section 3), varying amounts of Ca released from each mixture yield a significant difference in Ca solubility. Ca containing mineral phases in the fresh steel slag samples may have been transformed over the course of different aging periods into various weathering products (secondary minerals) with different dissolution rates (e.g., calcium-alumina silicates). Nonetheless, the aged S is still capable of producing extremely alkaline leachates with high concentrations of dissolved Ca (Figure 2.5). Yildirim and Prezzi (2009) also reported that the ultimate swelling ratios for aged BOF slag samples were higher than those of fresh BOF slag samples. The laboratory leaching test results provided in Chapter 3 show that 6MS leaches the highest Ca-concentrations, since Ca was washed away during the earlier aging periods. 2YS slag released more Ca than 1YS, which shows that prolonged aging may have negative effects on the solubility of Ca-containing minerals in S. These findings agree with the results of the swelling test, where for both 20% and 40% of sand amended mixtures, the maximum swelling was

observed in the 6MS sample, whereas the least swelling was measured for the 1YS mixtures (Table 2.3).

The amendment of 10% and 30% WTR by weight decreases the ultimate volumetric expansion ratio of steel slag from 3.57% to 1.15% and 0.98%, respectively (Figure 2.5 and Table 2.3). This indicates that mixing S with WTR can be used to prevent swelling in highway base/subbase applications. According to Figure 2.5, the expansion rates of the pure S are lower than those of their corresponding S30WTR mixtures in the first three days, which may be due to the fact that WTR itself exhibits an initial swelling. Wang et al. (2010) claimed that the hydration rate of free lime is initially slow due to the dense, or high calcining, structure of free lime in steel slag byproducts. Wang et al. (2010) also suggested that this phenomenon decreases the rate of reaction that occurs between water and free lime, which ultimately decreases the initial expansion rate. The swelling patterns for the S-WTR mixtures are in agreement with the ones observed in sand slag mixtures. WTR-treated 6MS exhibits the largest swelling behavior, whereas WTR-treated 1YS has the lowest ultimate swelling ratio. Increasing the amount of WTR reduces the ultimate swelling.

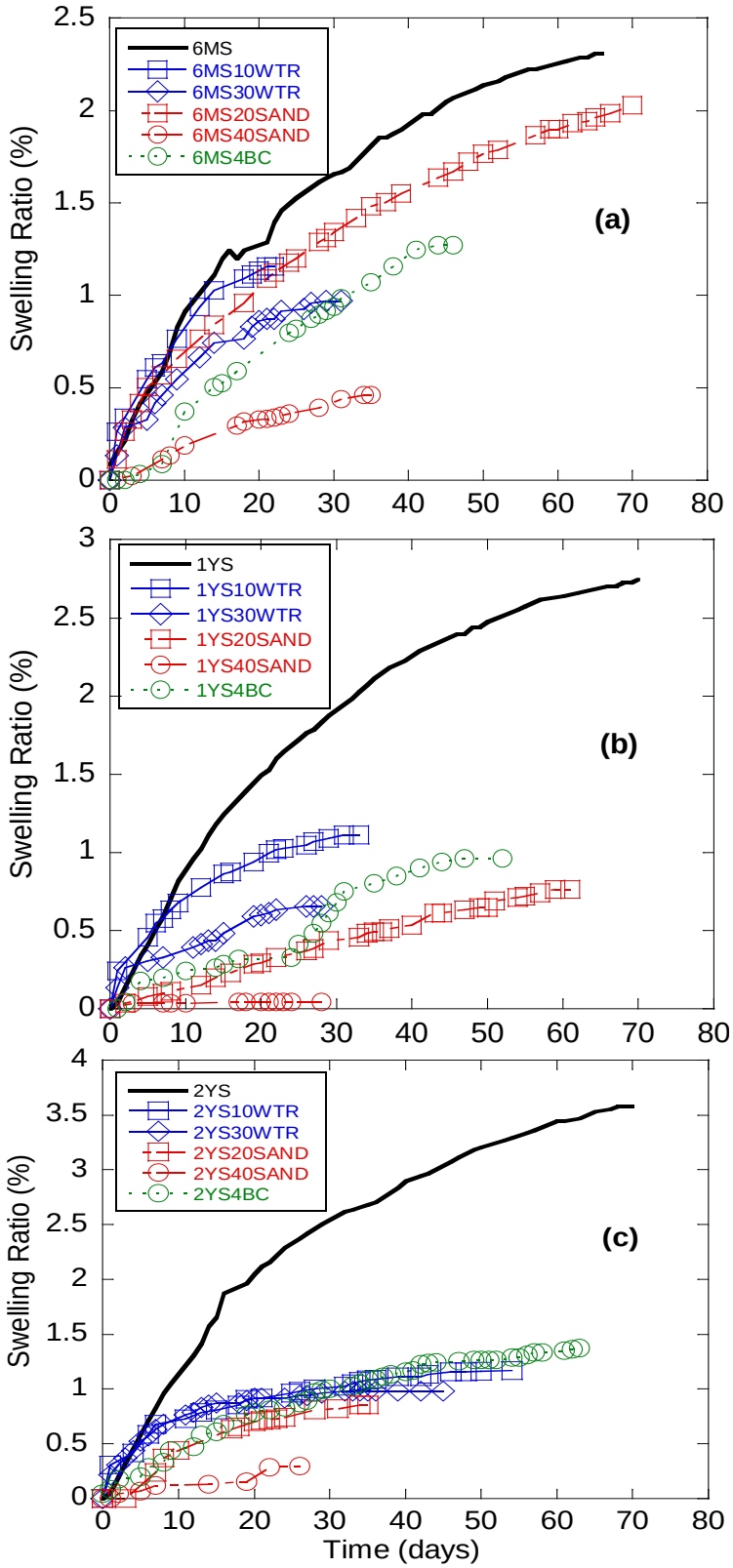

Figure 2.5 Swelling curves for of pure, bitumen-coated, and WTR or sand-amended steel slag aged for (a) 6 months, (b) 1 year, and (c) 2 years. (Note: S: steel slag, BC: bituminous coating, WTR: water treatment residual)

Table 2.3 Ultimate swelling ratios of the materials tested

Sample ID	Ultimate Swelling Ratio (%)
6 MS	2.61
1 YS	2.75
2 YS	3.57
6 MS4BC	1.27
1 YS 4BC	0.96
2 YS 4BC	1.27
6 MS10WTR	1.15
1 YS 10WTR	1.11
2 YS 10WTR	1.15
6 MS30WTR	0.97
1 YS 30WTR	0.65
2 YS 30WTR	0.98
6 MS20SAND	2.02
1 YS20SAND	0.76
2 YS20SAND	0.85
6 MS40SAND	0.45
1 YS40SAND	0.15
2 YS40SAND	0.05

2.5 CONCLUSIONS

A series of accelerated swelling tests and direct shear tests were performed on pure as well as bitumen coated, sand-amended, and water treatment residual (WTR)-mixed steel slag samples. The results can be summarized as follows:

- An increase in the amount of bituminous material decreased the maximum dry unit weight ($\gamma_{dry\text{-}max}$) and optimum moisture content (w_{opt}) of the bitumen coated steel slag. Addition of water treatment residual (WTR) to steel slag decreased the $\gamma_{dry\text{-}max}$ and increased w_{opt} due to high fines content of the WTR. Addition of sand resulted in a lower $\gamma_{dry\text{-}max}$ due to lower specific gravity of sand particles compared with steel slag but no significant change in optimum content was observed.
- All pure steel slag materials as well as mixtures used in this study had excellent shear strength properties based on direct shear tests. Both effective internal friction angle and effective cohesion generally decreased with WTR, bitumen, or sand addition. WTR addition caused the largest decrease in friction angles due to fine nature of the WTR particles.
- The results of the accelerated swelling (volumetric expansion) tests showed that all three methodologies (bituminous coating, sand amendment and WTR amendment) were very efficient in the prevention of significant expansion of the steel slag material. Mixing the steel slag material with 30% WTR by weight decreased the swelling (expansion) rate from 2.95% to approximately 1%. The steel slag materials coated with bituminous material do not exhibit excessive swelling, most likely due to the sealing off of the free lime and magnesia.

Even though the results of all three methods seem promising for supression of swelling, additional information on pH is needed. Thus, a series of batch tests were conducted to study the environmental suitability of the treatment methods. pH values obtained from thse tests provide a comparative evaluation of the three treatment methods.

3 EXPERIMENTAL EVALUATION OF TRACE METAL LEACHING FROM STEEL SLAG INTO SURFACE WATERS

3.1 INTRODUCTION

As mentioned in Chapter 2, processed steel slag (S) has favorable mechanical properties, such as good compatibility and high friction angle. However, one key issue that has prevented its use in embankments is the surface water impacts caused by metals in steel slag leachate. The steel slag is mainly composed of environmentally benign oxides of calcium, silicon and iron, but it may also contain low concentrations of potential toxic elements, including chromium and vanadium. The high calcium and iron levels create an environment that is generally conducive to sequestering these pollutants; however, as rainwater percolates through an embankment profile, trace elements leach from slag and may reach rivers and streams. Furthermore, pH conditions and pollutant leaching potential are highly influenced by the intended slag application.

As mentioned in Chapter 2, bituminous coating, WTR addition, and sand amendment methods have deemed as successful methods to suppress swelling. A series of pH measurements were conducted on the samples prepared using these three methods, and the results showed that the WTR treatment is the only one that is likely to effective on pH reduction (Figure 3.1). Accordingly, WTR amendment was chosen as the appropriate method for the leaching tests.

Limited information exists on the pollutant characteristics in surface waters during the construction of highway embankments (Boyer 1994, Banks et al. 2006, Mayes et al. 2008). In order to evaluate the metal leaching behavior of WTR-treated steel slag, a series of sequential water leach and column leach tests were conducted. A computer model was developed to study the effluent concentration within a stream adjacent to an embankment.

3.2 MATERIALS

The steel slag (S) material used in this study was produced via blast oxygen furnace (BOF). Only 2-year-old (2YS) steel slag was used in laboratory tests. Debris and foreign materials were removed by hand before testing.

The water treatment residual (WTR) was collected from the City of Rockville Water Treatment Plant, and air-dried and sieved through U.S. No. 40 sieve before being mixed with steel slag. The measurements conducted, according to EPA Method SW-846 Method 9045, showed that the pH of S and WTR materials were 12.4 and 6.9, respectively. WTR was added at 10%, 20% and 30% by weight to the S material.

A clayey, or borrow material, commonly used by SHA was utilized for simulating an encapsulation layer around pure or treated S materials in embankments. All mixtures prepared in the current study were compacted at their optimum moisture contents (w_{opt}) and maximum dry unit weights ($\gamma_{dry\text{-}max}$) using the standard Proctor effort (ASTM D698, 600 kN-m/m^3). Total elemental analyses (TEA) were performed by means of inductively coupled plasma optical emission spectrometer (ICP-OES) by the University of Wisconsin Soil and Plant Analysis Laboratory on all materials in

order to select the metal analytes of interest. Table 3.1 and Table 3.2 provide a summary of the physical and chemical properties of the materials used in this study.

3.3 METHODS

3.3.1 Sequential Water Leach Test (SWLT)

Sequential batch water leach tests (SWLT) were conducted on pure S and S-WTR mixtures in accordance with ASTM D3987 with slight modifications mentioned below. Pure S and pure WTR were also tested as control materials. The specimens were prepared at a liquid-to-solid ratio (L:S) of 20:1. All materials were air-dried and sieved through the No. 10 (2.0 mm) sieve before use. A 0.02 M NaCl solution was added to 2.5 grams of dry mixtures in 50 mL high-density polyethylene (HDPE) bottles. Next, the solutions were rotated at a rate of 29 rpm at room temperature (24 C^{o}) for 18 hours, in accordance with ASTM D3987. After rotation, the samples were centrifuged at 6000 rpm for 15 minutes. Upon centrifugation, the leachates were filtered through the 0.2-μm pore size, 25 mm diameter membrane disk filters fitted in a 25-mm Easy Pressure syringe filter holder by using a 60-mL plastic syringe. The pH and electrical conductivity (EC) measurements were conducted, and the volume of the filtrated solution was measured.

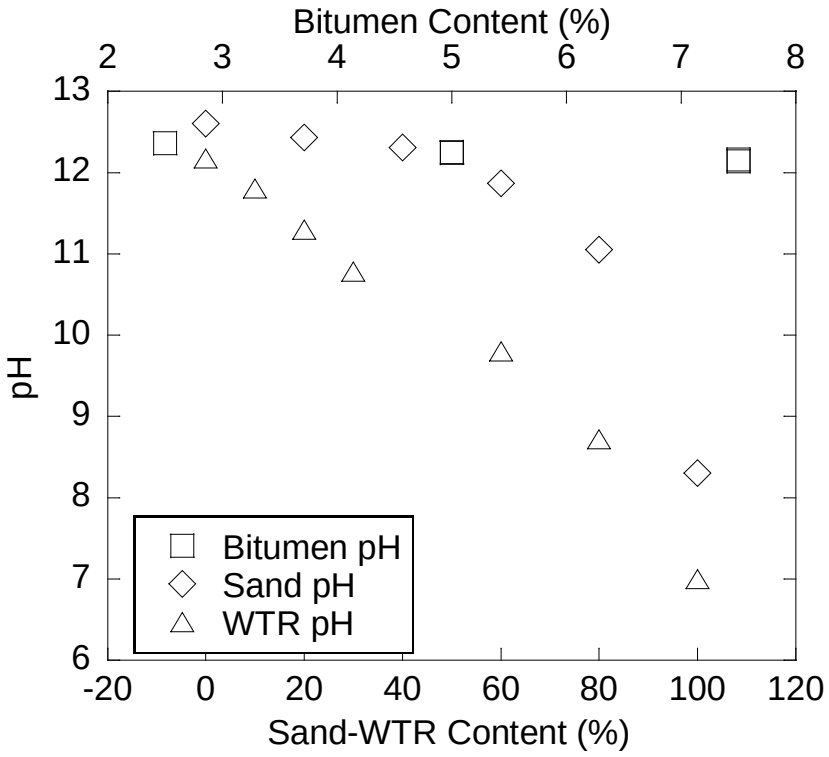

Figure 3.1 Results of preliminary batch water leach tests on swelling mitigation methods

Table 3.1 Physical properties of the steel slag, water treatment residual, and encapsulation soil.

Material	G_s	I_P (%)	w_n (%)	w_{opt} (%)	$\gamma_{dry\text{-}max}$ pcf (kN/m^3)
Steel Slag (S)	3.45	NP	10	13.5	141.2 (22.2)
Water Treatment Residual (WTR)	1.88	NP	385	42	65.3 (10.3)
Encapsulation Soil	2.66	18	17	26	104.4 (16.4)

Note: I_p: plasticity index, G_s: specific gravity NP: non-plastic, w_n: natural water content, w_{opt}: optimum moisture content, $\gamma_{dry\text{-}max}$: maximum dry unit weight.

Table 3.2 Elemental composition of the steel slag, water treatment residual, and encapsulation soil

Material	Steel Slag (2YS) (mg/L)	Water Treatment Residual (WTR) (mg/L)	Encapsulation Soil (mg/L)
P	2100	2100	262
K	19,400	2600	2350
Ca	173,000	5100	1940
Mg	50,900	3000	6300
S	617	4700	110
Zn	189	98.1	142
B	41.6	10.4	4.57
Mn	18,100	4300	885
Fe	113,900	22,600	53,700
Cu	19.7	56.4	61.7
Al	10,600	159,700	47,700
Na	299	284	106
Cd	<0.4	<0.4	<0.4
Co	1.90	12.2	29.1
Cr	1300	<0.1	37.0
Mo	1.57	2.41	<0.4
Ni	<0.3	6.18	17.4
Pb	16.0	<2	<2
Li	16.7	24.2	13
As	<3	13	3.24
Se	<3	<3	<3
Ba	68.5	210	98.6
V	500	41.5	138
Ag	<0.6	275	461
Sb	< 0.81	1.79	6.13
Si	457	516	847

To simulate the flow of leachate through an encapsulating clay layer, the leachate solution from the first water leach test was put into a centrifuge tube and dry clay was added to maintain an L:S of 20:1. The samples were rotated for another 18 hours and the steps mentioned above were repeated. After the pH and EC measurements were taken, the samples were acidified to pH <2 with 2% HNO_3. Before use, all equipment (centrifuge tubes, filter holders syringe, etc.) were washed with 2% HNO_3 acid solutions and rinsed with deionized (DI) water. All samples were stored at 4 C^o for chemical analysis. Duplicate SWLTs were conducted on all mixtures. The SWLT setup is schematically given in Figure 3.2.

3.3.2 Sequential Column Leach Test (SCLT)

In order to simulate the encapsulation of pure or treated S materials in a clayey soil, sequential column leach tests (SCLT) were conducted. In these tests, the effluent tubing of the first column, which contains pure or treated S materials, is connected to the second column that houses the encapsulating clay layer. Effluent samples were collected from both columns in order to compare the pH, EC and metal concentrations. The SCLT setup is shown in Figure 3.3 and the conceptual flow model is given in Figure 3.4.

The SCLTs were conducted on pure S and S-WTR mixtures. All specimens were compacted at their optimum moisture contents in a PVC mold with a 4-inch (101.6 mm) diameter and 4.6-inch (116.4 mm) height using standard Proctor effort (ASTM D698, 600 kN-m/m^3). In order to increase the surface area of the sample, air-dried steel slag was sieved from a 3/8-inch (9.5 mm) sieve to remove larger particles. PVC molds

were preferred because it minimizes the outside effects on effluent metal concentrations.

The columns were operated in an upflow mode using a peristaltic pump on the influent line. The polypropylene (PP) influent lines were connected both to the second column and to a polyethylene reservoir tank, which was filled with the 0.02 M NaCl solution. On the effluent end of the column, polypropylene (PP) tubing transferred the effluent solution into the collection bottle. An inflow rate of 15 mL/hr was used due to the low permeability of the encapsulating clay layer ($k= 1.01 \times 10^{-6}$ cm/s).

A 0.02 M NaCl solution, prepared with ASTM Type II water (resistivity greater than 1 megaohm-cm; ASTM D1193) was used to provide an influent with an ionic strength comparable to that of groundwater percolating through the embankment (Morar et al. 2012). The leachate samples were taken every hour for the first four hours and then daily throughout the test. The sample's pH and electrical conductivity measurements were recorded immediately after the sample collection. The suspended solids were filtered through the 0.2-μm pore size, 25-mm diameter membrane disk filters fitted in a 25-mm Easy Pressure syringe filter holder by using a 60-mL plastic syringe. A series of falling-head hydraulic conductivity tests were conducted on the specimens before dismantling the columns.

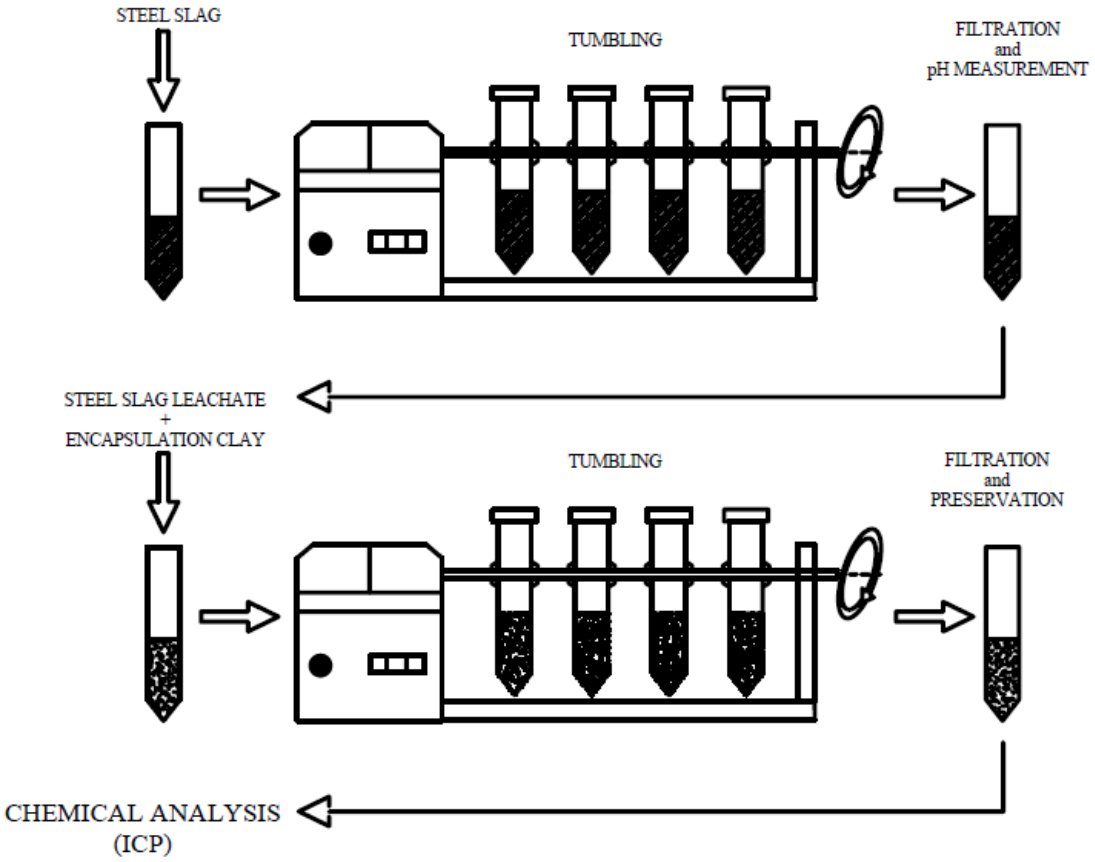

Figure 3.2 Sequential Water Leach Test Setup

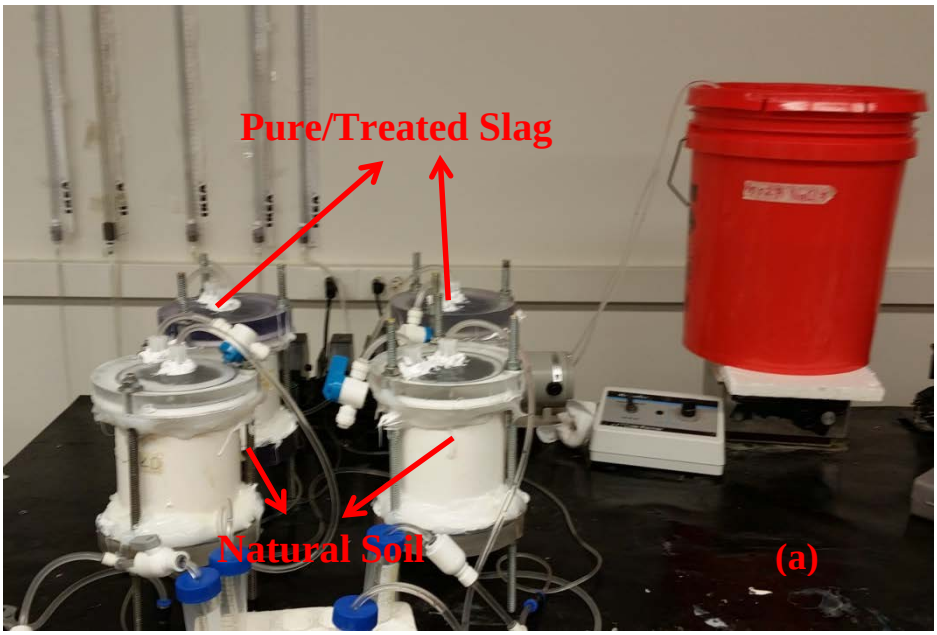

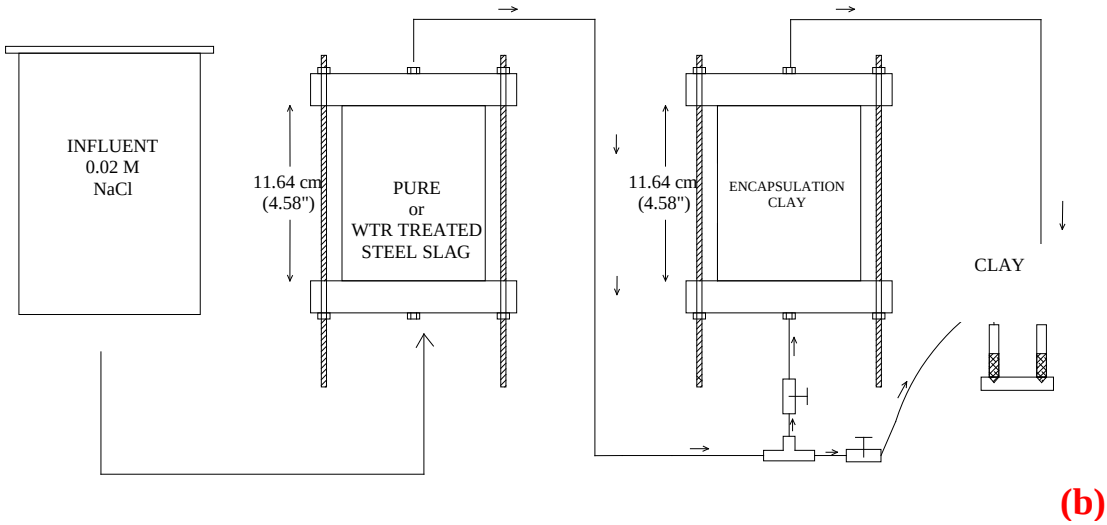

Figure 3.3 (a) Photo and (b) sketch of the sequential column leach test set-up.

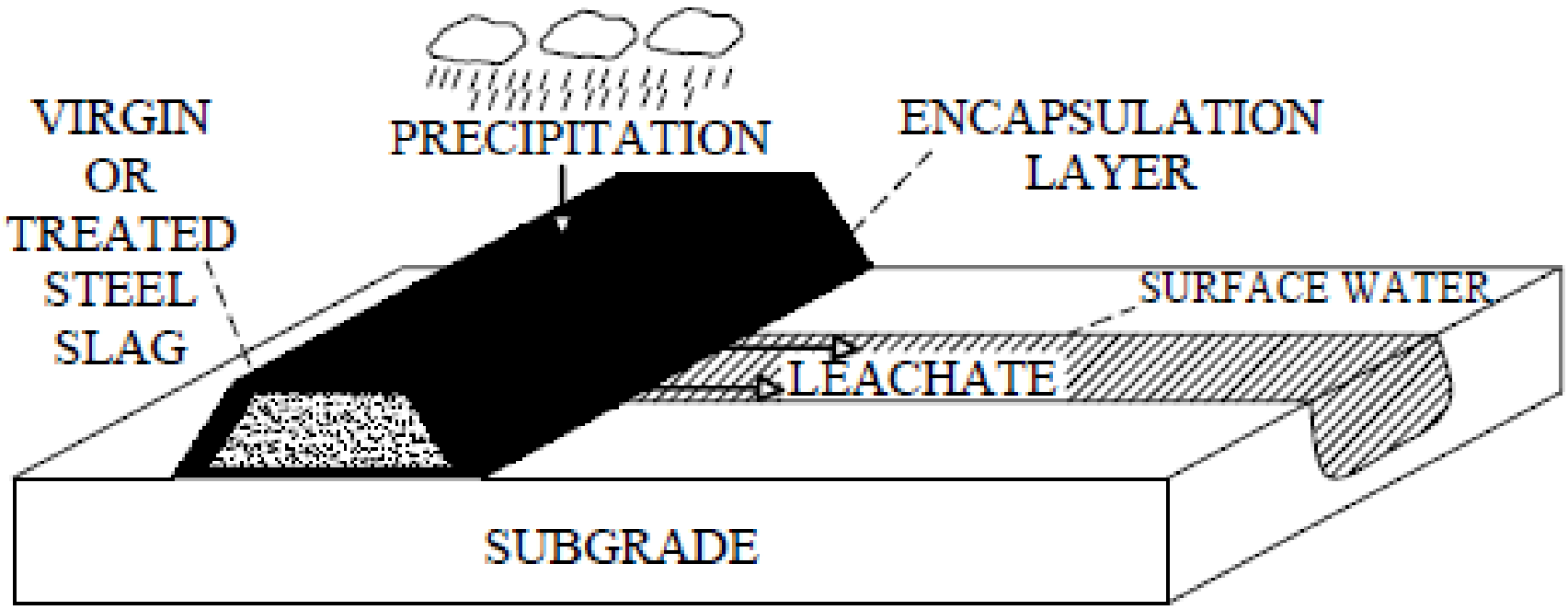

Figure 3.4 Conceptual model to analyze the flow of steel slag into surface waters.

3.3.3 Chemical Analysis

The total elemental analyses (TEA) method covers a digestion process and analysis of pure and treated slag (S) samples for major and minor element contents. The digestion process began by weighing the sample in a 50-mL glass digestion tube. In each tube, 5 mL of concentrated HNO_3 (trace element grade) was added and the tubes were loosely capped and placed on a digestion block that was heated to 1200° C. The slag, WTR and encapsulation clay samples were digested for 15 to 16 hours at 1200° C and then removed from the digestion block. After the samples were cooled down, 1mL of hydrogen peroxide (H_2O_2) was added to each tube, and the tubes were placed back on the block for 30 minutes. This step was repeated twice and the samples were then removed from the block to cool down. The sample volume was made sure to be brought to 50 mL, mixed and kept for three hours before the chemical analysis.

The concentration of all metals for TEA and the ones in SWLT/SCLT leachates were determined using a Varian Vista-MPX CCD Simultaneous ICP-OES (Thermo Jarrell Ash IRIS Advantage Inductively Coupled Plasma Optical Emission Spectrometer). All sampling equipment that contacted the leachate samples was acid-cleaned, dried and stored in clean, sealed bags. Every 20 samples a blank reagent and every 10 samples a spiked sample was tested for calibration purposes. Minimum detection limits (MDLs) for ICP-OES were determined for each metal, and a set of calibration standards, according to the U.S. Code of Federal Regulations Title 40, was followed.

SWLT/SCLT leachates were analyzed for Al, As, B, Ba, Ca, Cd, Co, Cr, Cu, Li, Mn, Ni, Pb, and V. The metals selected for further discussion were Al, Cr, and As.

These three metals were selected based on TEA (presented in Table 3.2), and due to their elevated concentrations in SWLT/SCLTs, their potential risk to the environment and human health as well as their documented mobilities in groundwater (Fällman and Aurell, 2000, Lim et al. 2004, Jankowski et al. 2006, Komonweeraket et al. 2010).

In humans and animals, sustained exposure to high levels of Al can cause bone abnormalities. Cases of adverse respiratory tract effects, such as asthma, neuropyschiatric symptoms, like loss of coordination and loss of memory (Alzheimer's disease), and problems with balance due to Al overexposure have also been reported in humans (U.S. FDA 2000, Healy et al. 2001, Krewski et al. 2007, Shaw and Tomljenovic 2013). Aluminum (Al) easily transits from solid to liquid phase at low pH values, and is quickly mobilized by acid rain, which results in its accumulation in plants and natural water systems. In plants, soluble Al can inhibit cell division and produce chromosomal aberrations and color changes due to phosphate deficiency and crop decrease (Manna and Parida 1965, Barabasz et al. 2002, ATSDR 2008).

Chromium (III) (Cr^{3+}) is nontoxic and provides necessary nutrition metal for plants and animals (Quina et al. 2009), whereas Cr (VI) is a toxic Cr species, an acute irritant for living cells and can be carcinogenic to humans from inhalation (Whalley et al. 1999).

Arsenic (As), which is found in several different chemical forms and oxidation states, causes acute and chronic adverse health effects including cancer (Hughes 2002). Arsenic is toxic to the majority of organ systems, the most sensitive target organ being the kidney (Cohen et al. 2006). While chronic arsenic exposure affects the vascular

system and causes hypertension and cardiovascular disease, acute arsenic toxicity may cause cardiomyopathy and hypotension (Jomova et al. 2010).

3.3.4 Modeling of Contaminant Transport in Surface Waters

In the case of steel slag-amended embankments, the contamination of surface waters like rivers and streams is of concern. Usually, computer programs designed to model the flow of groundwater through multiple soil layers ignore the surface runoff that may occur at the embankment surface and instead assume that the entire precipitated water infiltrates through the pavement structure and soil vadose zone.

Analytical solutions of the advection-dispersion equation (ADE) and related models are necessary to simulate contaminant transport processes in streams and rivers. The ADE distinguishes two transport modes: advective transport as a result of passive movement along with water, and dispersive/diffusive transport to account for diffusion and small-scale variations in the flow velocity, as well as any other processes that contribute to solute spreading.

Van Genuchten (2013) developed one- and multi-dimensional solutions for the adversion-dispersion equation to define advective, dispersive, longitudinal transports and lateral dispersion. These solutions were utilized to develop a numerical model, named UMDSurf herein, to estimate the concentration distributions as a function of distance.

For one-dimensional transport, the solute flux J_s can be written as;

$$J_s = uC - D_x \frac{\partial C}{\partial x} \tag{3.1}$$

where u is the longitudinal fluid flow velocity, C is the solute concentration expressed as mass per unit volume of water, D_x is the longitudinal dispersion coefficient accounting for the combined effects of ionic or molecular diffusion and hydrodynamic dispersion, and x is the longitudinal coordinate.

The mass balance equation is then formulated by considering the accumulation of the solute in a control volume over time as a result of the divergence of the flux (i.e., net inflow or outflow):

$$\frac{\partial C}{\partial t} = -\nabla \times J_s - R_s + R_w C_e \tag{3.2}$$

where t is time and R_s represents arbitrary sinks or sources of solute; i.e. $R_s<0$ means consumption, whereas $R_s>0$ means the feeding of solute, while the last term denotes injection (> 0) or pumping (< 0) of water with constituent concentration C_e at a rate R_w. If these two last terms are ignored, the generally used ADE is obtained using the following equation:

$$\frac{\partial C}{\partial t} = D_x \frac{\partial^2 C}{\partial x^2} - u \frac{\partial C}{\partial x}. \tag{3.3}$$

However, natural processes such as biodegradation or inactivation, radioactive decay and production may affect the concentration of contaminants, and can all be included in the sink/source term, R_s, in Eq. (3.2). As long as this term is described in terms of linear processes, the transport problem can still be solved analytically. For a case involving one or several sets of zero- and first-order rate expressions, the

governing equation can be represented in the following form, where μ is a general first-order decay rate, and γ is a zero-order production term:

$$\frac{\partial C}{\partial t} = D_x \frac{\partial^2 C}{\partial x^2} - u \frac{\partial C}{\partial x}. \tag{3.4}$$

In this study, a numerical one-dimensional solution of ADE with a third type inlet condition is used as (ω=1). The initial and boundary conditions are given below:

$$C(x, 0) = f(x) \tag{3.5}$$

$$\left(uC - \omega D_x \frac{\partial C}{\partial x}\right)_{x=0^+} = ug(t) \tag{3.6}$$

$$\frac{\partial C}{\partial x}(\infty, t) = 0 \; or \; \frac{\partial C}{\partial x}(L, t) = 0 \tag{3.7}$$

There is a semi-infinite domain with uniform initial concentration, $f(x) = C_i$, and no production or decay is assumed to exist. The inlet concentration function, $g(t)$, is of the pulse type (a Heaviside step function) with the constant concentration C_o, and is written as follows:

$$g(t) = \begin{cases} C_0, & 0 < t \leq t_0 \\ 0, & t \geq t_0 \end{cases} \tag{3.8}$$

The solution of Equation 3.4 is given below:

$$C(x,t) = \begin{cases} C_i + (C_0 - C_i)A(x,t), & 0 < t \leq t_0 \\ C_i + (C_0 - C_i)A(x,t) - C_0 A(x, t - t_0), & t \geq t_0 \end{cases} \quad (3.9)$$

Where

$$A(x,t) = \frac{1}{2} erfc\left[\frac{x - ut}{\sqrt{4D_x t}}\right] +$$

$$\sqrt{\frac{u^2 t}{\pi D_x}} exp\left[-\frac{(x-ut)^2}{4D_x t}\right] - \frac{1}{2}\left(1 + \frac{ux}{D_x} + \frac{u^2 t}{D_x}\right) exp\left(\frac{ux}{D_x}\right) erfc\left[\frac{x+ut}{\sqrt{4D_x t}}\right] \quad (3.10)$$

3.4 RESULTS

3.4.1 Sequential Water Leach Tests (SWLT)

Duplicate sequential batch water leach tests (SWLT) were conducted on steel slag (S), water treatment residual (WTR) and their mixtures. The leachates collected from the specimens were introduced into the encapsulation clay, and the tests were run for another 18 hours to simulate the flow of leachate through the encapsulation clay. Table 3.3 summarizes the pH values and the leached metal concentrations from SWLT.

Figure 3.5 shows that the addition of WTR decreases pH significantly; however, the rate of decrease drops with increasing WTR amounts. It is speculated that the WTR addition decreases the release of free lime (CaO), hydrated calcium silicate (C-S-H) and portlandite $Ca(OH)_2$ from the steel slag, resulting in a decrease in pH. The WTR used in this study is an aluminum-based material and, thus, the reduction in Ca releases for the WTR-treated steel slag might be due to the formation of less soluble secondary mineral phases as a result of excess aluminum in the solution. As stated by Juenger et

al. (2006) and Ozkok et al. (2015), the formation of an aluminosilicate layer may have encapsulated the slag particles and hindered CaO hydration.

The data in Table 3.3 show that the presence of an encapsulation layer can significantly influence the pH due to high adsorption and the buffering capacity of the clayey soils. Buffering capacity is the capacity of a soil to adsorb and/or desorb H^+ and OH^- ions. This means a soil can act as an acid or base, and thus show a resistance to pH changes. The buffer capacity is determined experimentally by measuring the pH change when a strong base or acid is added to a solution. Clay particles have a very large surface area compared to silt particles (Sparks, 2003). This relatively large surface area increases the contact time and influences the buffering effect, which ultimately reduces the pH and the concentration of the most elements (Sauer et al. 2012). Liu et al. (2008b) conducted column-leaching tests on several different types of soils and showed that clayey soils are likely to provide the largest buffering capacity for pH.

Table 3.3 shows the concentrations of thirteen metals for pure S, the S-WTR mixture and the S-WTR-encapsulation clay system. The results show that, with an exception for Al, higher metal concentrations were observed for pure S than its mixtures with WTR and/or encapsulation clay. All metal concentrations in leachates past through the S-WTR-encapsulation clay system are below the U.S. EPA maximum concentration limits for drinking waters (MCL), EPA water quality limits (WQL) and Maryland aquatic toxicity limits (ATL). The variation in concentrations of Al, Cr and As is plotted against WTR content in Figure 3.6. For Al and Cr, increasing WTR content results in decreased metal concentrations, and As concentrations remain below detection limits for all mixtures.

The rate of decrease in metal concentrations, however, is different without a recognizably consistent variation, which is partially due to differences on metal concentrations based on total elemental analysis (Table 3.2). The decrease in metal concentrations is not linear with increasing WTR content, even though the mass of metals in soil mixture decreases approximately linearly with increasing WTR content. Therefore, the use of linear dilution calculations will underestimate the resulting metal concentrations leached from the soil mixtures.

The effluent concentrations of aluminum (Al) are lower for the pure S than the S-WTR mixtures. This is due to very high aluminum content of the WTR compared with pure slag and the alkaline leachate pH. The solubility of Al is minimum at a pH of 6.5-7.0 and increases under alkaline conditions (Lim et al. 2004, Komonweeraket et al. 2010). The data in Figure 3.6 shows that the Al concentrations decrease even as the WTR amount is increased, since effluent pH decreases with increasing WTR content and Al remains insoluble.

Chromium (Cr) concentrations within the leachate decrease with the addition of WTR. As seen in Table 3.2., Steel slag contains a significant amount of Cr, whereas the amount in WTR is negligible (1,300 mg/L versus <0.1 mg/L). However, the decrease in Cr concentrations is not linear due to a variation in pH. The solubility of Cr is highly dependent on the pH of the aqueous solution. Cr solubility is reported in the literature to follow mostly an amphoteric pattern (Komonweeraket et al. 2010, Cetin et al. 2014), i.e. mobility is very low at a neutral pH, but increases significantly at both acidic and basic conditions (Sparks, 2003).

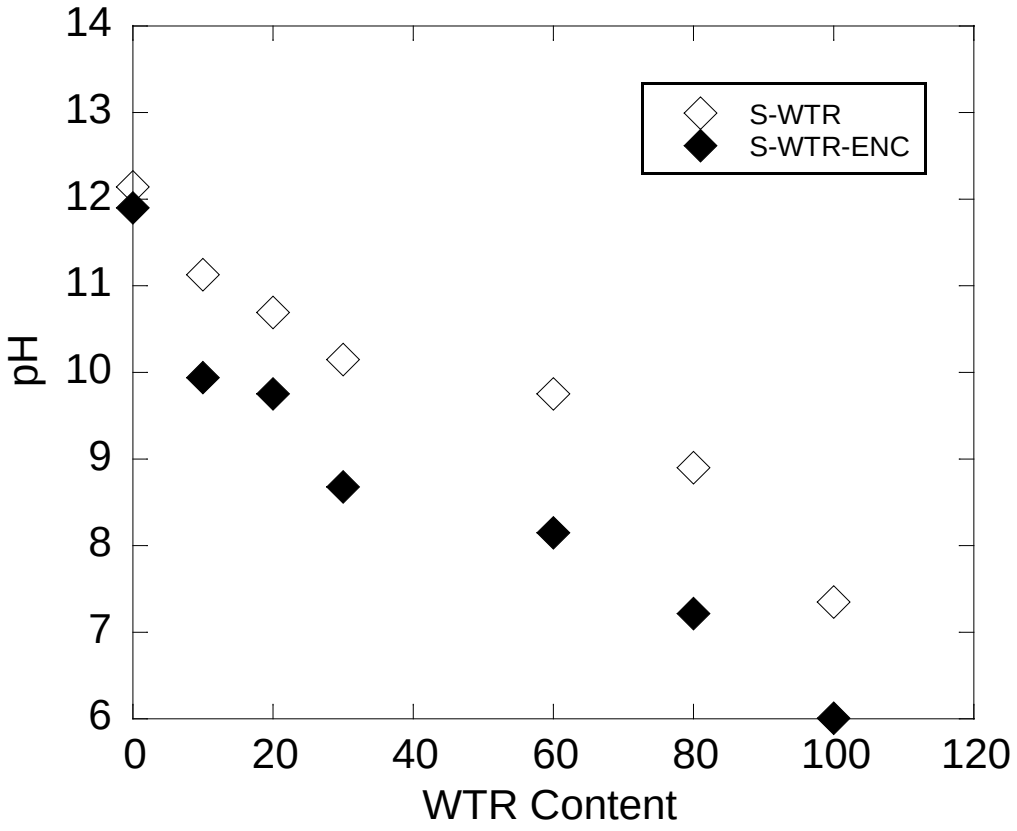

Figure 3.5 Effect of WTR content and presence of encapsulation clay on pH of the slag mixtures. Note: SWTR designate the specimens prepared with different WTR percentages whereas SWTR-ENC designates specimens that are prepared by mixing encapsulation clay and effluent leachates from SWTR mixtures.

Table 3.3 Aqueous metal concentrations in SWLTs. Concentrations exceeding EPA WQL are in **bold**

Sample	WTR Content	pH	Al (mg/L)	As (µg/L)	B (µg/L)	Ba (µg/L)	Cd (µg/L)	Co (µg/L)	Cr (µg/L)	Cu (µg/L)	Li (µg/L)	Mn (µg/L)	Ni (µg/L)	Pb (µg/L)	V (µg/L)
S-ENC	0	11.9	**3.66**	<10	36	35	<4	<3	51.95	<5	<2	**59**	45	385	25
S10WTR-ENC	10	9.94	**14.7**	<10	51	35	<4	<3	17.15	<5	<2	21	42	140	13
S20WTR-ENC	20	9.75	**9.08**	<10	35	37	<4	<3	15.8	<5	<2	23	35	120	10
S30WTR-ENC	30	8.68	**0.91**	<10	20	45	<4	<3	13	<5	<2	30	34	112	10
S60WTR-ENC	60	8.15	**1.42**	<10	16	35	<4	<3	15	<5	<2	32	29	216	14
S80WTR-ENC	80	7.22	<0.05	<10	3	76	<4	<3	12	<5	<2	**750**	32	325	15
WTR-ENC	100	6.01	<0.05	<10	5	170	<4	<3	<1	<5	<2	**2810**	30	136	13
U.S .EPA MCL			0.2	10	NA	2000	5	NA	100	1300	NA	50	NA	15	NA
U.S .EPA WQL			0.75	340	NA	NA	2	NA	570	13	NA	NA	470	65	NA
MD ATL			NA	NA	NA	NA	2	NA	570	13	NA	NA	470	65	NA
MDL			0.05	10	5	10	4	3	1	5	2	1	10	5	10

Notes: MCL= maximum contaminant levels for drinking water; MCL for Al is based on a secondary non-enforceable drinking water regulation; WQL= water quality limits for protection of aquatic life and human health in fresh water. MD ATL = Maryland State aquatic toxicity limits for fresh water; Concentrations exceeding MCLs in bold. NA=Not available; MDL= minimum detection limit.

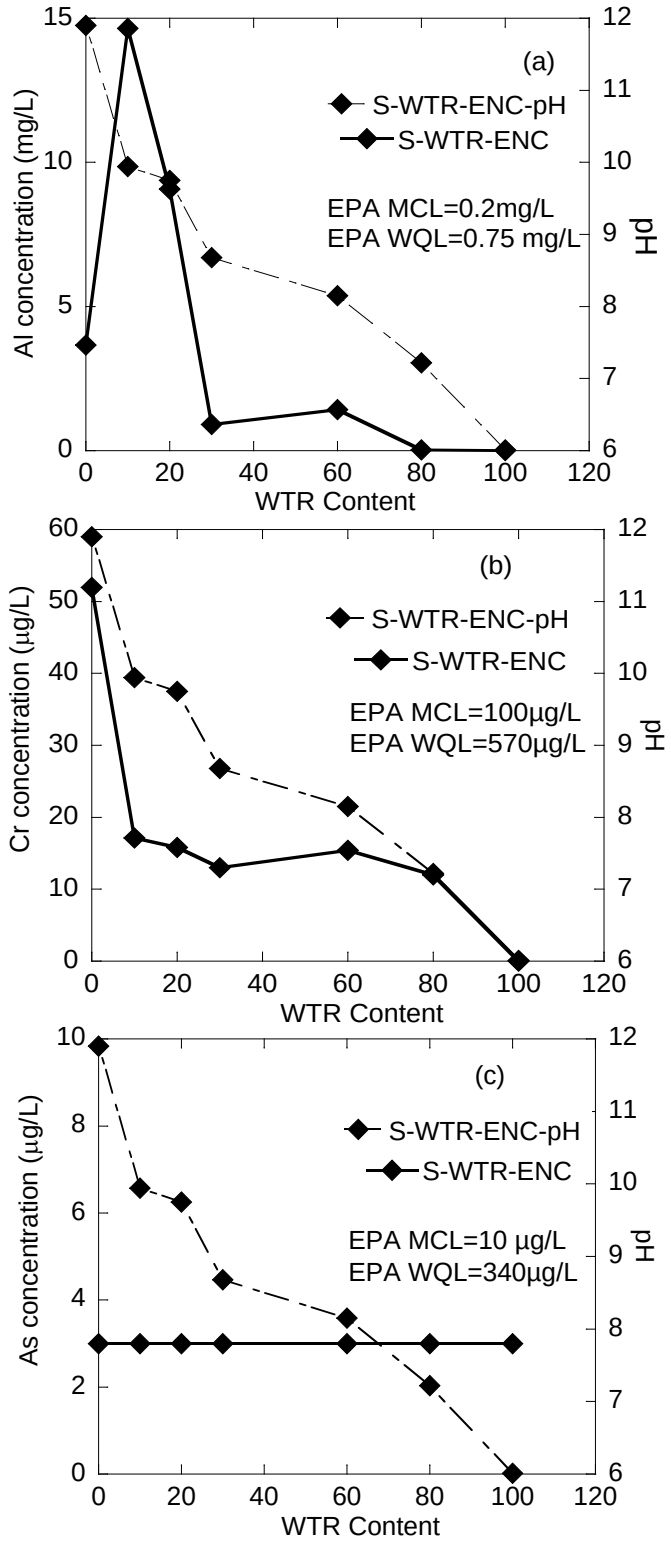

Figure 3.6 Effect of WTR content on sequential water leach test concentrations of a) aluminum (Al), b) chromium (Cr), and c) arsenic (As). 0% and 100% WTR content corresponds to pure S and pure WTR specimens, respectively.

3.4.2 Sequential Column Leach Tests (SCLT)

Figure 3.7 shows the temporal characteristics of effluent pH of the pure S and the S-WTR mixtures, as well as the effluent pH after leaching through the encapsulation clay material. Considering the low hydraulic conductivity of the clay material (k= 1.01 x 10^{-6} cm/s) compared with that of the pure slag (k= 9.3 x 10^{-4} cm/s) and S-WTR mixtures (k= 4.2 x 10^{-5} cm/s to 3 x 10^{-6} cm/s), all tests were continued until a minimum of 20 pore volumes (PV) of flow were obtained to examine the behavior and persistency of pH. Even though the pH levels of the influent solutions were kept between 6 and 6.5, the stabilized pH levels of the effluent solutions of pure or treated S were significantly high (pH>11).

Pure steel slag has the highest pH (~12.6) and pH decreases with increasing WTR amounts (Figure 3.7). Similar to the observations made in SWLTs, the addition of WTR appears to have a significant effect on pH, and further decreases in pH can be obtained when the leachate passes through the encapsulating clay layer. These results also show that the clay reduces the system pH, regardless of the WTR percentage in the mixture, mainly due to the high buffering capacity of the clayey soils. It is speculated that the addition of WTR might have resulted in a decrease in pH, due to the formation of ettringite by coating the particles and preventing Ca^{2+} leaching (Ozkok et al. 2015). The elution curves for Ca^{2+}, a significant indicator of change in pH, are given in Figure 3.8.

Table 3.4 shows that concentrations of some of the metals that leach from pure slag or S-WTR mixtures exceed the groundwater quality limits set by EPA, but the concentrations decrease significantly after leachate percolates through the

encapsulating clay layer. The leaching mechanisms are further discussed below in detail.

Figure 3.9 shows a series of CLT elution curves for Al, Cr and As. Similar trends were observed for the remaining metals. Leaching of the Cr and As exhibits a first-flush leaching pattern, followed by stabilized concentrations. The first-flush pattern is related to release of the metals from the water-soluble fraction as well as from the sites which have lower adsorption energies (Bin-Shafique et al. 2006, Morar 2008). Sauer et al. (2012) reported that materials with a higher CaO content were more likely to exhibit a first-flush leaching pattern. The relatively high Ca content in steel slag (173,000 mg/L,Table 3.2) may be responsible for the first-flush behavior observed in the current study.

Al exhibits an amphoteric pattern, i.e., higher leaching concentrations at extreme pH levels and lower concentrations at a near-neutral pH level (Langmuir 1997, Kenkel 2003). A mixed trend in Al leaching is observed with the WTR amendment to steel slag due to relatively higher amounts of Al in the WTR (159,700 mg/L versus 10, 600 mg/L, Table 3.2). The WTR addition decreases the effluent pH below 12; however, large amounts of WTR (about 80% of total composition based on TEA) contribute to higher leached Al concentrations. The data in Table 3.5 show that the Al concentrations are elevated with an increase in WTR content; however, the concentrations decrease below detection limits when the effluent solution passes through the encapsulation clay layer and the pH drops below 7.5. This agrees with the results of other studies that showed Al leaching is the lowest at pH~7 and is the highest under very alkaline conditions (Lim et al. 2004, Komonweeraket et al. 2010). Sparks

(2003) also showed that aluminum is very insoluble at a neutral pH, and its solubility is controlled by dissolution-precipitation oxide and hydroxide minerals. Fällman and Aurell (2000) performed CLTs and field lysimeter tests on steel slag and reported that the field Al concentrations were significantly lower than those in column tests, due to lower pH levels measured in the field. Fällman and Aurell (1994) also reported that a pH change of approximately four units between column and lysimeter tests, resulting in a 100 times decrease in Al concentrations.

Figure 3.9 shows that a decrease in the initial Cr metal concentrations occurs with an increasing WTR content. The solubility of Cr is highly dependent on the pH of the aqueous solution; i.e., Cr concentration is very low at a neutral pH, but increases significantly under very acidic and basic conditions. As seen in Table 3.4, the high pH of the slag leachate (pH ~12.6) causes an increase in peak Cr concentrations. Fällman (2000) performed a study to determine the controlling mechanism for chromium leaching from steel slag and showed that there are interdependencies between concentrations of barium, chromium, sulphur and calcium. Fruchter et al. (1990) indicated that aqueous concentrations of chromate (Cr^{6+}) is controlled by solid solutions of barium sulphate ($BaSO_4$) and solid solutions of $Ba(S,Cr)O_4$. However, none of these are reported to exist as primary minerals in steel slag. No testing was conducted to identify the oxidation state of Cr speciation in the CLT leachates collected in the current study; however, Chaurand et al. (2007) claimed that Cr generally appears as Cr^{3+} in steel slag leachates due to the absence of pre-edge peak in the spectra, or an indicator of hexavalent chromium in the X-ray absorption near edge structure spectroscopy analysis (XANES). Pourbaix diagrams for the Cr-O-H system indicate

that the Cr measured in WLT and CLT leachates is likely to exist as $Cr(OH)_3$ or $Cr(OH)_4^-$ for the pH conditions of between 7 and 12.5 present in the current study (Stumm and Morgan, 1996). This oxyanionic species cannot be adsorbed and is soluble; thus, Cr concentrations of the pure slag leachate are higher than the S-WTR mixtures. Increasing WTR content also decreases the pH; thus, Cr^{3+} exists in an amorphous $Cr(OH)_3$ form, and the Cr concentration for both the effluent of slag-WTR mixture and the effluent passing through the encapsulation clay are below the detection limits.

Jankowski et al. (2006) and Komonweeraket et al. (2010) pointed out that a change in pH from neutral to alkaline conditions also increases the As concentrations. The pH-dependency of As observed in the current study agrees with these findings (Table 3.4). The leaching of As tends to show an amphoteric leaching pattern and has a high affinity to exist in its anionic forms, such as $HAsO_4^{2-}$ or $HAsO_3^-$ (Narukawa et al. 2005, Ettler et al. 2009). At near-neutral pH conditions (pH=6-7.5), leaching of As is minimal due to the maximum adsorption of As metals onto soil surfaces. In addition, Kim et al. (2009) and Pandey et al. (2011) also indicated that As adsorption onto metal oxide minerals is very likely to occur at neutral pH levels minimizing the As concentration within the leachate. Fe-oxides have a strong affinity for the As species due to a rapid adsorption reaction between As and Fe-oxides (Sadiq et al. 2002). Aluminum and iron oxides may have coated the surface of steel slag grains in the current study, reducing the leaching of trace metals at pH=6.8-7.0 when the leachate flowed through the encapsulation layer. Van der Hoek and Comans (1996) reported an over 100 times decrease in As concentrations when the pH was changed from 12 to 6

and showed that As leaching was controlled by adsorption onto hydrous ferric oxides (HFO).

A chemical equilibrium modelling software, Visual MINTEQ v3.0, was utilized for estimating $CaCO_3$ precipitation in slag leachates containing different Ca^{2+} concentrations. Input Ca concentrations were determined based on the measured dissolved Ca^{2+} concentrations in the leachates from the column tests. 0.02 M Na^+ and Cl^- (background electrolytes) were entered for all estimations (no atmospheric CO_2 exposure, T=20ºC). pH was calculated based on "mass and charge balance". Equilibrium conditions with the atmospheric CO_2 was assumed and CO_2 pressure was set to 0.00038 atm. Default databases that were available with the original software were used.

Calcium carbonate ($CaCO_3$) precipitation, also called "tufa formation", occurs when steel slag leachates containing high concentrations of dissolved calcium are exposed to atmosphere. Calcium carbonate is a sparingly soluble compound and over time thick layers of calcium carbonate may result in clogging of the drainage system. The estimated amount of $CaCO_3$ precipitation for the effluent leachates are given in Table 3.6. The results indicate that the $CaCO_3$ precipitation significantly decreases with increasing WTR amount. Furthermore, no $CaCO_3$ (tufa) precipitation occurs when steel slag is used as a S30-WTR mixture and the pH values as well as metal concentrations are stabilized.

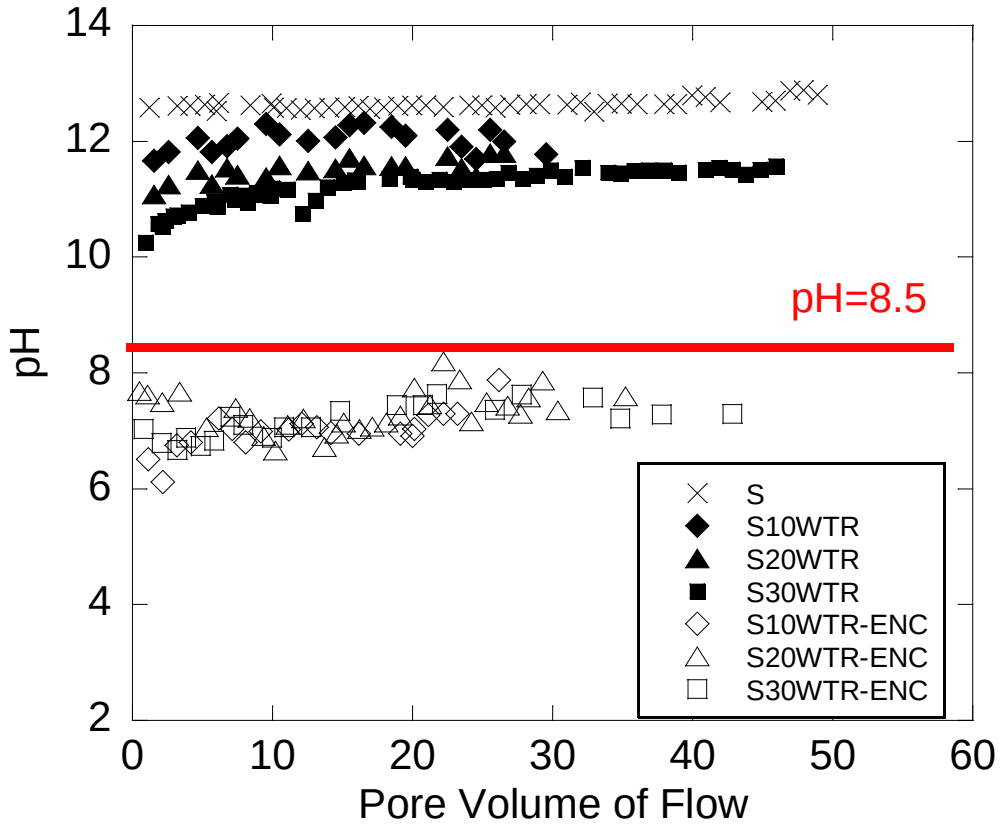

Figure 3.7 Effluent pH in SCLTs**.**

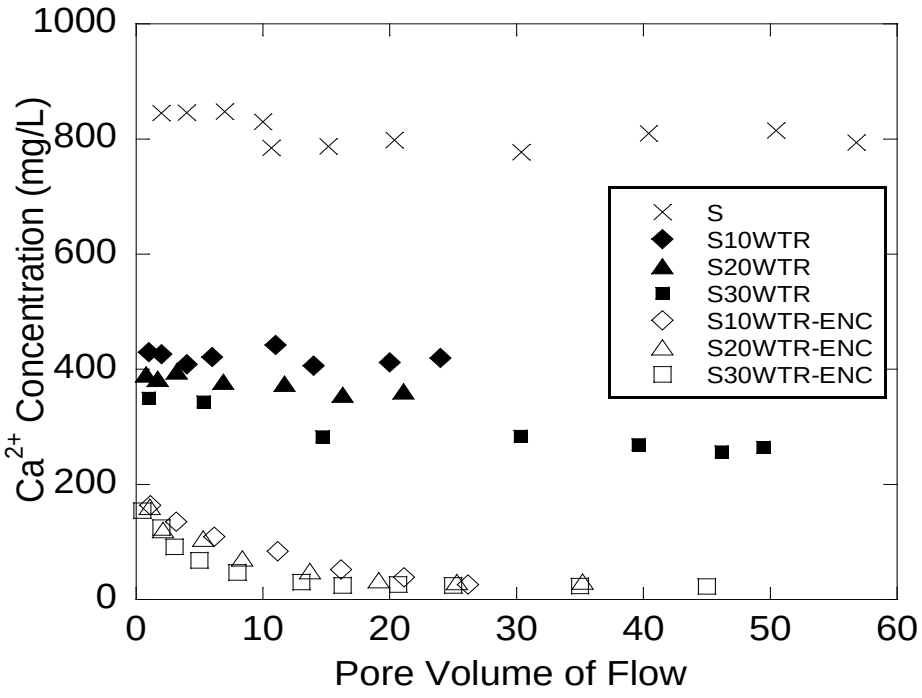

Figure 3.8 Elution curves for Ca^{2+}.

Table 3.4 Peak effluent pH and metal concentrations in SCLTs. Concentrations exceeding MCLs in **bold**.

Sample	WTR Content	pH	Al (mg/L)	As (µg/L)	B (µg/L)	Ba (µg/L)	Cd (µg/L)	Co (µg/L)	Cr (µg/L)	Cu (µg/L)	Li (µg/L)	Mn (µg/L)	Ni (µg/L)	Pb (µg/L)	V (µg/L)
S	0	12.59	**0.6**	**170**	410	1000	<4	<3	73	14	230	1.4	<10	**22**	30
S10WTR	10	12.23	**173**	**146**	290	840	<4	<3	18	58	81	6	15	**15**	30
S20WTR	20	11.51	**213**	**102**	175	630	<4	<3	15	36	48	11	30	11	25
S30WTR	30	11.10	**240**	**70**	73	120	<4	<3	3	100	20	35	40	8	20
S10WTR-ENC	10	7.30	**0.70**	<10	42	1081	<4	113	<1	<5	<2	**23,000**	60	<5	20
S20WTR-ENC	20	7.28	**0.85**	<10	40	1042	<4	109	<1	<5	<2	**22,400**	65	<5	20
S30WTR-ENC	30	7.23	**0.81**	<10	40	1070	<4	92	<1	<5	<2	**23,500**	60	<5	20
U.S .EPA MCL			0.2	10	NA	2000	5	NA	100	1300	NA	50	NA	15	NA
U.S .EPA WQL			0.75	340	NA	NA	2	NA	570	13	NA	NA	470	65	NA
MD ATL			NA	NA	NA	NA	2	NA	570	13	NA	NA	470	65	NA
MDL			0.05	10	5	10	4	3	1	5	2	1	10	5	10

Notes: MCL= maximum contaminant levels for drinking water; MCL for Al is based on a secondary non-enforceable drinking water regulation; WQL= water quality limits for protection of aquatic life and human health in fresh water. MD ATL = Maryland State aquatic toxicity limits for fresh water; NA=Not available; MDL= minimum detection limit

Table 3.5 Stabilized effluent pH and metal concentrations in SCLTs. Concentrations exceeding MCLs in **bold**.

Sample	WTR Content	pH	Al (mg/L)	As (µg/L)	B (µg/L)	Ba (µg/L)	Cd (µg/L)	Co (µg/L)	Cr (µg/L)	Cu (µg/L)	Li (µg/L)	Mn (µg/L)	Ni (µg/L)	Pb (µg/L)	V (µg/L)
S	0	12.50	**0.43**	**70**	410	530	<4	<3	15	10	160	0.8	<10	**21**	10
S10WTR	10	12.28	**89**	**41**	270	400	<4	<3	5	10	35	1.5	<10	13	10
S20WTR	20	11.49	**116**	**36**	170	240	<4	<3	5	10	20	2	<10	10	10
S30WTR	30	11.01	**188**	**10**	70	90	<4	<3	3	10	10	5	<10	8	10
S10WTR-ENC	10	7.24	<0.05	<10	30	420	<4	10	<1	<5	<2	**6,580**	<10	<5	10
S20WTR-ENC	20	7.24	<0.05	<10	30	410	<4	10	<1	<5	<2	**6,650**	<10	<5	10
S30WTR-ENC	30	7.23	<0.05	<10	30	400	<4	15	<1	<5	<2	**6,500**	<10	<5	10
U.S .EPA MCL			0.2	10	NA	2000	5	NA	100	1300	NA	50	NA	15	NA
U.S .EPA WQL			0.75	340	NA	NA	2	NA	570	13	NA	NA	470	65	NA
MD ATL			NA	NA	NA	NA	2	NA	570	13	NA	NA	470	65	NA
MDL			0.05	10	5	10	4	3	1	5	2	1	10	5	10

Notes: MCL= maximum contaminant levels for drinking water; MCL for Al is based on a secondary non-enforceable drinking water regulation; WQL= water quality limits for protection of aquatic life and human health in fresh water. MD ATL = Maryland State aquatic toxicity limits for fresh water; NA=Not available; MDL= minimum detection limit

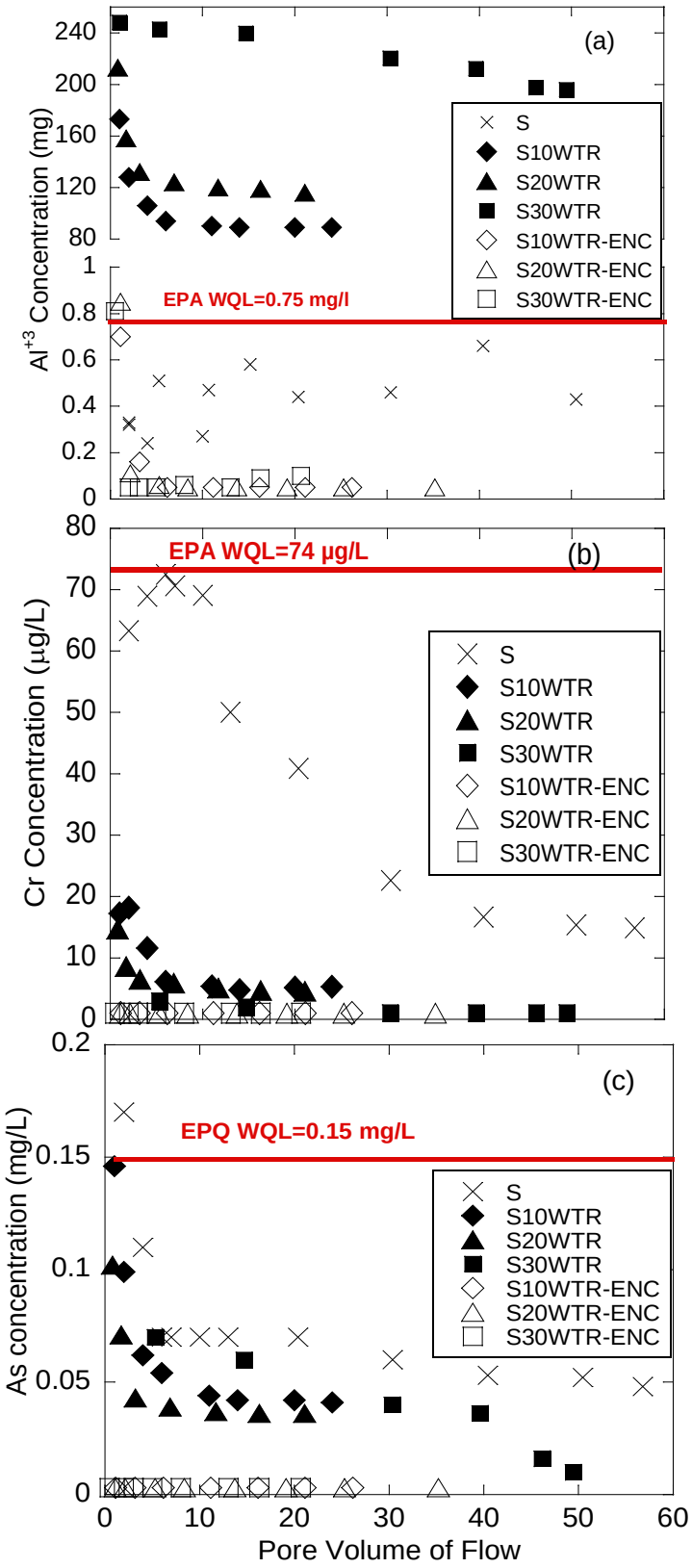

Figure 3.9 CLT elution curves for a) aluminum, b) chromium, c) arsenic.

Table 3.6 Estimation of $CaCO_3$ precipitation for the effluent leachates

Sample	Peak Ca^{2+}-concentration (mg/L)	Estimated Peak $CaCO_3$ Precipitation (mg/L)	Stabilized Ca^{2+}-concentration (mg/L)	Estimated Stabilized $CaCO_3$ Precipitation (mg/L)
S	848	2050	796	1920
S30WTR	341	782	284	639
S30WTR-ENC	189	402	10	0

Note: S=Steel slag; WTR=water treatment residual; ENC= encapsulation clay. Calcium carbonate precipitation was estimated based on measured Ca^{2+} concentrations using Minteq Visual v3.1

3.4.3 Chemical Transport Modeling (UMDSurf)

Figure 3.10 presents the UMDSurf-predicted concentrations of aluminum, chromium and arsenic in the stream after 20, 50, 100, 200, 500 and 1000 seconds. The results are obtained based on the assumptions of an instantaneous injection (t= 10 s) of 2.2 lbs (1 kg) solute in the main channel of a river having a cross-section of 107 ft^2 (10 m^2), an average flow velocity of 3.2 ft/s (1 m/s) and a dispersion coefficient of 54 ft^2/s (5 m^2/s) per recommendations of De Smedt et al. (2005) and van Genuchten (2013). The maximum concentrations obtained by the column tests are used as the input concentration at t=0 sec.

The variation of Al, Cr and As concentrations at different horizontal distances from the point of contact, the corner of the embankment, is presented in Figure 3.10. As expected, metal concentrations decrease significantly with time and distance from the surface of the S-WTR-ENC system. For all cases, at 20 m horizontal distance from the corner of the embankment, the concentrations decrease to 50% of the initial concentration. Moreover, concentrations of all metals are lower than the EPA WQLs at all locations.

For pure steel slag, Al concentrations at 1000 m away from the corner of the embankment decrease to 13 μg/L, which is significantly lower than the EPA MCL limit (200 μg/L). For steel slag leachate, EPA MCL can be achieved at 50 m, whereas the leachate of S30WTR percolating through encapsulation layer decreases to the EPA MCL at 80 m from the corner of the embankment. The data in Figure 3.10 also suggests that the first-flush effect is minimized by the addition of WTR to slag, with the exception of aluminum due to very high Al content of the WTR material itself.

Encapsulation of the embankment with a clayey soil (borrow material) decreases the concentrations to acceptable limits in surface waters.

Similar trends can be observed for the Cr concentrations. At 20 m from the corner of the embankment, both the EPA MCL and WQL are satisfied. It should be noted that the rate of decrease increases if the initial concentration is higher. When S30WTR instead of 100% slag is used, the concentrations in surface waters are below the EPA MCL and WQL. The presence of an encapsulation clay layer further decreases the Cr concentrations.

As concentrations in a stream, will be strongly affected by the treatment and the method of construction. If pure S is used, the concentrations would decrease to EPA MCL at approximately 500 m from the corner of the embankment, whereas for the S30WTR mixture, it would take 100 m to reach the same concentration levels. When S30WTR leachate percolates through the encapsulation layer, As concentrations throughout the length of the stream remain below the EPA MCL.

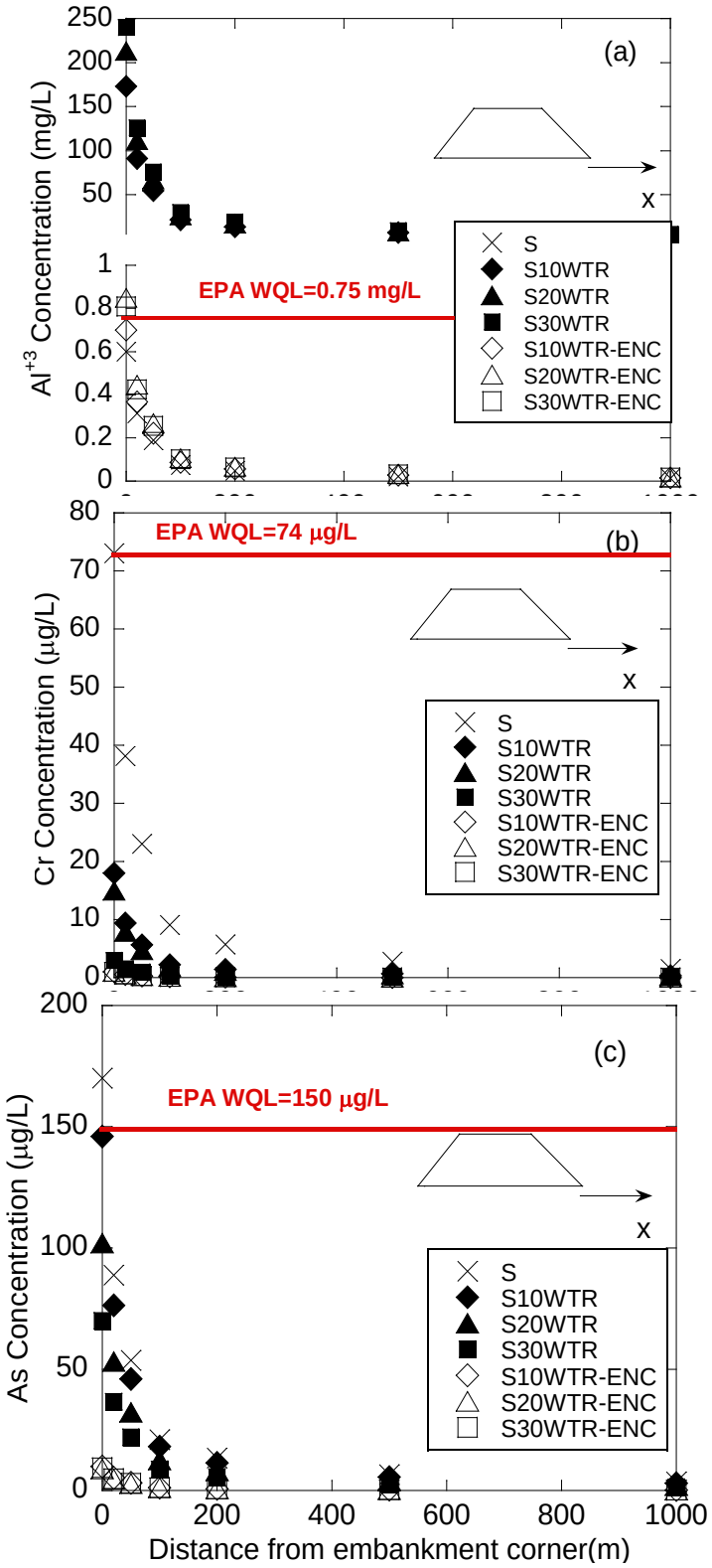

Figure 3.10 Surface water concentrations of a) aluminum, b) chromium, c) arsenic with increasing horizontal distance.

3.5 CONCLUSIONS

A laboratory study was conducted to investigate the leaching characteristics of pure or WTR-amended steel slag in surface waters near highway embankments. The effects of WTR addition to steel slag, and presence of an encapsulating clay layer on pH and metal concentrations were studied through laboratory leaching tests. The observations from the current study are as follows:

- The results of sequential water leach tests showed that increasing WTR percentage results in a decrease in pH. Flow of this leachate past through an encapsulation clay further decreases the pH.
- Aluminum concentration increased when WTR amount increased from 0 to 10 % due to high alum content of WTR, however, then decreased with increasing WTR percentage due to its amphoteric nature. Chromium concentrations decreased with increasing WTR content, whereas As concentrations remained below the EPA MCLs.
- The results of sequential column leach tests indicated that an increase in WTR decreased the pH; however, WTR percentage did not have a significant effect on final pH values once the leachate percolated through the encapsulation layer.
- Al-concentrations increased dramatically with addition of alum-rich WTR but decreased significantly once the leachate past through the encapsulation clay layer. It should be noted that Al is on the EPA list of secondary drinking water regulations, and there are no limits for Al specified in Maryland groundwater

protection guidelines. Both Cr and As concentrations were below EPA MCLs after percolating through the encapsulation layer.

- The results of chemical transport model showed that approximately 40 m away from the corner of the embankment, metal concentrations decreased by 50%. At that distance, Al concentrations also remained below the EPA limits.

4 EXPERIMENTAL EVALUATION OF TRACE METAL LEACHING FROM STEEL SLAG INTO GROUNDWATER

4.1 INTRODUCTION

Utilization of steel slag in embankment construction has been documented in earlier studies (van der Sloot 1991, Ghionna et al. 1996, Havanagi et al. 2012). Most of these studies focused on the mechanical improvement of steel slag and limited information was available for its chemical behavior when used in embankment construction (Gomes and Pinto et al. 2006, Grubb et al. 2013). Water quality is a critical measure of the Chesapeake Bay's health, thus strict limits on pH (6.5-8.5) and leached metal concentrations have been set by the Maryland Department of Environment (MDE).

Previous research has shown that steel slag can be a good alternative to natural aggregates; however, it contains low to medium level concentrations of potential toxic elements, including chromium and arsenic (Apul et al. 2005, Cornelis et al. 2011, Grubb et al. 2011). As rainwater percolates down through the profile, trace elements that leach from steel slag may migrate downward through the subgrade soils and may contaminate the groundwater table. Thus, effect of subgrade soil characteristics on the leachate should be evaluated carefully.

The objective of this study was to evaluate the leaching potential of pure or treated steel slag and to assess their potential impact on groundwater through laboratory tests and computer modeling. The effect of underlying foundations on potential field

performance was evaluated through inclusion of five Maryland subgrades with varying physicochemical characteristics in the testing program.

4.2 MATERIALS

The same steel slag (S), water treatment residual (WTR) and encapsulation clay (borrow material-ENC) employed in the testing described in Chapter 3 were used. In addition, five subgrade soils with different plasticity and cation exchange capacities were used to simulate the flow of steel slag leachate through subgrade layers and to evaluate the effect of soil plasticity on the contaminant behavior. The physical and chemical properties of all materials are summarized in Table 4.1 and Table 4.2. Table 4.3 provides the list of slag-WTR mixtures that are used in the current study along with their leaching test combination.

4.3 METHODS

4.3.1 Laboratory Leaching Tests

The procedures listed in Section 3.3.1 for the sequential water leach tests (SWLTs) were followed. To simulate the flow of leachate through subgrade soil, the leachate collected from encapsulating clay was put into another centrifuge tube, dry subgrade soil was added, and the samples were rotated for another 18 hours. After pH and EC measurements, the samples were acidified to pH <2 with 2% HNO_3. A sketch for the SWLT is given in Figure 4.1. Before use, all equipment (centrifuge tubes, filter holders, syringes, etc.) were washed with 2% HNO_3 acid solutions and rinsed with DI water. All samples were stored at 4 C^o before the chemical analysis. Duplicate WLTs were conducted on all mixtures for each soil specimen.

Table 4.1 Physical properties of the steel slag, water treatment residual, encapsulation clay and subgrade soils.

Material	G_s	FC (%)	LL (%)	I_P (%)	USCS Classification	w_n (%)	w_{opt} (%)	$\gamma_{dry\text{-}max}$ pcf (kN/m^3)
Steel Slag (S)	3.45	12	NP	NP	SP-SM	10	13.5	141 (22.2)
Water Treatment Residual (WTR)	1.88	77	NP	NP	SM	385	42	65 (10.25)
Encapsulation Soil	2.66	71	50	22	CL-CH	17	26	104 (16.4)
Subgrade Soil 1	2.68	53	24	6	CL-ML	12	17	114 (17.95)
Subgrade Soil 2	2.68	66	30	12	CL	10	12	121 (19.35)
Subgrade Soil 3	2.70	75	37	18	CL	13	16	115 (18.08)
Subgrade Soil 4	2.66	69	29	16	OL	-	24	93 (14.65)
Subgrade Soil 5	2.72	93	62	37	CH	-	19	103 (16.1)

Note: G_s: specific gravity FC: Fines Content LL: Liquid Limit I_p: plasticity index, NP: non-plastic, w_n: natural water content, w_{opt}: optimum moisture content, $\gamma_{dry\text{-}max}$: maximum dry unit weight.

Table 4.2 Chemical properties of the steel slag, water treatment residual, encapsulation clay and subgrade soils.

Material	Steel Slag (2YS) (mg/L)	Water Treatment Residual (WTR) (mg/L)	Encapsulation Soil (mg/L)
pH	12.4	6.9	5.9
Cation Exchange Capacity, CEC (meq/100gr)	-	32.6	72.5
P	2100	2100	262
K	19400	2600	2350
Ca	173000	5100	1940
Mg	50900	3000	6300
S	617	4700	110
Zn	189	98.1	142
B	41.6	10.4	4.57
Mn	18100	4300	885
Fe	113900	22600	53700
Cu	19.7	56.4	61.7
Al	10600	159700	47700
Na	299	284	106
Cd	<0.4	<0.4	<0.4
Co	1.90	12.2	29.1
Cr	1300	<0.1	37.0
Mo	1.57	2.41	<0.4
Ni	<0.3	6.18	17.4
Pb	16.0	<2	<2
Li	16.7	24.2	13.0
As	<3	13.0	3.24
Se	<3	<3	<3
Ba	68.5	210	98.6
V	500	41.5	138

Table 4.2 (cont'd) Chemical properties of the steel slag, water treatment residual, encapsulation clay and subgrade soils.

Material	Soil 1 (CL-ML) (mg/L)	Soil 2 (CL-Acidic) (mg/L)	Soil 3 (CL-Neutral) (mg/L)	Soil 4 (OL) (mg/L)	Soil 5 (CH) (mg/L)
pH	6.3	3.8	6.2	6.0	5.8
Cation Exchange Capacity, CEC (meq/100gr)	38.4	69.1	58.5	63.7	117.1
P	760	115	428	3600	569
K	3040	900	4975	7500	5900
Ca	9300	250	1494	24600	30730
Mg	3000	245	4527	3500	4306.7
S	238	99	55	-	407.7
Zn	50.4	26.3	70.2	132.5	67.6
B	<2	<2	<2	46	12
Mn	893	32	1,623	216	443.2
Fe	40300	14700	43293	6010	27016
Cu	44.6	16.2	22	29.1	16.0
Al	39000	9050	34000	13500	40239
Na	495	46	75	1100	1150
Cd	<0.4	<0.4	<0.4	0.7	<0.4
Co	26.9	7.3	33.9	2.2	9.8
Cr	40.5	240.9	58.7	17.1	57.1
Mo	<0.4	<0.4	<0.4	1.4	<0.4
Ni	12.8	10.3	22.1	11.2	18.5
Pb	4.3	<2	21.8	53.2	<2
Li	21.9	6.4	80.6	-	30.0
As	<3	<3	11.8	3.2	8.9
Se	<3	<3	<3	1.4	<3
Ba	141.8	35	91.7	139.0	171.1
V	52.9	49	65.1	20.0	55.0

Table 4.3 Legend and Combination of the Materials and Mixtures

Legend of Mixture	Slag Content (%)	WTR Content (%)	Subgrade Soil Type
S-1	100	0	Soil 1-CL-ML
S10WTR-1	90	10	Soil 1-CL-ML
S20WTR-1	80	20	Soil 1-CL-ML
S30WTR-1	70	30	Soil 1-CL-ML
S60WTR-1	40	60	Soil 1-CL-ML
S80WTR-1	20	80	Soil 1-CL-ML
WTR-1	0	100	Soil 1-CL-ML
S-2	100	0	Soil 2-CL-Acidic
S10WTR-2	90	10	Soil 2-CL-Acidic
S20WTR-2	80	20	Soil 2-CL-Acidic
S30WTR-2	70	30	Soil 2-CL-Acidic
S60WTR-2	40	60	Soil 2-CL-Acidic
S80WTR-2	20	80	Soil 2-CL-Acidic
WTR-2	0	100	Soil 2-CL-Acidic
S-3	100	0	Soil 3-CL-Neutral
S10WTR-3	90	10	Soil 3-CL-Neutral
S20WTR-3	80	20	Soil 3-CL-Neutral
S30WTR-3	70	30	Soil 3-CL-Neutral
S60WTR-3	40	60	Soil 3-CL-Neutral
S80WTR-3	20	80	Soil 3-CL-Neutral
WTR-3	0	100	Soil 3-CL-Neutral
S-4	100	0	Soil 4-OL
S10WTR-4	90	10	Soil 4-OL
S20WTR-4	80	20	Soil 4-OL
S30WTR-4	70	30	Soil 4-OL
S60WTR-4	40	60	Soil 4-OL
S80WTR-4	20	80	Soil 4-OL
WTR-4	0	100	Soil 4-OL
S-5	100	0	Soil 5-CH
S10WTR-5	90	10	Soil 5-CH
S20WTR-5	80	20	Soil 5-CH
S30WTR-5	70	30	Soil 5-CH
S60WTR-5	40	60	Soil 5-CH
S80WTR-5	20	80	Soil 5-CH
WTR-5	0	100	Soil 5-CH

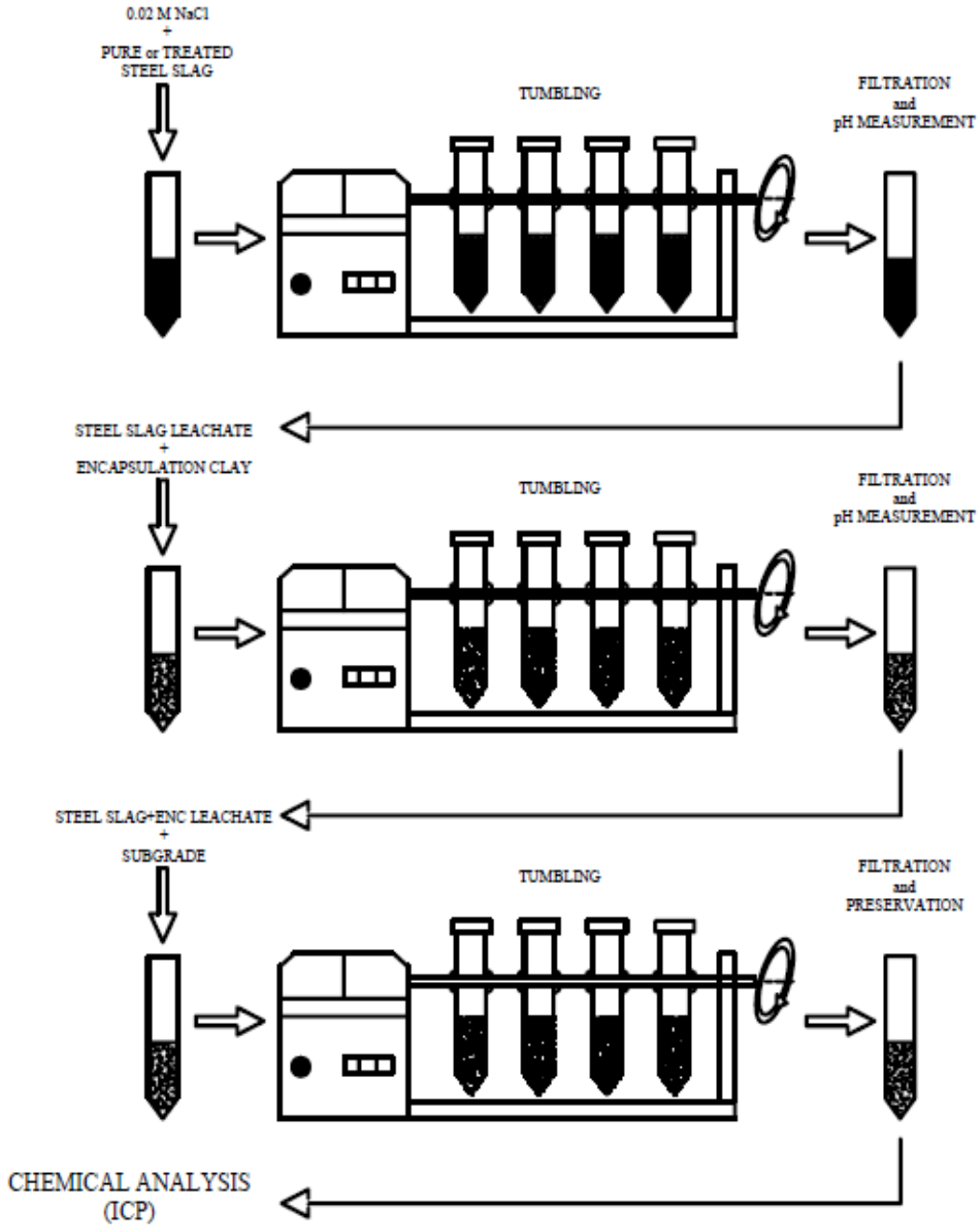

Figure 4.1 Sequential Water Leach Test (SWLT) setup

The procedures listed in Section 3.3.2 were followed for the sequential column leach tests (SCLTs), with an exception of the second column being filled with both the encapsulation and subgrade clays. SCLT setup is shown in Figure 4.2, whereas the conceptual model for flow of leachate through the subgrade soil is given in Figure 4.3.

The chemical analyses were conducted in conformance with the methodology provided in Chapter 3.3.3. SWLT/SCLT leachates were analyzed for Aluminum (Al), Arsenic (As), Boron (B), Barium (Ba), Calcium (Ca), Chromium (Cr), Copper (Cu), Lithium (Li), Manganese (Mn), Nickel (Ni). Lead (Pb) and Zinc (Zn). The metals selected for further discussion were Al, Zn, Pb, Cu, Ba and B. These six metals were selected based on the total elemental analyses presented in Table 4.2, due to their elevated concentrations in SWLT/SCLTs, their potential risk to the environment and human health, as well as their documented mobilities in groundwater (Praharaj et al. 2002, Bankowski et al. 2004, Kim 2006, Jankowski et al. 2006, Goswami and Mahanta 2007, Quina et al. 2009, Chavez et al. 2010). In humans, Boron (B) can cause many effects such as vomiting, redness of the skin, nausea, difficulty swallowing and diarrhea. In animals, fast and excessive exposure to B may result in rapid respiration, inflammation of body parts, swelling of the paws and potential effects to the reproductive organs (Ischii et al. 1993, Wegman et al. 1994, U.S. EPA 2008). Hypertension is reported as a side effect of long-term Barium (Ba) exposure in humans (Perry et al. 1989, Wones et al. 1990). Exposure to Potassium (K) in conjunction with Ba may result in adverse cardiac, gastroenteritial and skeletal effects in human body (U.S. EPA 1990). Copper (Cu) and zinc (Zn) metals are listed in the priority list by

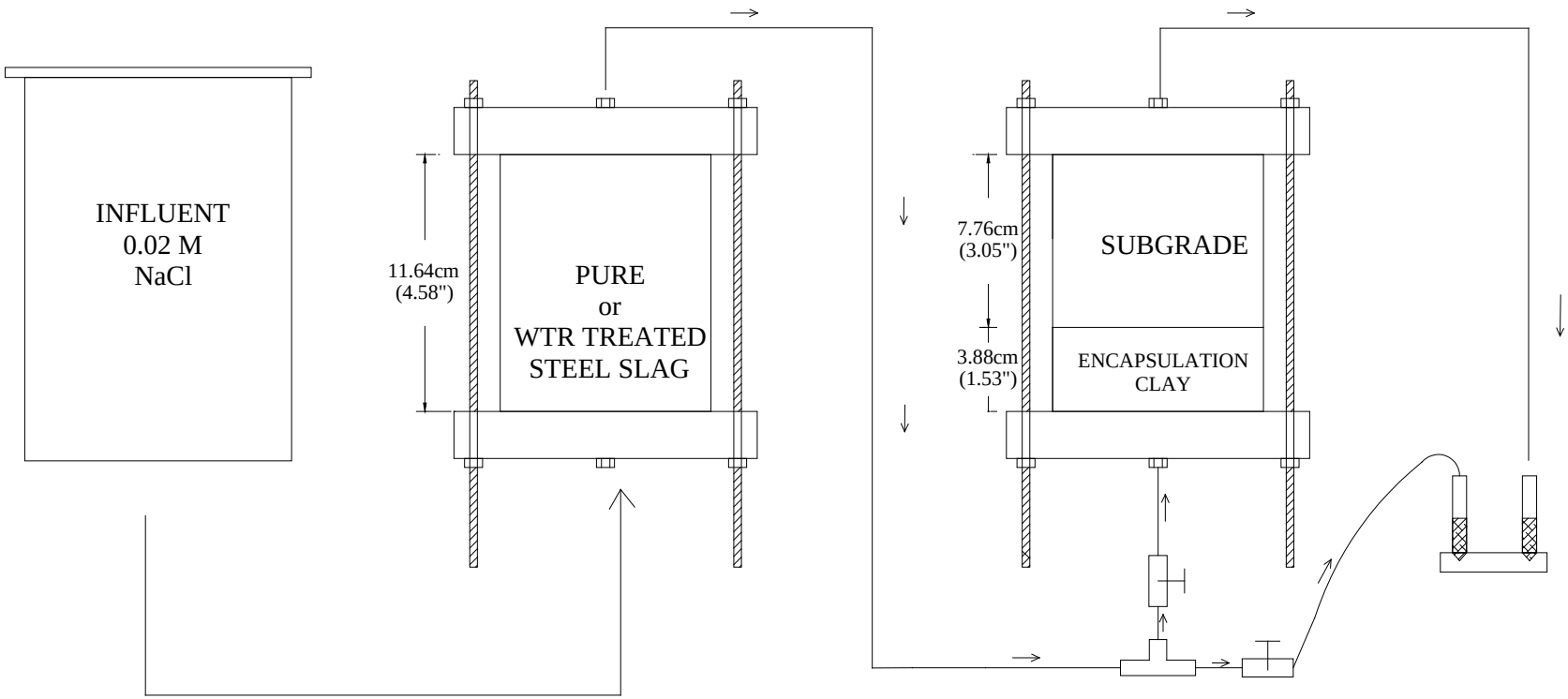

Figure 4.2 Sequential Column Leach Test (SCLT) setup

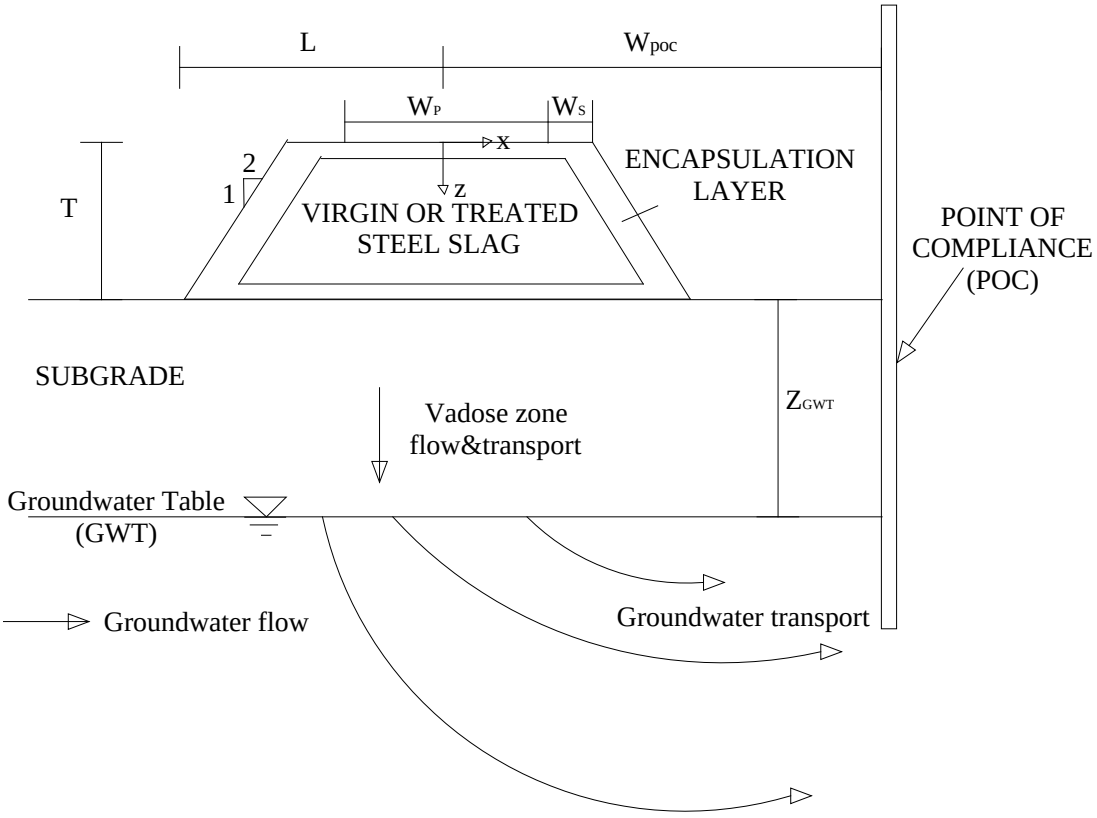

.

Figure 4.3 Conceptual model for flow of leachate into groundwater (Adapted from Cetin et al, 2013)

U.S.EPA. These two metals are very soluble, do not easily degrade in the nature and can accumulate in animals, plants or humans in long term (Svilovic et al. 2009, Elsayed-Ali et al. 2011).

The metals also represent different mobilities. For instance, at the pH values typical of pure and WTR-treated steel slag (pH = 10.0–12.5), Aluminum (Al) forms hydroxyl compounds and their attachment to the soil surface depends on its solubility level (Sparks 2003), whereas Ba and B concentrations mostly depend on the presence of the metal source within the mixture (Bankowski et al. 2004). Lead (Pb) was chosen as the sixth metal because it is a persistent pollutant in solid and aqueous phases, and is considered a major environmental hazard. Pb has been recognized for many adverse health effects, and yet the molecular processes underlying lead toxicity are still poorly understood. Due to the general nature of the symptoms, Pb poisoning is quite difficult to diagnose (U.S. EPA 2006). Lead toxicity affects the central and peripheral nervous systems, renal function and the vascular system (Patrick 2012). Arsenic (As) and Chromium (Cr) were not selected for analysis because of their very low aqueous concentrations measured in SCLTs in Chapter 3.

4.3.2 Modeling of Contaminant Transport in Groundwater

The transport of metals in a highway environment was simulated using WiscLEACH, a numerical model for simulating water and solute movement in two-dimensional variably saturated media (Li et al. 2007, Cetin et al. 2014). Three analytical solutions to the advection-dispersion-reaction equation (ADRE) were combined in WiscLEACH to develop a method for assessing impacts to groundwater caused by leaching of trace elements from steel slags used in highway layers. WiscLEACH simulations were

conducted to study the concentration profiles in soil vadose zones and in groundwater (e.g., at the centerline of the pavement structure and at the vicinity of point of compliance). Contours of trace metals were developed at different years as a function of the depth to groundwater, the thickness of the base layer, the percent steel slag by weight, the hydraulic conductivity of the base layer, the hydraulic conductivity of the aquifer material and the initial concentration of the metal in steel slag. Input to the model included the annual precipitation rate in Maryland, obtained from the National Weather Service records, the point of compliance and physical properties of the pavement layers, which were selected according to the Maryland SHA roadway design manual (MD-SHA, 2004), and transport parameters and hydraulic conductivities, which were determined via laboratory tests conducted in the current study.

WiscLEACH assumes all materials in the profile are homogeneous and isotropic. Precipitation falling on the pavement surface, the shoulders and the surrounding ground either infiltrates into the ground surface or runs off (Li et al. 2007). As water percolates down through the profile, trace elements leach from the steel slag migrate downward through the subgrade soils until they reach the groundwater table. Flow in the slag and subgrade is assumed to occur only in the vertical direction. Steady one dimension (1D) unit gradient flow is assumed to occur in the pavement layers and the vadose zone, with the net infiltration rate controlled by both the least conductive layer in the profile and by the annual precipitation rate. Surface runoff and evaporation are not considered. Infiltration of runoff along the edges of the pavement structure is not considered.

Transport in the vadose zone is assumed to follow ADRE for 1D steady state vertical flow with 2D dispersion and linear, instantaneous and reversible adsorption. Trace elements that reach the groundwater table are transported horizontally and vertically, although the flow of groundwater is assumed to occur predominantly in the horizontal direction. Steady saturated groundwater flow is assumed, and transport in groundwater is assumed to follow ADRE. Chemical and biological reactions that may consume or transform trace elements are assumed to be absent. Further details on WiscLEACH are provided by Li et al. (2007).

4.4 RESULTS

4.4.1 Sequential Water Leach Tests (SWLT)

Table 4.4 to Table 4.8 show that adding WTR to slag decreases pH significantly with all types of subgrade soils; however, the rate of decrease reduces with an increasing WTR amount (Figure 4.4). As mentioned in Chapter 3, an increase in WTR amount decreases the release of free lime (CaO), hydrated calcium silicate (C-S-H) and portlandite $Ca(OH)_2$ from slag. The formation of an aluminosilicate layer, which encapsulated slag particles and hindered CaO hydration, results in a drop in pH.

Figure 4.4 shows that the pH value of the leachate passed through the encapsulation and subgrade soils decreases drastically. The effluent leachate pH values are in agreement with the material pH values of the subgrade soils. Consequently, Soil 2, which is a clayey subgrade (CL, I_p= 12) consistently provides a lower pH than all the other subgrades. Sparks (2003), and Wan Zuhairi et al. (2008) also showed that plastic soils exhibit higher buffering capacities for pH. In addition to its relatively

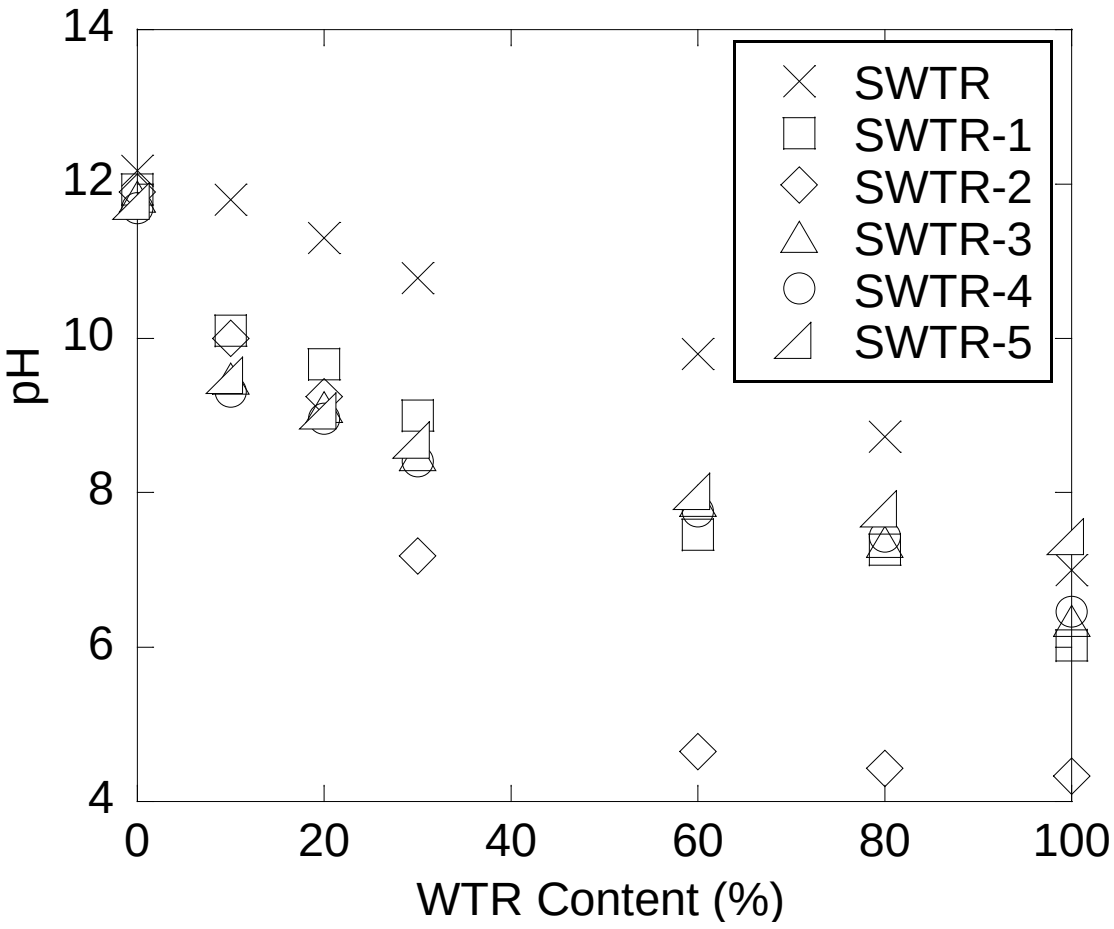

Figure 4.4 Effect of WTR content and subgrade properties on pH of the leachates past through the subgrade soils . Note: SWTR designate the specimens prepared with different WTR percentages whereas SWTR-1,2,3,4 and 5 designate specimens that are prepared by mixing effluent leachates from the SWTR mixtures with subgrade soils 1 to 5.

Table 4.4 Aqueous metal concentrations in SWLTs for Subgrade Soil 1 (CL-ML). Concentrations exceeding MCLs in **bold**.

Sample	WTR Content	pH	Al (mg/L)	Zn (mg/L)	Pb (µg/L)	Cu (µg/L)	Ba (µg/L)	B (µg/L)	As (µg/L)	Cr (µg/L)	Li (µg/L)	Mn (µg/L)	Ni (µg/L)
S-1	0	11.93	**3.98**	2.3	**387**	80	19	36	<10	46	<2	58.2	39
S10WTR-1	10	10.1	**13.65**	2.02	**135**	65	12.5	139	<10	25	<2	13.9	37
S20WTR-1	20	9.66	**7.6**	1.71	**109**	41	21	63	<10	16.4	<2	20.1	32
S30WTR-1	30	9.00	**3.96**	1.16	**69**	28	30	52	<10	13.7	<2	31.0	29
S60WTR-1	60	7.46	0.02	0.72	**168**	7.26	12.9	7.02	<10	7.1	<2	34.3	26
S80WTR-1	80	7.27	0.03	0.69	**175**	5.67	3	0.235	<10	6.6	<2	**179.8**	24
WTR-1	100	6.02	0.3	0.9	**136**	15	91	4.7	<10	4.2	<2	**2755**	24
U.S .EPA MCL			0.2	5.0	15	1300	2000	NA	10	100	NA	50	NA
U.S .EPA WQL			0.75	0.12	65	13	NA	NA	340	570	NA	NA	470
MD ATL			NA	0.12	65	13	NA	NA	NA	570	NA	NA	470
MDL			0.05	0.001	5	5	10	5	10	1	2	1	10

Notes: S=Slag; 1=Soil 1; MCL= maximum contaminant levels for drinking water; MCL for Al is based on a secondary non-enforceable drinking water regulation; WQL= water quality limits for protection of aquatic life and human health in fresh water; MD ATL = Maryland State aquatic toxicity limits for fresh water; MDL = Minimum detection limits; NA = Not available.

Table 4.5 Aqueous metal concentrations in SWLTs for Subgrade Soil 2 (CL-Acidic). Concentrations exceeding MCLs in **bold**.

Sample	WTR Content	pH	Al (mg/L)	Zn (mg/L)	Pb (µg/L)	Cu (µg/L)	Ba (µg/L)	B (µg/L)	As (µg/L)	Cr (µg/L)	Li (µg/L)	Mn (µg/L)	Ni (µg/L)
S-2	0	11.9	**4.1**	2.25	**400**	75	17.8	36	<10	44	<2	55	<10
S10WTR-2	10	10.0	**13.56**	1.98	**110**	62	11.53	141	<10	20	<2	9.7	<10
S20WTR-2	20	9.25	**7.1**	1.45	**63**	32	24.6	73	<10	13.8	<2	13.6	<10
S30WTR-2	30	7.18	**0.3**	0.82	**45**	8	50.4	45	<10	8.7	<2	29.3	<10
S60WTR-2	60	4.65	**1.22**	2.36	**138**	65	53	13	<10	6.2	<2	**79.2**	<10
S80WTR-2	80	4.43	**0.86**	3.28	**149**	68	69.9	6.82	<10	3.4	<2	**1898**	<10
WTR-2	100	4.33	**1.55**	4.6	**145**	68	112	5	<10	32.7	<2	**2325**	<10
U.S .EPA MCL			0.2	5.0	15	1300	2000	NA	10	100	NA	50	NA
U.S .EPA WQL			0.75	0.12	65	13	NA	NA	340	570	NA	NA	470
MD ATL			NA	0.12	65	13	NA	NA	NA	570	NA	NA	470
MDL			0.05	0.001	5	5	10	5	10	1	2	1	10

Notes: S=Slag; 2=Soil 2; MCL= maximum contaminant levels for drinking water; MCL for Al is based on a secondary non-enforceable drinking water regulation; WQL= water quality limits for protection of aquatic life and human health in fresh water; MD ATL = Maryland State aquatic toxicity limits for fresh water; MDL = Minimum detection limits; NA = Not available.

Table 4.6 Aqueous metal concentrations in SWLTs for Subgrade Soil 3 (CL-Neutral). Concentrations exceeding MCLs in **bold**.

Sample	WTR Content	pH	Al (mg/L)	Zn (mg/L)	Pb (µg/L)	Cu (µg/L)	Ba (µg/L)	B (µg/L)	As (µg/L)	Cr (µg/L)	Li (µg/L)	Mn (µg/L)	Ni (µg/L)
S-3	0	11.8	**4.16**	2.46	**456**	86	23	39	<10	41.4	<2	**72.4**	43
S10WTR-3	10	9.48	**10.86**	2.18	**269**	79	22.6	102	<10	32.0	<2	40.9	40
S20WTR-3	20	9.11	**8.41**	1.79	**174**	44	36.1	56	<10	20.6	<2	33.6	31
S30WTR-3	30	8.49	**3.90**	0.79	**128**	17	56.2	43	<10	17.24	<2	36.7	27
S60WTR-3	60	7.89	**1.01**	0.65	**71**	11	79.0	17	<10	11.45	<2	**67.1**	23
S80WTR-3	80	7.37	**0.90**	0.60	**61**	14	86.0	7.6	<10	10.56	<2	**126.1**	22
WTR-3	100	6.34	**0.94**	0.61	**64**	16	103	6.9	<10	14.49	<2	**2996**	23
U.S .EPA MCL			0.2	5.0	15	1300	2000	NA	10	100	NA	50	NA
U.S .EPA WQL			0.75	0.12	65	13	NA	NA	340	570	NA	NA	470
MD ATL			NA	0.12	65	13	NA	NA	NA	570	NA	NA	470
MDL			0.05	0.001	5	5	10	5	10	1	2	1	10

Notes: S=Slag; 3=Soil 3; MCL= maximum contaminant levels for drinking water; MCL for Al is based on a secondary non-enforceable drinking water regulation; WQL= water quality limits for protection of aquatic life and human health in fresh water; MD ATL = Maryland State aquatic toxicity limits for fresh water; MDL = Minimum detection limits; NA = Not available.

Table 4.7 Aqueous metal concentrations in SWLTs for Subgrade Soil 4 (OL). Concentrations exceeding MCLs in **bold**.

Sample	WTR Content	pH	Al (mg/L)	Zn (mg/L)	Pb (μg/L)	Cu (μg/L)	Ba (μg/L)	B (μg/L)	As (μg/L)	Cr (μg/L)	Li (μg/L)	Mn (μg/L)	Ni (μg/L)
S-4	0	11.7	**3.84**	3.18	**478**	89	41	40	<10	37.9	<2	**69.1**	<10
S10WTR-4	10	9.31	**12.15**	3.06	**312**	82	30.7	109	<10	31.1	<2	30.93	<10
S20WTR-4	20	8.96	**8.70**	2.24	**232**	56	29.6	64	<10	19.6	<2	36.8	<10
S30WTR-4	30	8.41	**4.05**	2.12	**179**	16	59.0	47	<10	14.2	<2	32.1	<10
S60WTR-4	60	7.76	**1.44**	1.43	**124**	13	80.2	19	<10	9.98	<2	46.2	<10
S80WTR-4	80	7.43	**1.16**	0.96	**86**	16	87.4	10.3	<10	10.01	<2	**103.8**	<10
WTR-4	100	6.46	**1.01**	0.91	**91**	10	106.4	8.5	<10	9.56	<2	**2644**	<10
U.S .EPA MCL			0.2	5.0	15	1300	2000	NA	10	100	NA	50	NA
U.S .EPA WQL			0.75	0.12	65	13	NA	NA	340	570	NA	NA	470
MD ATL			NA	0.12	65	13	NA	NA	NA	570	NA	NA	470
MDL			0.05	0.001	5	5	10	5	10	1	2	1	10

Notes: S=Slag; 4=Soil 4; MCL= maximum contaminant levels for drinking water; MCL for Al is based on a secondary non-enforceable drinking water regulation; WQL= water quality limits for protection of aquatic life and human health in fresh water; MD ATL = Maryland State aquatic toxicity limits for fresh water; MDL = Minimum detection limits; NA = Not available.

Table 4.8 Aqueous metal concentrations in SWLTs for Subgrade Soil 5 (CH). Concentrations exceeding MCLs in **bold**.

Sample	WTR Content	pH	Al (mg/L)	Zn (mg/L)	Pb (µg/L)	Cu (µg/L)	Ba (µg/L)	B (µg/L)	As (µg/L)	Cr (µg/L)	Li (µg/L)	Mn (µg/L)	Ni (µg/L)
S-5	0	11.8	**4.27**	2.46	**369**	81	51.15	36	<10	41.4	<2	**36.4**	<10
S10WTR-5	10	9.52	**14.45**	2.31	**128**	69	49.8	144	<10	31.1	<2	15.2	<10
S20WTR-5	20	9.06	**7.98**	2.02	**96**	55	54.6	103	<10	27.0	<2	16.4	<10
S30WTR-5	30	8.68	**4.12**	1.89	**57**	21	62.1	84	<10	19.1	<2	18.0	<10
S60WTR-5	60	8.02	**1.69**	1.74	**49**	20	79.4	46	<10	12.4	<2	29.1	<10
S80WTR-5	80	7.79	**1.54**	1.45	**32**	18	92.0	32	<10	7.6	<2	**69.85**	<10
WTR-5	100	7.43	**1.14**	1.04	**24**	16	136.9	21	<10	6.55	<2	**1760**	<10
U.S .EPA MCL			0.2	5.0	15	1300	2000	NA	10	100	NA	50	NA
U.S .EPA WQL			0.75	0.12	65	13	NA	NA	340	570	NA	NA	470
MD ATL			NA	0.12	65	13	NA	NA	NA	570	NA	NA	470
MDL			0.05	0.001	5	5	10	5	10	1	2	1	10

Notes: S=Slag; 5=Soil 5; MCL= maximum contaminant levels for drinking water; MCL for Al is based on a secondary non-enforceable drinking water regulation; WQL= water quality limits for protection of aquatic life and human health in fresh water; MD ATL = Maryland State aquatic toxicity limits for fresh water; MDL = Minimum detection limits; NA = Not available.

higher plasticity, the lower initial pH of the CL soil (pH 3.8, Table 4.2) may be the reason for observing lower leachate pHs with this soil during SWLTs.

According to the Maryland Soil Map, CL soils are identified as B1 type soils with pH "varying largely from neutral to extremely acidic" (Maryland Department of State Planning 1973). Johnson and Zhang (2004) indicated that different factors, such as rainfall, acidic parent material, organic matter decay or the harvest of high yielding crops may cause a drop in soil pH values. This hypothesis is also enhanced by the data obtained from SWLT with Soil 3, 4 and 5, where the material pH strongly affects the effluent pH.

The data in Table 4.4 to Table 4.8 show that Al concentrations increase when the WTR percentage is elevated to 10% by weight due to high Al contents of the WTR itself (159,700 mg/L versus 10,600 mg/L, Table 4.2). Even though the source of metal content increases with WTR addition, Al concentrations decrease when the pH drops from 12 to neutral values (Figure 4.5). However, due to amphoteric leaching pattern of the material, the low pH leachates generated by Soil 2 (pH=4.33) increase Al concentrations in the leachate and Komonweeraket et al. (2010) and Cetin et al. (2012a) also reported a higher release of Al at extreme pHs.

Zinc (Zn) is widely known to exhibit an amphoteric pattern (Lim et al. 2004, Cetin et al. 2013). Jegadeesan et al. (2008) showed that a decrease in the leaching of Zn in a neutral pH is due to its surface complexation with Fe–Al-oxide or silicate material, or the formation of insoluble hydroxides. Beyond a neutral pH, the Zn metals precipitate as $Zn(OH)_2$ and under very alkaline conditions Zn species dissolve completely as $Zn(OH)_3^-$ (Cotton and Wilkinson, 1999). The highest Zn concentrations

can be observed in leachates of pure steel slag (pH=11.93), and Zn concentrations decrease with an increasing WTR content in the leachates passed through Soil 1 (Figure 4.5). The Soil 2 provides a similar trend (lower Zn concentrations with decreasing pH) for WTR amounts 10-80% by weight. However, for the 100% WTR specimens that contain no slag, Zn concentrations are elevated due to an acidic environment generated by the Soil 2 (pH=4.33). Leachates of Soil 3, 4 and 5 exhibit a similar behavior to Soil 1 due to their similar material pH values.

Jagedeesan et al. (2008) and Komonweeraket et al. (2010) showed that Cu and Pb are amphoteric metals that have high leachability at extreme pH conditions and low leachability at a neutral pH. They not only form cations at acidic pH, but also form soluble hydroxides at alkaline pH, and, thus, are released both at low and high pH, resulting in a V-shaped solubility curve (Sabbas et al. 2003, Fedje 2010). When the pH value is at about 8, minimum solubility is reached for most of the solid phases controlling the leaching of Pb, Zn and Cu (Meima and Comans 1999). Figure 4.5 and Figure 4.6 show that the addition of WTR to slag results in lower pH values, and generally lowers the solubility of Cu and Pb. The only exception was the pure WTR specimen in Soil 2. The pH of the 100% WTR effluent past through the CL subgrade was measured as 4.33 and elevated Cu and Pb concentrations were observed. For the Subgrade Soil 1, the effluent solutions had a near-neutral pH (pH=6), and very low solubilities of Cu and Pb are evident. Table 4.2 shows that CL-ML soil has a higher Fe content compared with the CL subgrade, which might have resulted in surface complexations of Cu and Pb with Fe-oxides. Meima and Comans (1998, 1999) also reported Fe and Al (hydr)oxides being reactive adsorptive minerals for Cd, Zn, Cu, Pb

and Mo. The amphoteric leaching pattern can be clearly observed for Soils 3, 4 and 5, where the increasing WTR content lowers the pH from highly alkaline to neutral values and both the Pb and Cu concentrations in the leachate decrease significantly. The elevated Pb concentrations from Soil 3 and 4 leachates are probably due to the high Pb content in the elemental composition of these soils.

Barium (Ba) concentrations tend to decrease with an increase in pH (Bankowski et al. 2004, Cetin et al. 2013). When leachates passed through a subgrade, pure slag produced a higher pH than S10WTR (pH 11.9 versus 10.1, Figure 4.4); however, the measured Ba concentrations for slag samples are slightly higher than those measured for S10WTR mixtures (17.8-19 μg/L versus 11.5-12.5 μg/L, Table 4.4). The slag may have formed complexes with silicates present in WTR, resulting in slightly lower Ba concentrations, similar to the observations made by Bankowski et al. (2004). In general, Ba concentrations passed through the CL subgrade are higher than the ones passed through the CL-ML subgrade due to lower pH values of the leachate (pH 6.02-11.93 versus 4.33-11.9, respectively).

As seen in Figure 4.5, B concentrations increase with the introduction of 10% WTR and thus elevated pH. However, B concentrations start to decrease at higher WTR contents, which is contrary to the findings of Elseewi et al. (1980). This may be related to lower percentage of slag which has a higher B content than WTR (41.6 mg/L versus 10.4 mg/L, Table 4.2). Furthermore, ettringite may form when WTR was added to the slag. Solem-Tishmack et al. (1995) reported that the presence of ettringite decreases the B concentrations by substitution of boron in oxyanion form for sulfate.

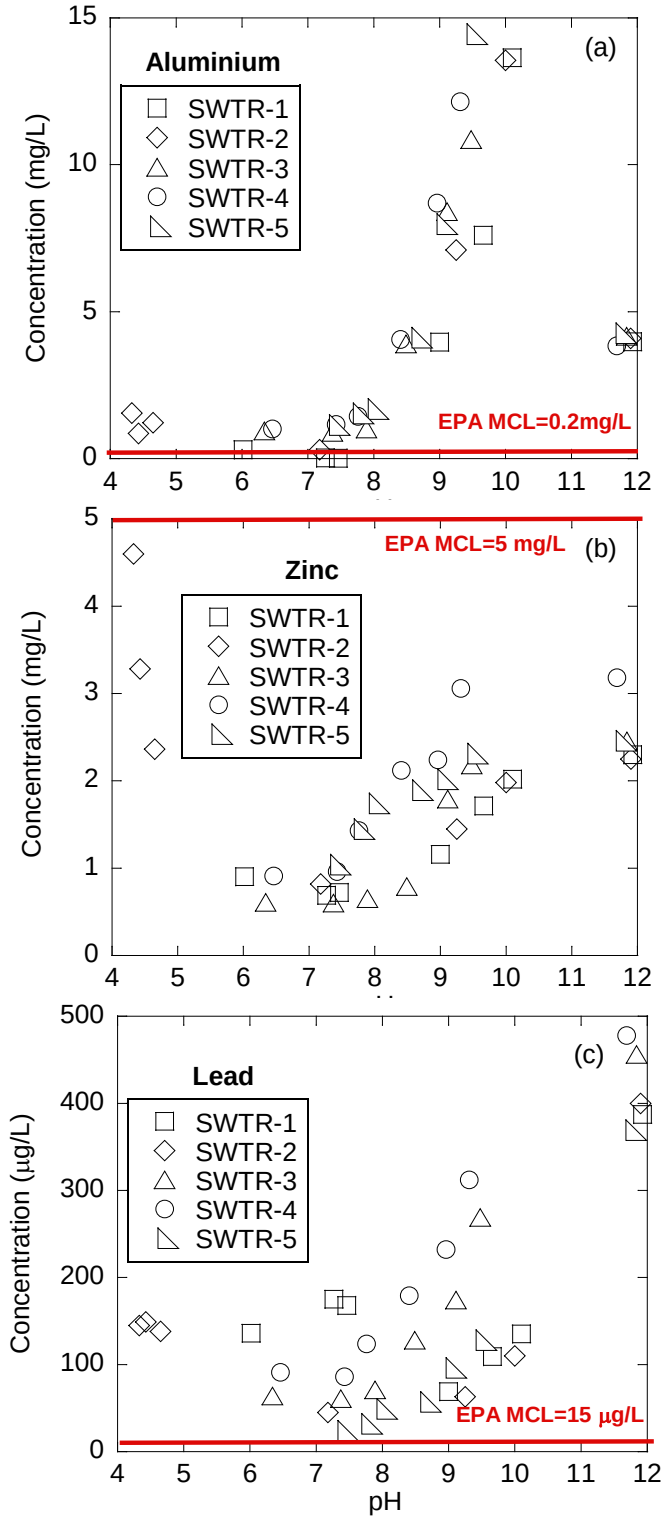

Figure 4.5 Effect of pH on SWLT concentrations of a) aluminum, b) zinc and c) lead. Leachates of mixtures prepared with 10%, 20% 30%, 60% and 80% WTR are run for another 18 hours with subgrade soils 1,2,3,4 and 5. 0% and 100% WTR content corresponds to steel slag only and WTR only specimens, respectively.

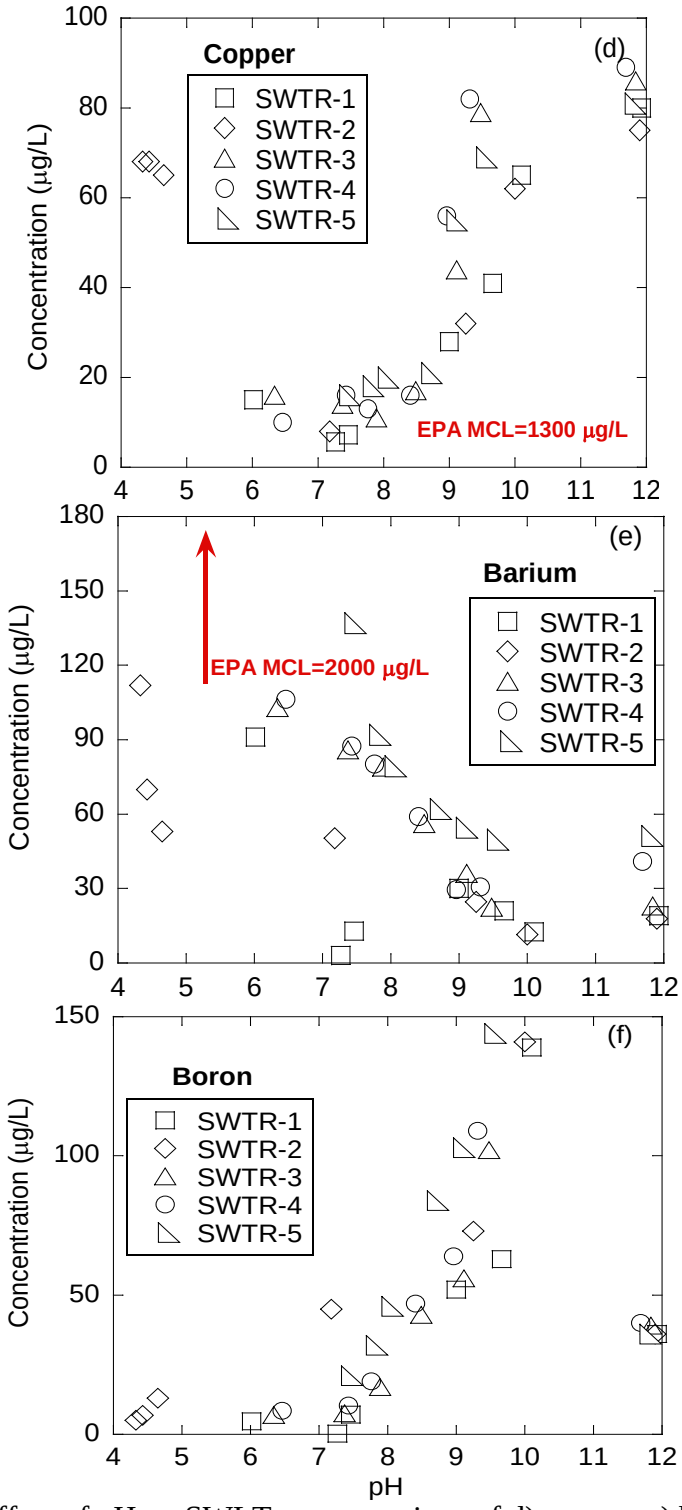

Figure 4.6 Effect of pH on SWLT concentrations of d) copper, e) barium and f) boron. Leachates of mixtures prepared with 10%, 20% 30%, 60% and 80% WTR are run for another 18 hours with subgrade soils 1,2,3,4 and 5. 0% and 100% WTR content corresponds to steel slag only and WTR only specimens, respectively.

4.4.2 Sequential Column Leach Tests (SCLT)

Figure 4.7 shows the effluent pH of the materials included in testing. For brevity, only 30WTR mixtures are provided for the second column test data hereby. The results indicate that pure slag results in the highest pH (~12.6), and pH decreases with increasing WTR amounts. As mentioned earlier, the addition of WTR coated the slag particles, limiting Ca^{2+} leaching and also cause the formation of ettringite. The data in Figure 4.7 also shows that the pH decreases when the leachate passes through all the subgrades and the effluent leachate pH is controlled by the pH of the subgrade soil. Elution curves for Ca^{2+}, a significant indicator for pH changes, are given in Figure 4.8.

A comparison of the data in Tables 4.4 to 4.8 and Table 4.9 indicates that the effluent pH values of sequential column leach test (SCLT) and sequential water leach test (SWLT) are not in agreement. The difference is more apparent for Soil 2 (pH 7.18 in SWLT versus peak and stabilized pHs of 4.09 and 4.03, respectively, in SCLTs) which has low pH (pH=3.8) associated with low Ca^{2+} concentrations (250 mg/L, Table 4.2). It is believed that the dynamic conditions in SCLTs played a significant role in a drop in pH and Ca^{2+} over several pore volumes of flow (Figure 4.7 and Figure 4.8).

An analysis of Figures A-1 to A-8 in Appendix A show that two distinct leaching patterns can be observed in column leach tests: first-flush and steady-state leaching. First-flush leaching is characterized by high initial concentrations followed by monotonically decreasing concentrations with increasing pore volumes of flow, whereas steady state leaching pattern does not exhibit any significant changes throughout the test.

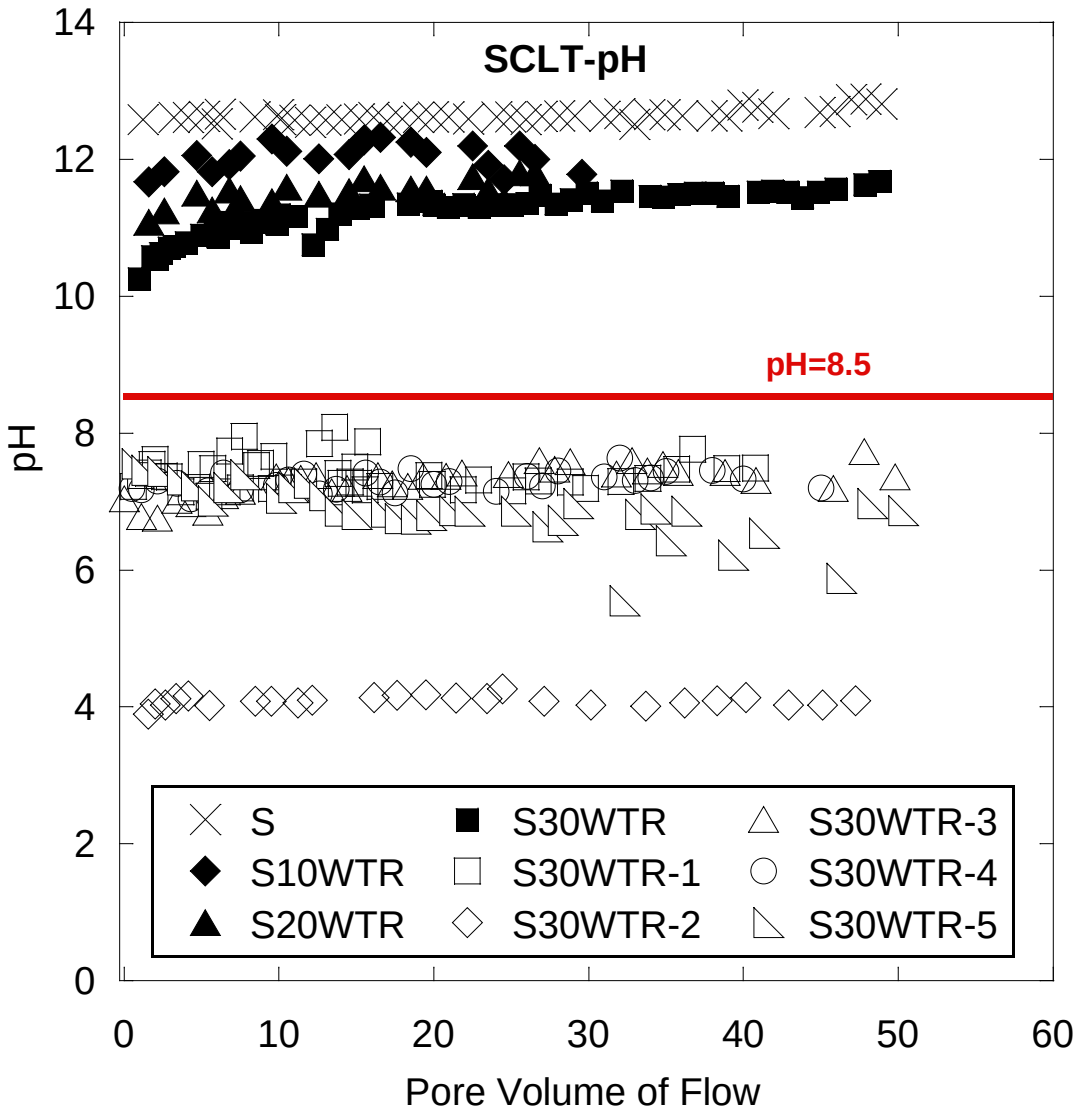

Figure 4.7 Effluent pH in CLTs on SWTR mixtures and subgrade soils

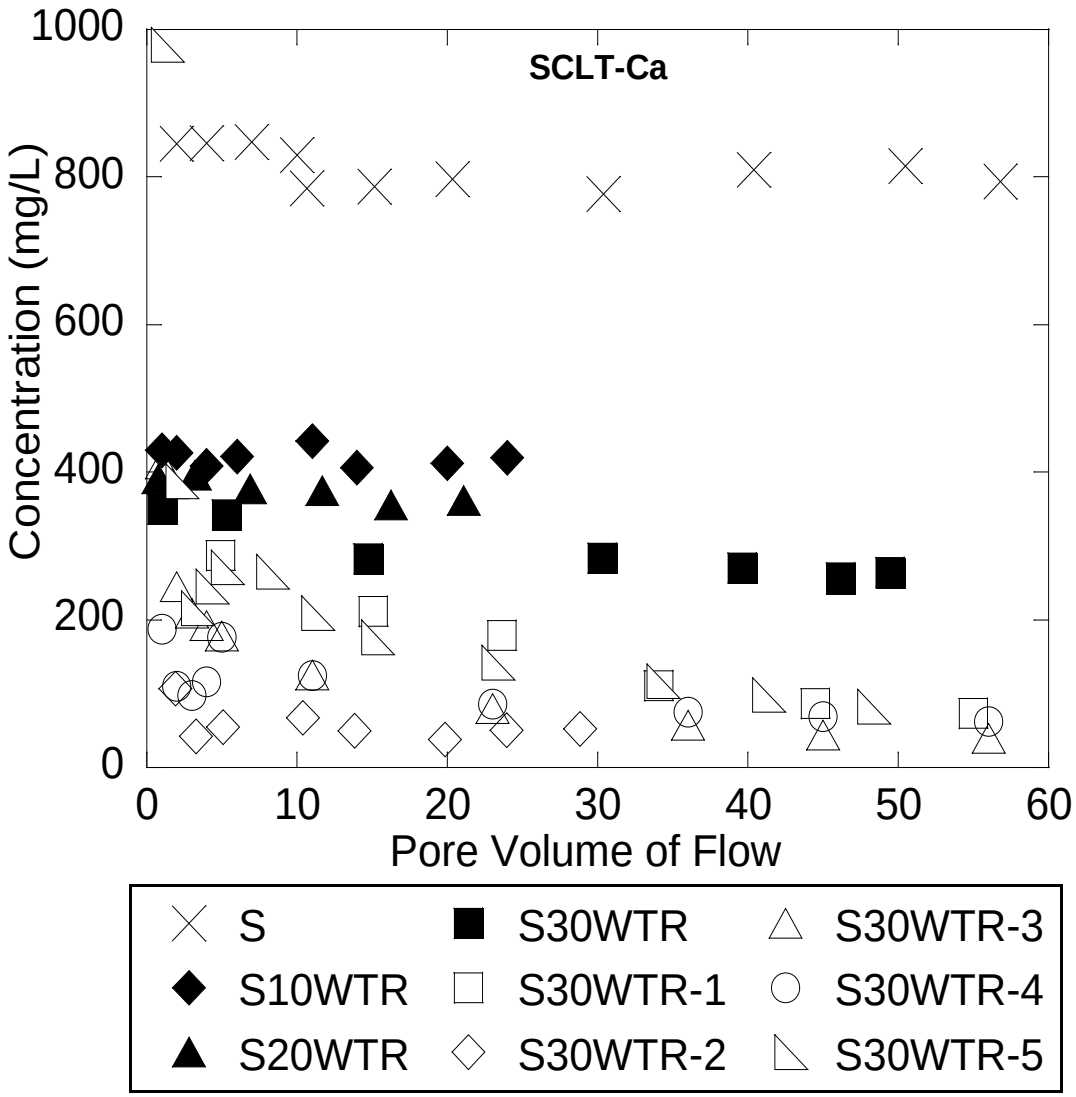

Figure 4.8 Ca^{2+} concentrations in CLTs on SWTR mixtures and subgrade soils

Figure 4.9 to Figure 4.12 show effect of subgrade type and WTR content on the peak and stabilized concentrations for Al, Zn, Cu, Pb, Ba and B. Al generally exhibits an amphoteric leaching pattern, i.e., higher leaching concentrations at extreme pH levels and lower concentrations at near-neutral pH (Langmuir 1997, Kenkel 2003). High concentrations of Al were measured in steel slag leachates because of its alkaline nature (pH 12.6). Due to the presence of large amounts of Al in WTR (159,700 mg/L, Table 4.2), Al concentrations were further elevated with the addition of WTR (Figure 4.9). When the effluent solution passes through the subgrade soil layer and the pH dropped below 7.5, a significant decrease in Al concentrations was observed. However, when the Soil 2 was used as a subgrade soil, Al concentrations were elevated again due to very low pH of the effluent (pH=4.03), confirming the amphoteric pattern.

Johnson et al. (1999) also showed that an increase in pH increases the Al concentrations leached from MSWI bottom fly ash, consistent with the findings of the current study. Considering the pH range in the CLT effluents (pH = 3.96 – 12.6, Figures A-1 to A-8 in Appendix A), it is very likely that Al is available in the leachates in both its cationic and anionic species. Aluminum is very insoluble at a neutral pH (Sparks 2003), and its solubility is controlled by the dissolution-precipitation of oxide and hydroxide minerals (Komonweeraket et al. 2010). At pH = 5.75- 9, free Al^{3+} starts precipitating as $Al(OH)_3$ (gibbsite) and $Al(OH)_3$ (amorphous), which reduces the Al^{3+} concentrations in the leachate (Astrup et al. 2006). At pH>9, $Al(OH)^{4-}$ becomes the dominant species. Under these alkaline conditions, the surface charge of steel slag particles are negative and anionic forms of Al metal tends to be released, which raises Al concentrations in the aqueous environment (Gitari et al. 2009).

The amphoteric behavior of Zn^{2+} in waste leachates has been extensively studied (Eighmy et al. 1995, Garrabrants et al. 2004, Lim et al. 2004, Camacho and Munson-McGee 2006, and Fernandez Olmo et al. 2007). Malviya and Chaudhary (2006) studied leaching behavior and the immobilization of heavy metals in cement solidified/stabilized hazardous sludge from a steel processing plant, and they found that Zn^{2+} forms hydroxides at pH>8, which functions both as an acid and a base. Figure 4.9 shows that the highest Zn concentrations are observed in S30WTR-2 leachate, which has a pH of 4.09. As the pH increases to neutral values the lowest solubility levels are expected to be reached for Zn. However, Soils 3 and 5 exhibit metal concentrations larger than expected. This may be due to larger metal content in the solid composition of the metals compared with the other subgrade soils (Table 4.2). The Zn concentrations in pure slag and slag-WTR mixtures are higher due to an elevated pH (pH 11.1-12.6), which is in agreement with the amphoteric nature of the metal. Metal oxides contained in wastes derived from thermal processes, e.g., steel slag, are usually present in hydroxide forms after the hydration reactions take place. $Zn(OH)_2$ forms beyond neutral pH values and controls the Zn^{2+} solubility. The hydroxy complexes $Zn(OH)_4^{2-}$ and $Zn(OH)_5^{3-}$ can be present in a strong alkaline solution. Their anionic properties preclude their adsorption onto the negative surfaces of the slag particles, increasing the soluble Zn^{2+} fraction. Fernandez-Olmo et al. (2009) studied the solubility of amphoteric heavy metals in stabilized/solidified steel foundry dust, a waste product of steel industry, and found out that Zn^{2+} exhibits an amphoteric pattern.

The data in Figure 4.9 and Figure 4.10 show how the addition of WTR and the inclusion of five subgrade soils influence the CLT Cu concentrations. Previous studies

indicated that Cu exhibits either an amphoteric (Fernandes Olmo et al. 2009, Komonweeraket et al. 2010) or cationic (Liu et al. 2008a, Cetin et al. 2012b) pattern. However, the patterns observed in this study were somewhat contradictory. There may be two reasons responsible for the observed behavior. First, WTR consists of large amounts of Cu compared to the S (56.4 mg/L vs 19.7 mg/L, Table 4.2) and its addition also contributes to Cu leaching. An initial increase in Cu concentrations can be observed when the leachate passes through the acidic CL subgrade (pH~4), and Cu concentrations immediately drop with WTR addition — possibly due to the precipitation of Cu. Second, large amounts of Fe-oxides that exist within the steel slag material (Table 4.2) may have also enhanced the adsorption of Cu onto slag surfaces.

Lead is amphoteric in nature, and its theoretical lowest solubility point occurs at pH 8.5 (Malviya and Chaudhary 2006). Pb concentrations measured in the current study tend to follow a pattern that is consistent with previous studies (Dijkstra et al. 2004, Fernandes-Olmo et al. 2009). At low pHs, $PbOH^+$ is the dominant dissolved Pb(II) species, and Pb forms hydroxide precipitates with an increase in pH. At neutral pH values, lower Pb concentrations are obtained, possibly due to the precipitation of Pb as a silicate species (alamosite and Pb_2SiO_4). When pH increases to higher values, soluble Pb increases, as hydroxy complexes ($Pb(OH)_3^-$ and $Pb(OH)_2$) and silicate precipitation remains the controlling mechanism for Pb stability (Halim et al. 2005). Voglar and Lestan (2010) tested cement solidified/stabilized contaminated soils and reported that Cu concentrations increase at pH >12 due to the formation of soluble hydroxide complexes.

The leaching pattern of Ba does not show a clear pH-dependency (Table 4.9 and Table 4.10). Previous studies showed that Ba leachability is controlled by the ubiquitous Ca in a solution, which would promote the precipitation of more insoluble sulphate and to co-precipitate as $(Ba,Sr)SO_4$, rather than as $BaSO_4$ or $SrSO_4$ (Fruchter et al. 1990, Izquierdo and Querol 2012). In the current study, Ba concentration remains at very low levels and almost constant at a pH of between 4 and 10; however, it exhibits a dramatic increase for the pure slag sample (pH=12.6). Even though steel slag includes small amounts of Ba (68.5 mg/L, Table 4.2), Cornelis et al. (2008) indicated that barium-metalates, which has low solubility products, may contribute to the release of Ba at such high pHs. Fällman (2000) and Huijgen (2006) studied the controlling mechanisms of Ba leaching and concluded that leaching of Ca and Ba are almost proportional since a decrease in the SO_4^{2-} solubility increases the solubility of Ba and Ca. Relatively higher Ba and Ca concentrations are observed with the pure steel slag used in the current study. Fällman (2000) and Huijgen and Comans (2006) also claimed that Ba solubility is controlled by Barite ($BaSO_4$). The addition of WTR in the current study might have elevated the SO_4^{2-} concentrations, contributed to barite formation, and decreased the solubility of Ba^{2+}. Bankowski et al. (2004) also indicated that the precipitation of Ba or the complexation with silicates might have decreased the Ba concentration within the leachate when the main metal source is treated.

Leached boron (B) concentrations from steel slag stay in a narrow range of 0.4-0.44 mg/L, and are independent of pH. When leachate of steel slag passes through the subgrade layers, B concentrations drop further and remain stable throughout the test (Figure 4.9 and Figure 4.10). Myeni et al. (1998) also reported that the formation of

ettringite, a stable mineral at pH> 10.7, could lead to a reduction in B concentrations due to the entrapment of B that exists as oxy-anion in the alkaline solution (Solem-Tishmack et al. 1995, Iwashita et al. 2005). These results show that the leaching pattern of B is independent of pH and is mainly dominated by the source of the metal.

Table 4.9 shows the peak concentrations of Al, Zn, Pb, Cu, Ba and B obtained from SCLTs. All metal concentrations are lower than the U.S. EPA limits after passing through the soil 1. The concentrations are higher when an acidic subgrade (Soil 2, CL, pH ~4) or a subgrade with a high solid content was employed (Soil 3, Soil 4 and Soil 5, Table 4.2); however, it should be recognized that the overwhelming majority of the concentrations are well below the EPA limits when stabilized concentrations are considered (Table 4.10). The variation in concentrations obtained from the SCLTs indicates that a better approach is necessary for the prediction of actual field behavior. Computer models, such as WiscLEACH, become useful in developing concentration profiles in the field.

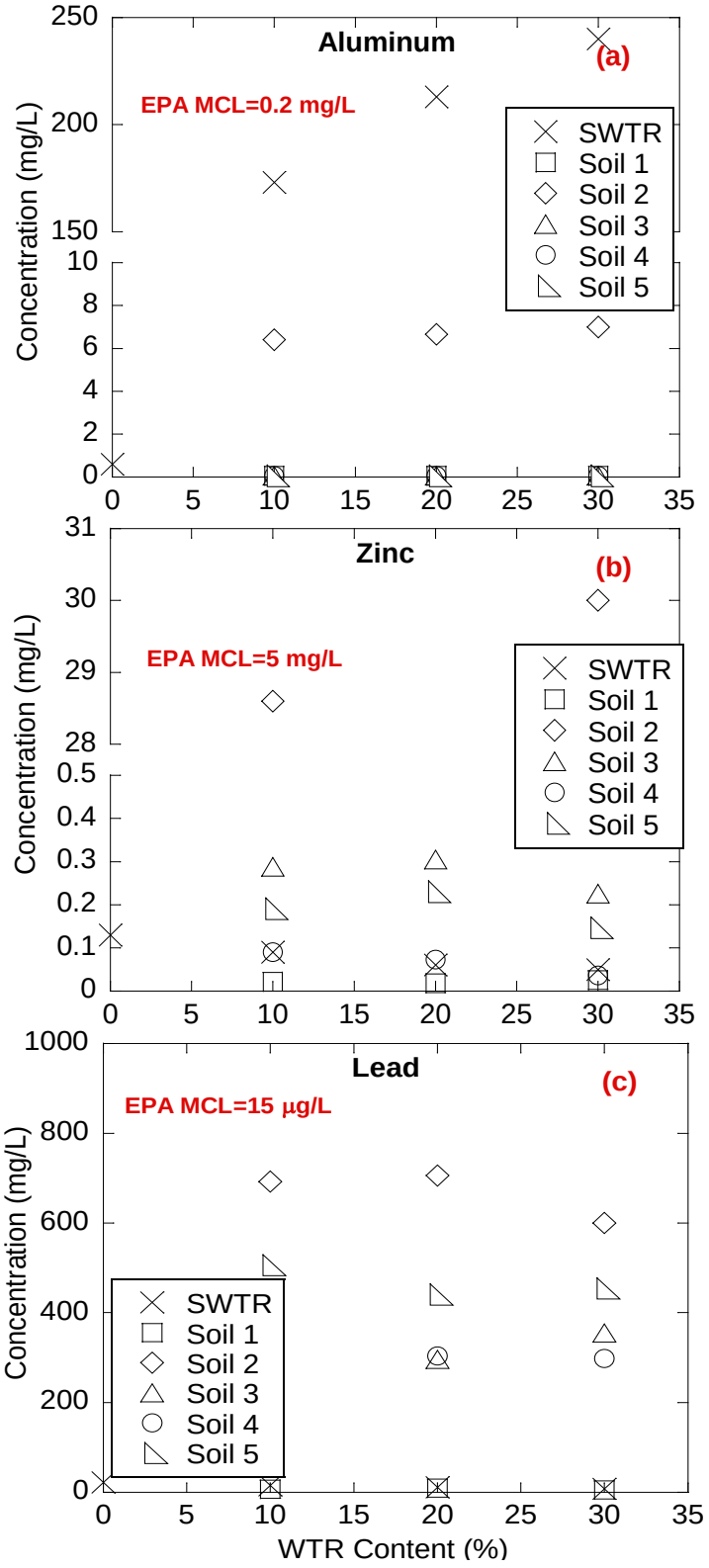

Figure 4.9 Effect of WTR content and subgrade type on peak SCLT concentrations of a) aluminum, b) zinc and c) lead

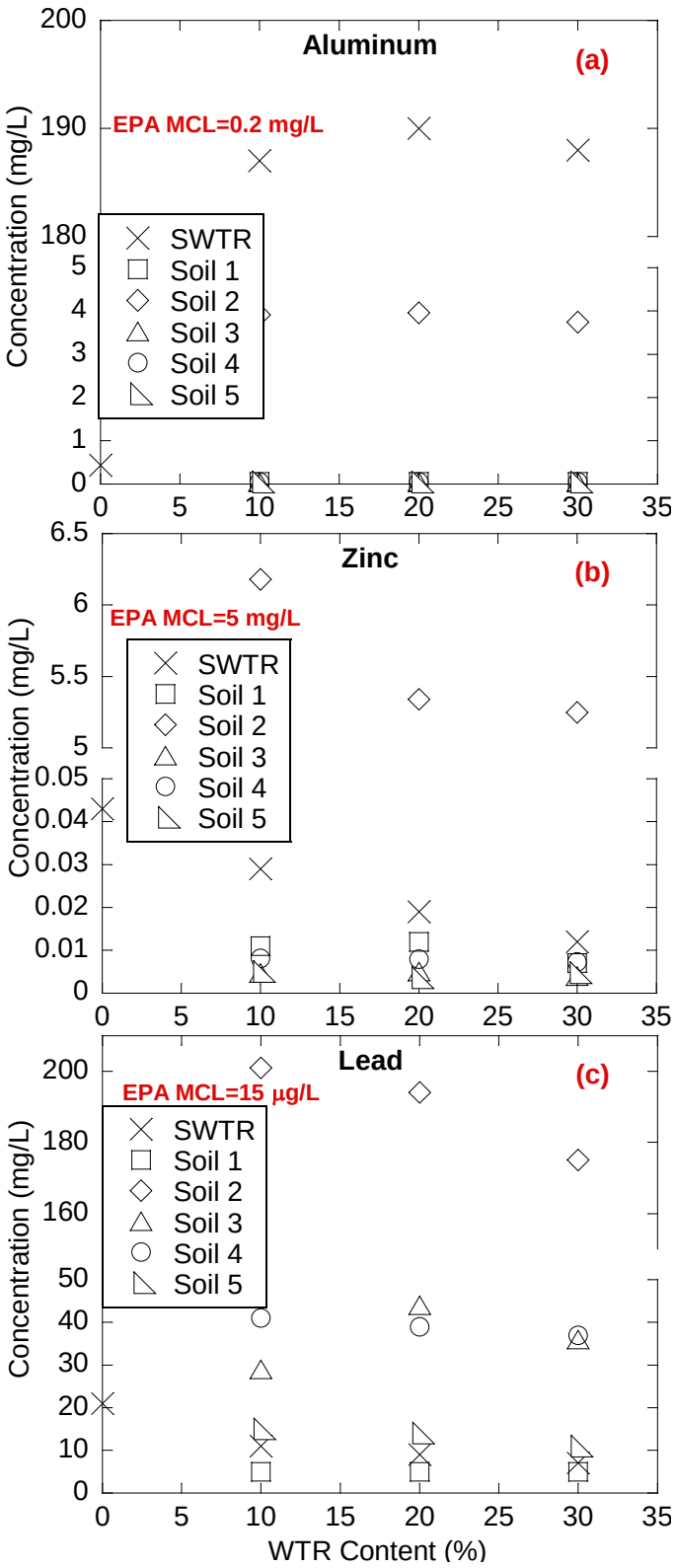

Figure 4.10 Effect of WTR content and subgrade type on stabilized SCLT concentrations of a) aluminum, b) zinc and c) lead

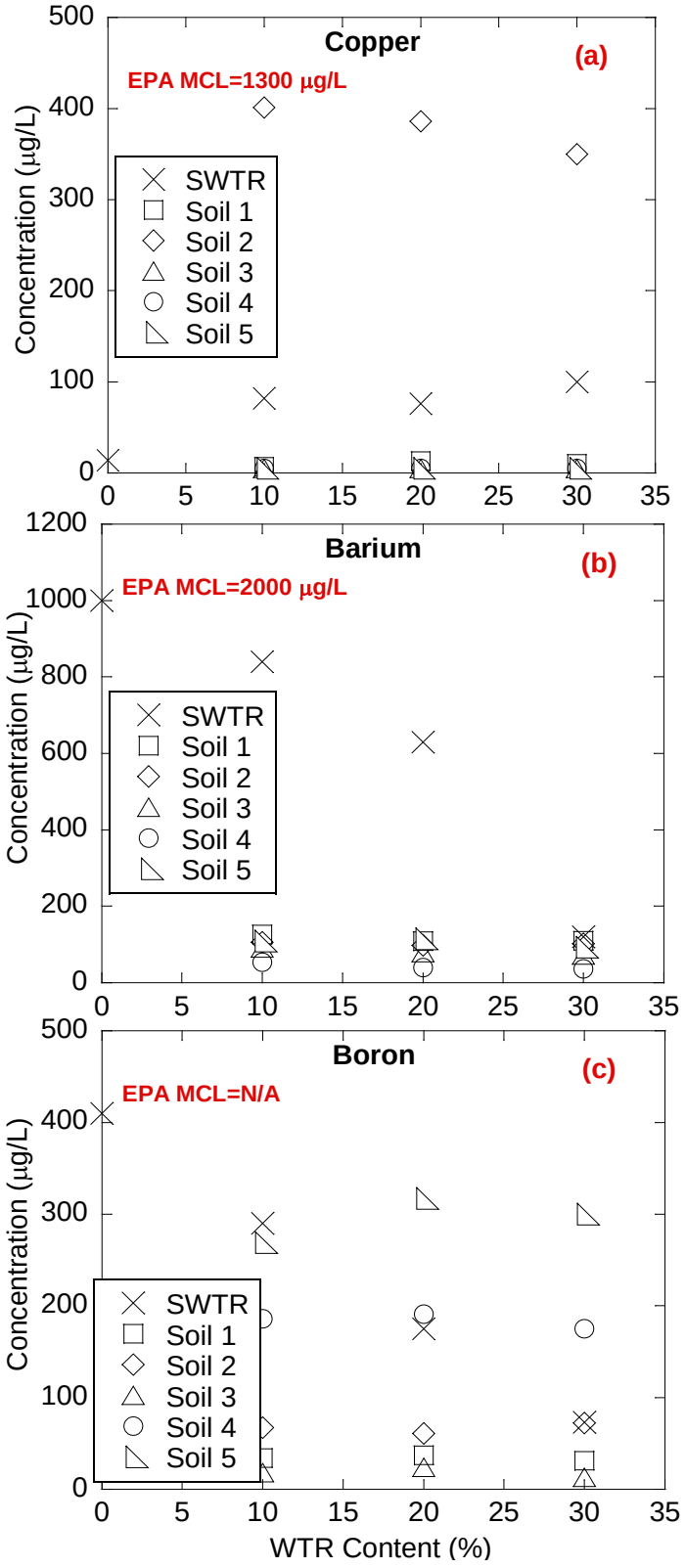

Figure 4.11 Effect of WTR content and subgrade type on peak SCLT concentrations of a) copper, b) barium and c) boron

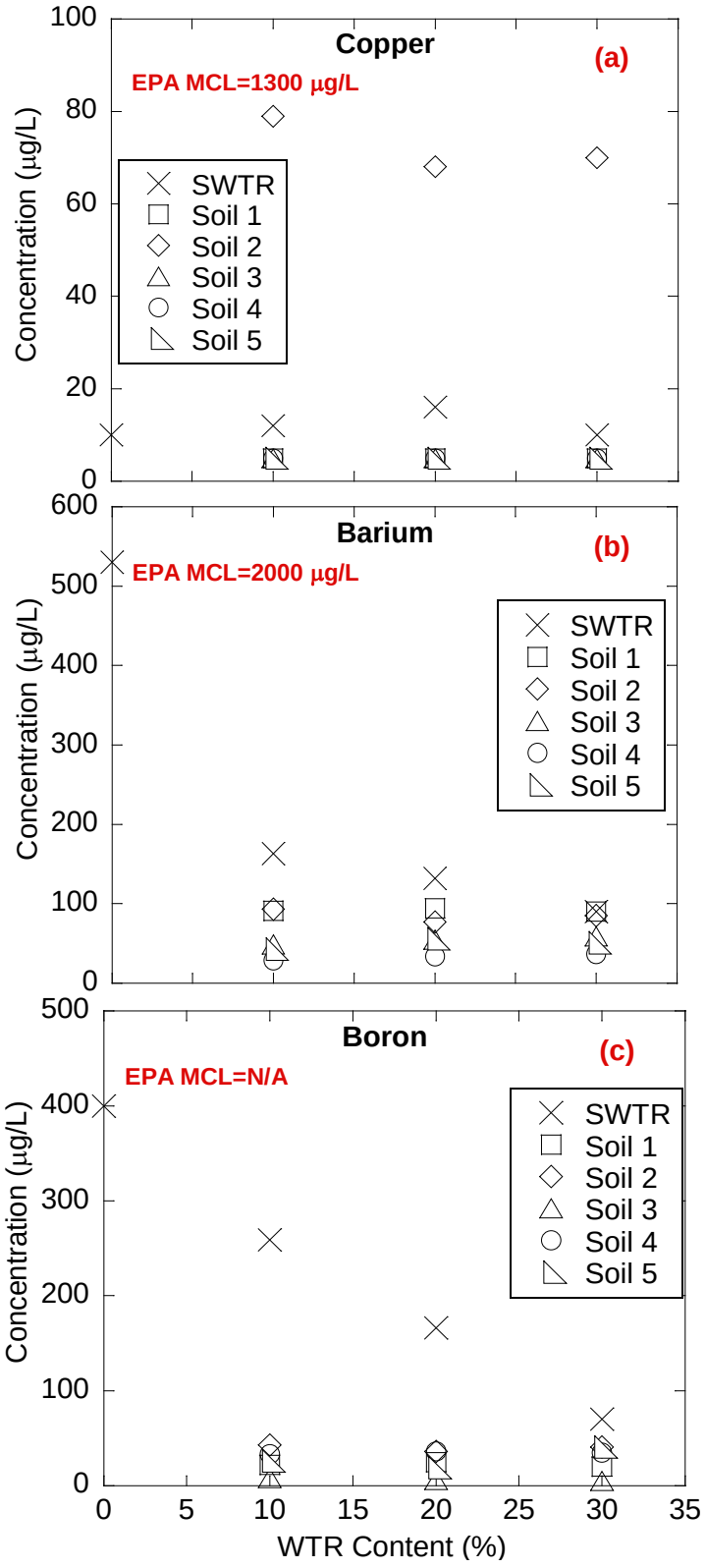

Figure 4.12 Effect of WTR content and subgrade type on stabilized SCLT concentrations of a) copper, b) barium and c) boron

Table 4.9 Peak effluent pH and metal concentrations in SCLTs. Concentrations exceeding MCLs in **bold**

Sample	WTR Content	pH	Al (mg/L)	Zn (mg/L)	Pb (μg/L)	Cu (μg/L)	Ba (μg/L)	B (μg/L)	As (μg/L)	Cr (μg/L)	Li (μg/L)	Mn (μg/L)	Ni (μg/L)
S	0	12.6	**0.6**	0.13	**22**	14	1000	410	**170**	73	230	1.4	<10
S30WTR	30	11.10	**240**	0.05	8	100	120	73	**70**	3	20	35	40
S30WTR-1	30	7.61	<0.05	0.025	5	10	110	31	**40**	<1	20	**11,360**	<10
S30WTR-2	30	4.09	**7**	**30**	**600**	350	102	72	**79**	5.2	129	**11,500**	8,050
S30WTR-3	30	7.60	<0.05	0.226	**355**	<5	73	13	<10	<1	<2	**7,130**	291
S30WTR-4	30	7.64	<0.05	0.037	**298**	<5	36	175	<10	<1	<2	**5,600**	646
S30WTR-5	30	7.55	<0.05	0.147	**454**	<5	93	300	<10	<1	145	**2,380**	383
U.S .EPA MCL			0.2	5.0	15	1300	2000	NA	10	100	NA	50	NA
U.S .EPA WQL			0.75	0.12	65	13	NA	NA	340	570	NA	NA	470
MD ATL			NA	0.12	65	13	NA	NA	NA	570	NA	NA	470
MDL			0.05	0.001	5	5	10	5	10	1	2	1	10

Notes: MCL= maximum contaminant levels for drinking water; MCL for Al is based on a secondary non-enforceable drinking water regulation; WQL= water quality limits for protection of aquatic life and human health in fresh water; MD ATL = Maryland State aquatic toxicity limits for fresh water; MDL = Minimum detection limits; NA=Not available.

Table 4.10 Stabilized effluent pH and metal concentrations in SCLTs. Concentrations exceeding MCLs in **bold.**

Sample	WTR Content	pH	Al (mg/L)	Zn (mg/L)	Pb (µg/L)	Cu (µg/L)	Ba (µg/L)	B (µg/L)	As (µg/L)	Cr (µg/L)	Li (µg/L)	Mn (µg/L)	Ni (µg/L)
S	0	12.6	**0.43**	0.043	**21**	10	530	410	**70**	15	160	0.8	<10
S30WTR	30	11.10	**188**	0.012	7	10	90	70	10	3	10	5	<10
S30WTR-1	30	7.06	<0.05	0.007	<5	<5	90	20	<10	<1	3	**5,536**	<10
S30WTR-2	30	4.03	**3.74**	**5.25**	**175**	70	85	41	**24**	3.5	15	**1,160**	1,500
S30WTR-3	30	7.15	<0.05	0.004	**36**	<5	59	<5	<10	<1	<2	**11,400**	25
S30WTR-4	30	7.20	<0.05	0.007	**37**	<5	37	35	<10	<1	<2	**5,360**	32
S30WTR-5	30	6.22	<0.05	0.005	11	<5	51	41	<10	<1	2	**783**	26
U.S .EPA MCL			0.2	5.0	15	1300	2000	NA	10	100	NA	50	NA
U.S .EPA WQL			0.75	0.12	65	13	NA	NA	340	570	NA	NA	470
MD ATL			NA	0.12	65	13	NA	NA	NA	570	NA	NA	470
MDL			0.05	0.001	5	5	10	5	10	1	2	1	10

Notes: MCL= maximum contaminant levels for drinking water; MCL for Al is based on a secondary non-enforceable drinking water regulation; WQL= water quality limits for protection of aquatic life and human health in fresh water; MD ATL = Maryland State aquatic toxicity limits for fresh water; MDL = Minimum detection limits; NA=Not available.

4.4.3 Modeling of Chemical Transport in Groundwater

The transport parameters and hydraulic conductivities, the two sets of inputs to WiscLEACH, were determined from the laboratory Br tracer and the falling-head hydraulic conductivity (BS 1377-6) tests, respectively (Table 4.11). Effective porosities and dispersion coefficients for each material and metal were determined by fitting the Ogata-Banks (1961) equation to the effluent Br concentrations in tracer tests. The calculated effective porosities and dispersion coefficients were then used to obtain the retardation factor for each metal by fitting the van Genuchten (1981) equation to the CLT elution curves. The annual precipitation rate was selected as 1 m/year, the average annual rainfall in State of Maryland, according to the U.S. Geological Survey. The remaining site parameters are listed in Table 4.12. For metals below the detection limits, since no leaching pattern could be observed, Rd=3.5 was assumed for all subgrades.

Figure 4.16 through Figure 4.13 show the contour plots of the predicted concentrations of Zn in the soil vadose zone, as well as the groundwater. For brevity, the plots for Zn for only Subgrades 1 and 2 are provided herein, and the concentration profiles for all metals and all subgrades are given in the Appendix B. The contour plots provide predictions of the metal concentrations after 5, 20, 50 and 100 years of construction. WiscLEACH simulations indicate that Zn concentrations within both subgrade 1 and 2 were below the EPA MCL of 5 mg/L. The results indicated that the maximum Zn concentrations were reached in approximately 20 years; however, they were significantly below the EPA MCL at the groundwater table.

As shown in Figure 4.16 through Figure 4.13, Zn concentrations decreased away from the steel slag-WTR embankment due to the dispersion of metals in the soil vadose zone. A high annual precipitation rate may have also caused an initial increase in leaching of the metals originating from the mixture; however, most of the metals are absorbed into subgrades. Even though the permeabilities and peak metal concentrations of steel slag and S30WTR are significantly different, the metal concentrations within the vadose zones and in groundwater only change minimally. This is due to the fact that hydraulic conductivity of the compacted clay layer and subgrades are very low and provide good attenuation to the leachate comprising trace metals.

In addition to the groundwater modeling, also a chemical equilibrium modelling software, Visual MINTEQ v3.0, was utilized for estimating $CaCO_3$ precipitation in slag leachates containing different Ca^{2+} concentrations. Calcium carbonate ($CaCO_3$) precipitation, also called “tufa formation”, occurs when steel slag leachates containing high concentrations of dissolved calcium are exposed to atmosphere. Calcium carbonate is a sparingly soluble compound and over time thick layers of calcium carbonate may result in clogging of the drainage system. The procedures are listed in Section 3.4.2 and estimated amount of $CaCO_3$ precipitation for the effluent leachates are given in Table 4.13.The results indicate that the $CaCO_3$ precipitation significantly decreases with increasing WTR amount. When the stabilized effluent of S30WTR mixture goes through Soil 2, which has a pH of 3.8 and Ca^{2+} content of 250 mg/L, the predicted $CaCO_3$ concentration decreases approximately to 0.5% of the original predicted leachate.

Table 4.11 Hydraulic and transport input parameters for pavement, embankment, subgrade and aquifer structures

Specimen	Hydraulic Conductivity K, (m/year)	Effective Porosity, n_e	Hydraulic Gradient, i	Longitudinal Dispersivity, α_L (m)	Transverse Dispersivity, α_T (m)	Retardation Factor R_d, for Zn
S	295	0.32	0.001	0.588	0.059	28
S30WTR	0.95	0.343	0.001	0.368	0.037	20.5
Subgrade 1	2.24	0.33	0.001	0.130	0.010	16
Subgrade 2	0.36	0.27	0.001	0.147	0.015	7.3
Encapsulation Layer	0.32	0.25	0.001	0.1	0.01	7.2
Pavement	18.29	0.35	0.001	0.1	0.01	1
Aquifer	3784	0.30	0.001	0.1	0.01	1

Table 4.12 Input site parameters

W_{POC} (m)	W_P (m)	W_S (m)	Z_{GWT} (m)	Prcpt (m/year)	T_{max} (m)	T (m)	Side Slope (2:1)
30	6	2	5	1.00	200	7	2:1

Notes: W_{POC}: Point of compliance, W_P: Pavement width, W_S: Shoulder width, Z_{GWT}: Depth to groundwater table, Prcpt: Annual precipitation rate in m/year, T_{max}: 50 years, T: Thickness of embankment structure

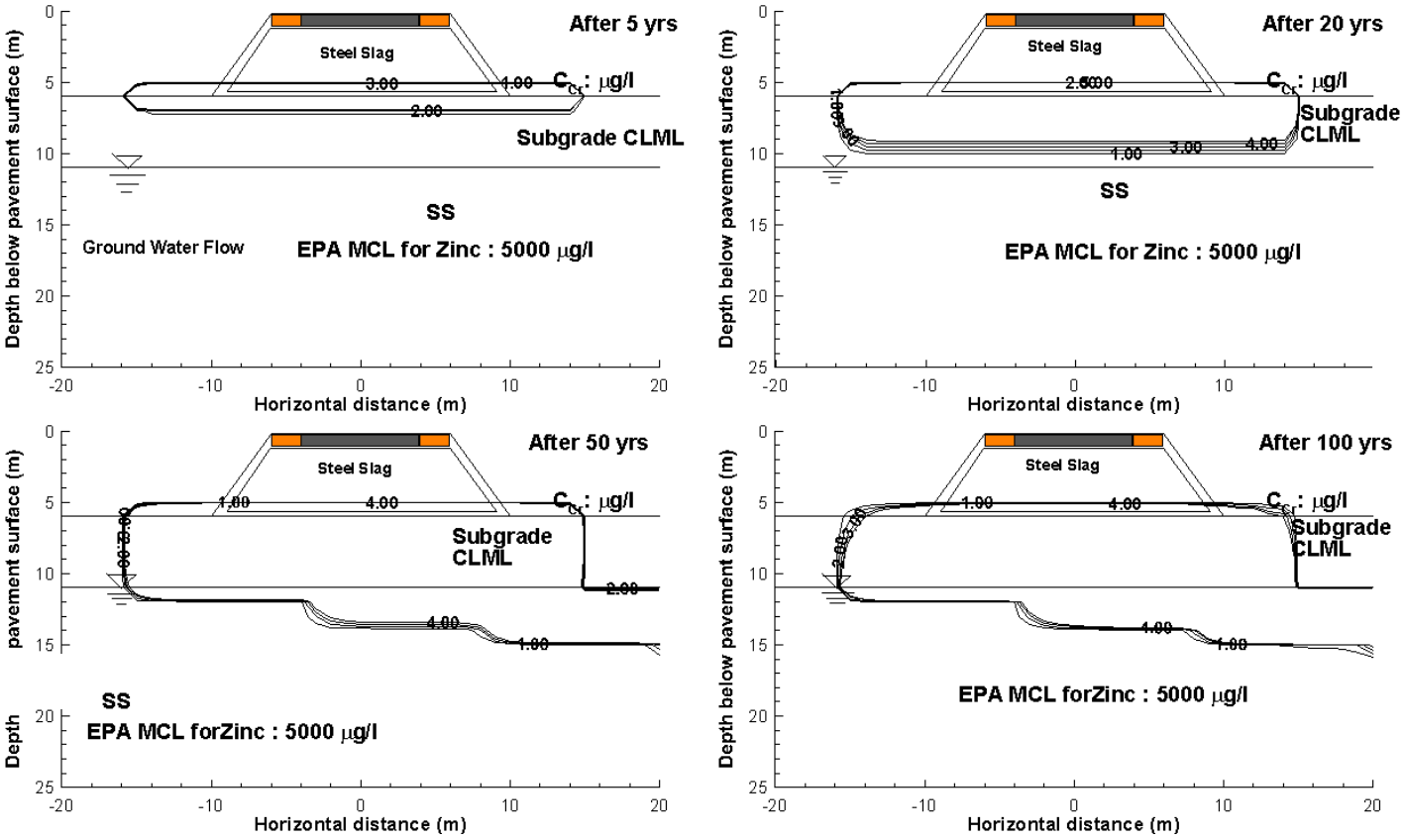

Figure 4.13 Predicted Zn concentrations in vadose zone and groundwater for simulating flow of S leachate through subgrade 1.

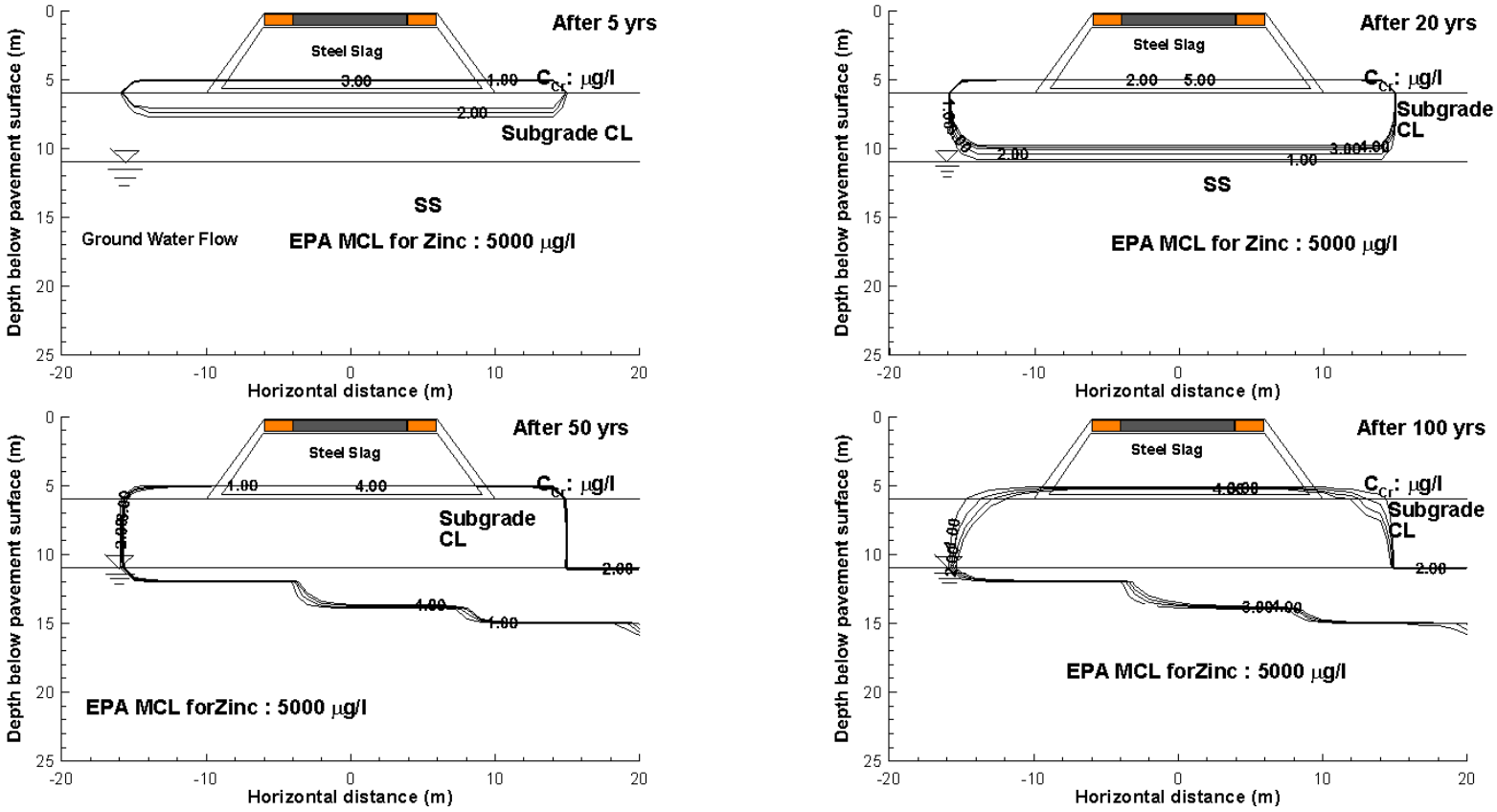

Figure 4.14 Predicted Zn concentrations in vadose zone and groundwater for simulating flow of S leachate through subgrade 2

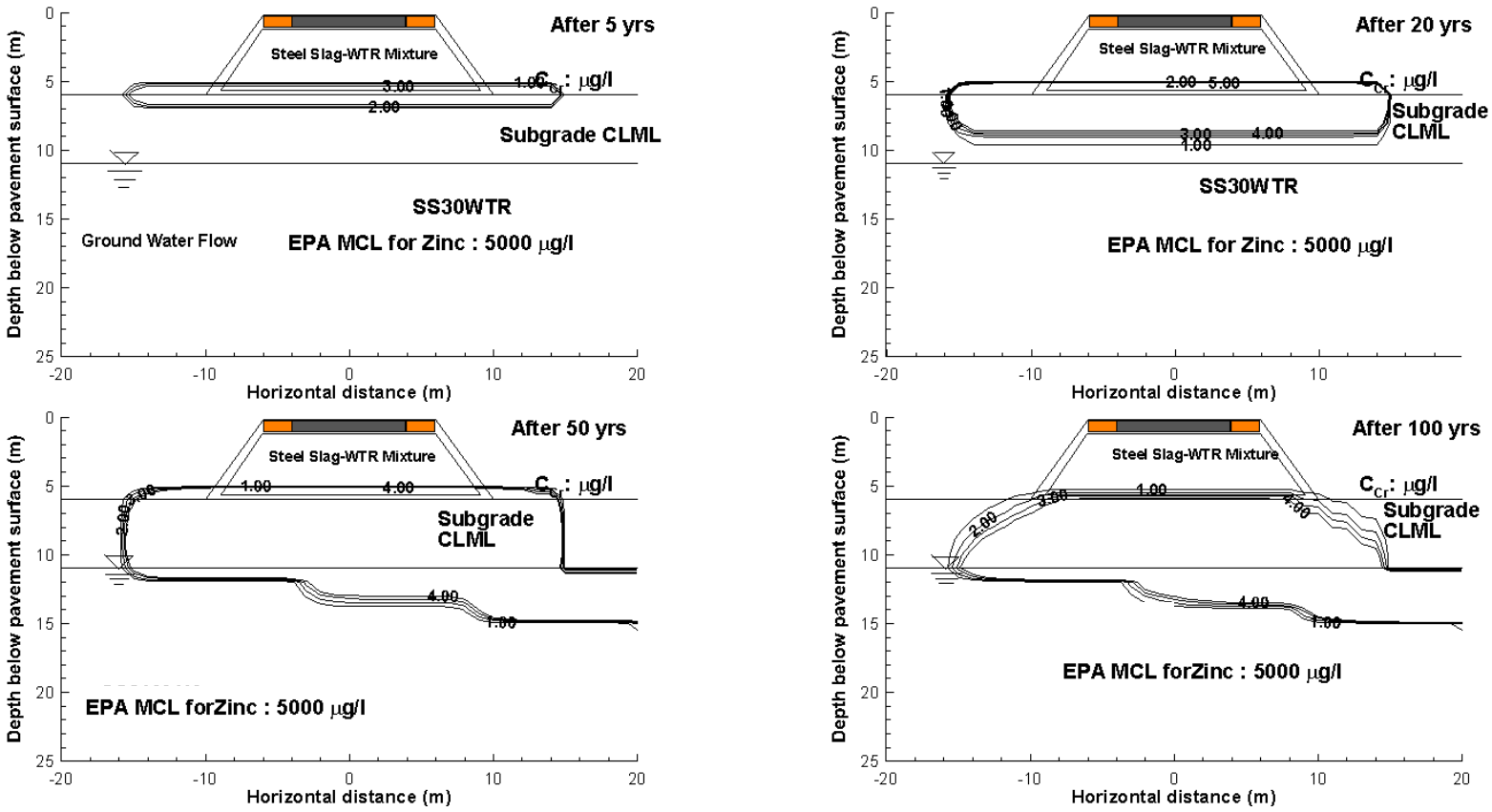

Figure 4.15 Predicted Zn concentrations in vadose zone and groundwater for simulating flow of S30WTR leachate through subgrade 1.

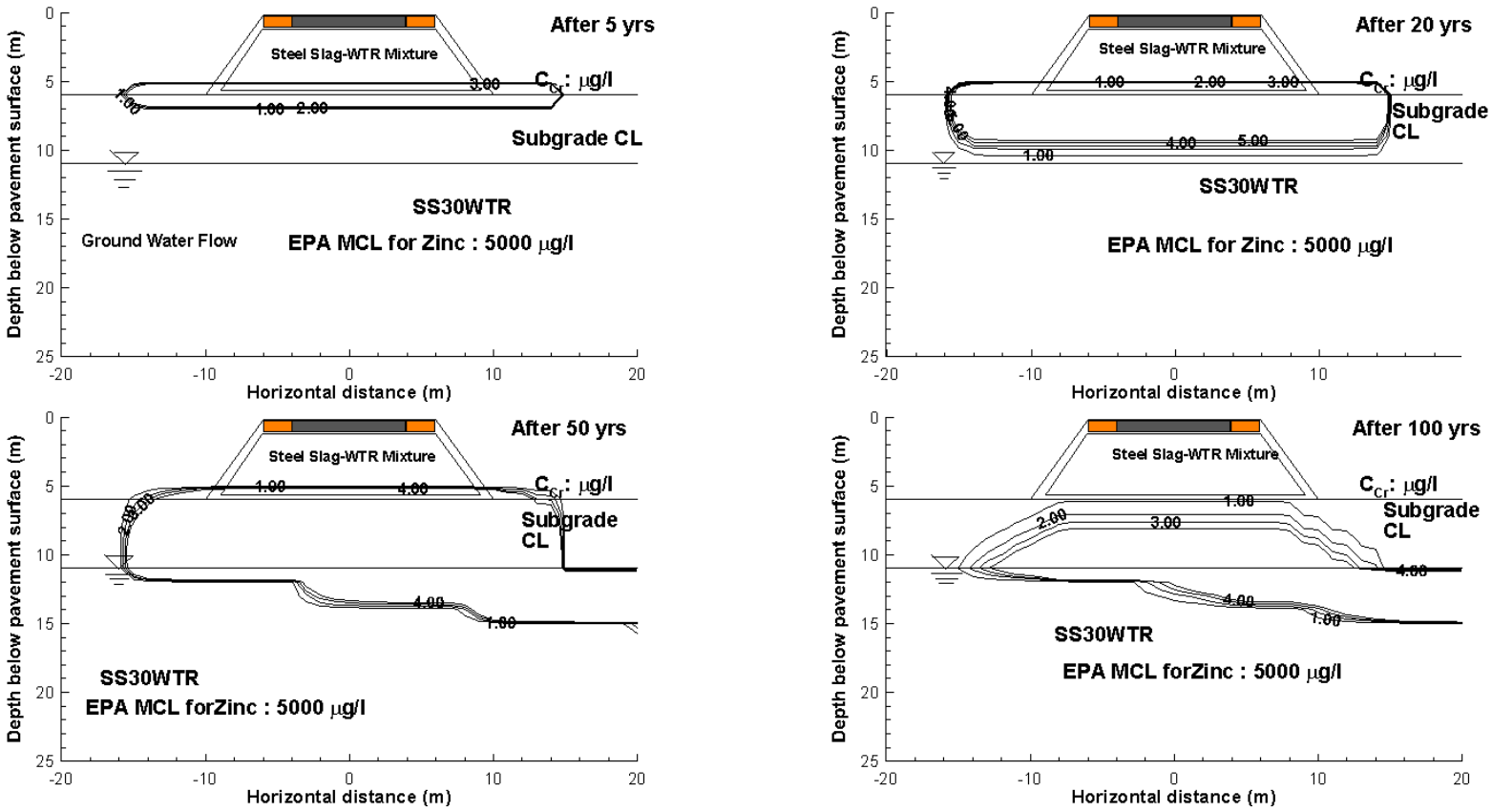

Figure 4.16 Predicted Zn concentrations in vadose zone and groundwater for simulating flow of S30WTR leachate through subgrade 2.

Table 4.13 Estimation of $CaCO_3$ precipitation for the effluent leachates

Sample	Peak Ca^{2+}-concentration (mg/L)	Estimated Peak $CaCO_3$ Precipitation (mg/L)	Stabilized Ca^{2+}-concentration (mg/L)	Estimated Stabilized $CaCO_3$ Precipitation (mg/L)
S	848	2050	796	1920
S30WTR	341	782	284	639
S30WTR-1	293	662	45	43.0
S30WTR-2	106	195	32	10.6

Note: S=Steel slag; WTR=water treatment residual; 1=Soil 1; 2= Soil 2. Calcium carbonate precipitation was estimated based on measured Ca^{2+} concentrations using Minteq Visual v3.1

4.5 CONCLUSIONS

A laboratory study was conducted to investigate the leaching characteristics of pure or WTR-treated steel slag in groundwater. The effects of WTR addition, presence of an encapsulating layer in the embankment, and type of the subgrade on pH and leached concentrations of Al, Ba, B, Cu, Pb and Zn metals were studied through laboratory leaching tests. The observations from the current study are as follows:

- The results of the sequential water leach tests showed that increasing WTR percentage resulted in a decrease in pH. Flow of the leachate past through the subgrade decreased the pH further with the effluent pH significantly depending on the natural pH of the soil.
- Aluminum concentration initially increased when WTR amount was increased from 0 to 10 % due to high alum content of WTR; however, then decreased with increasing WTR percentage due to amphoteric nature of Al. Pb, Cu and Zn exhibited a clear amphoteric pattern, whereas Ba concentrations increased with decreasing pH. The dominant factor for B leaching was the source of metal instead of pH.
- The results of sequential column leach tests indicated that an increase in WTR decreased the pH; however, WTR percentage did not have a significant effect on final pH values once the leachate percolated through the encapsulation layer.
- Al-concentrations increased dramatically with addition of WTR in the sequential column leach tests, but the concentration in the leachate was strongly pH-dependent, yielding higher metal concentrations for CL subgrade (natural pH=3.8). The same amphoteric nature could also be observed with Pb, Zn and

Cu. However, the highest metal concentrations for Ba and B were observed with pure slag leachates, indicating that the metal source was the dominant factor characterizing the leaching pattern instead of solubility. Stabilized metal concentrations of the leachates from the subgrade CL-ML were below the EPA MCL, however, As and Pb concentrations of the CL subgrade leachate were above those. This clearly emphasized that the natural pH of the subgrade played a significant role in the leachate characteristics.

• WiscLEACH numerical simulations suggest that the metal concentrations decreased over time and distance and that all the metals were sufficiently dispersed in the vadose zone. WiscLEACH results also indicated that the predicted metal concentrations were much lower than those measured in the column leach tests suggesting that the results of laboratory tests are likely to provide a conservative estimate of field metal leaching.

5 CONCLUSIONS AND RECOMMENDATIONS

5.1 CONCLUSIONS

Highway constructions pose great potential for the beneficial reuse of large volumes of steel slag (S). The research study was completed to investigate the mechanical and environmental suitability of slag-amended highway embankments. In order to decrease the material pH to acceptable levels, steel slag was mixed with water treatment residual (WTR), a non-hazardous residue obtained from drinking water treatment facilities. Accelerated swell tests were performed on mixtures prepared with different percentages of WTR to obtain the best slag-to-WTR ratio. A battery of laboratory sequential water leach tests (SWLT) and sequential column leach tests (SCLT) were conducted to determine the environmental suitability of steel slag and to simulate the leachate flow from pure steel slag or SWTR mixtures into groundwater or surface waters. A clayey borrow material, commonly used by the SHA in embankment construction and proposed herein as a soil to encapsulate steel slag in an embankment setting, and five subgrade soils with different plasticities were included in the leaching tests to study the influence of the buffering capacity of clayey soils on metal leaching and pH. A series of numerical analyses via WiscLEACH and UMDSurf were conducted to predict the leached metal concentrations in groundwater and surface waters, respectively, as a function of depth and time. The following onclusions are reached:

1. The addition of WTR to steel slag decreased the maximum dry unit weight ($\gamma_{dry\text{-}max}$), increased the optimum moisture content (w_{opt}) and lowered the ultimate swelling ratios of the mixtures. However, due to a significant difference between the specific gravities of steel slag and WTR (G_s=3.45 versus 1.88), usage of WTR greater than 30% by weight decreases the steel slag amount in the mixture significantly (by more than 44%).
2. All pure steel slag materials, as well as the mixtures used in this study, have excellent shear strength properties based on direct shear tests. Effective internal friction angle generally decreases with WTR, bitumen, or sand addition with a 30% WTR addition yielding in the largest decrease. The effective cohesion values are very small, and their largest decrease was observed with an addition of 30% WTR.
3. Steel slag can be treated using three different methods, bituminous coating, sand amendment, and water treatment residual (WTR) addition, to mitigate the swelling. Accelerated swelling test results show that all three methods can decrease the ultimate swelling ratio. However, leaching tests indicated that bituminous coating and sand amendment can not change the effluent pH of pure steel slag.
4. WTR amendment as high as 30% by weight to slag did not satisfy the Maryland Department of Environment (MDE) pH limit of 8.5 in either SWLTs or SCLTs. However, when the steel slag-WTR leachate passes through the encapsulation soil, SWLT and SCLT pH levels drop below 8.5.
5. The concentrations of the metals studied in this research are greatly influenced by the pH of the effluent solution, which suggests that mixing slag with an acidic or alum-rich additive, such as WTR, is essential for the reduction of pH levels and

metal concentrations to acceptable limits. High concentrations are reduced to acceptable limits when leachate passes through the subgrade soils with neutral natural pH. When an acidic subgrade soil is used, the difference between the leached Al concentrations and EPA Water Quality Limit (WQL) is less than one order of magnitude. It should be noted that Al is on the EPA list of secondary drinking water regulations, and no limits for Al are specified in Maryland groundwater protection guidelines.

6. WiscLEACH simulations for steel slag-amended embankments indicated that all metals can be sufficiently dispersed in the vadose zone, and the metal concentrations decrease over time and distance to negligible levels in groundwater. WiscLEACH results also indicate that the metal concentrations are much lower than those obtained in the laboratory leaching tests, suggesting that laboratory tests are likely to provide a conservative estimate of field metal leaching. UMDSurf results show that the metal concentrations decrease to 50% of their initial values at a 40 m distance from the contact point (i.e., the corner of the embankment). The rate of decrease slows down with increasing distance; and eventually all metal concentrations are below the EPA limits at 1000 m from the corner of the embankment.
7. Based on the findings obtained from the laboratory tests and numerical analyses, WTR-treated steel slag would not pose any hazard to surface waters in the vicinity of an embankment or groundwater below or within typical subgrades with close to neutral pH. In order to keep both swelling and metal leaching at acceptable levels, steel slag can be mixed with 30% WTR by weight before use.

5.2 RECOMMENDATIONS FOR FUTURE STUDIES

The experimental evaluation of both the mechanical and environmental impacts of using steel slag in highway embankments indicated that treated steel slag yields in lower ultimate swelling ratios and effluent pH values when passing through a clayey soil. However, performing all those tests is a time- and material-consuming as well as troublesome process. Thus, developing numerical models that can provide the needed parameters with only basic input would be extremely valuable. For instance, instead of performing accelerated or long term swelling tests on steel slag samples where app 6-7 kg material is used for each test sample, using a mathematical model providing the ultimate swelling value with only the Ca^{2+} data as the input would save significant time and labor.

Simultaneously, models that predict the metal concentrations within the leachate of column or pH-dependent tests would both save time and prevent issues such as contamination. However, it should be remembered that waste materials are extremely heterogenous and both the physical and the chemical features may vary from batch to batch, thus it is very difficult to come up with successful predictions. Especially when the mixtures of two waste materials are dealt with, it becomes incredibly difficult to predict both the leaching from the pure materials as well as the reaction mechanisms that will take place between the two materials.

Finally, performing large-scale field leaching tests on slag and mixtures utilized in the current study would help to compare field leaching to that observed in the laboratory. A field leaching study would help to validate the results obtained from numerical models and check the accuracy and efficiency of the treatment methods.

APPENDICES

APPENDIX A: METAL CONCENTRATIONS OF SEQUENTIAL COLUMN LEACH TESTS

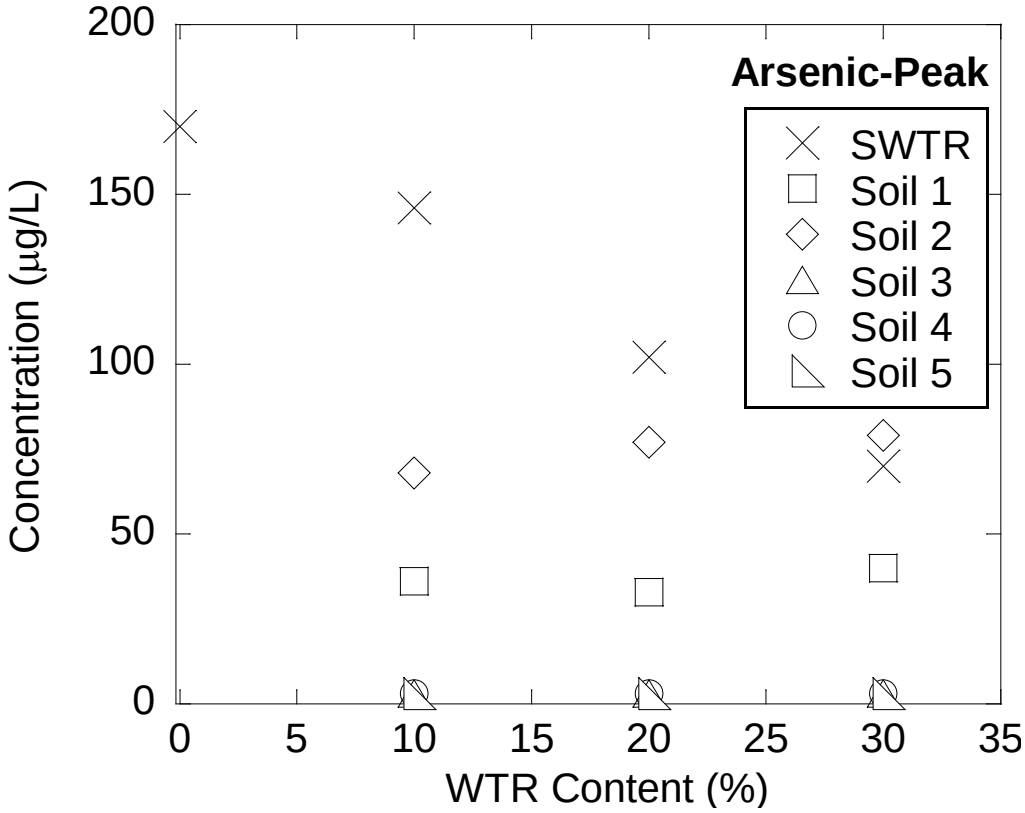
Arsenic-Peak
SWTR
Soil 1
Soil 2
Soil 3
Soil 4
Soil 5
Concentration (µg/L)
WTR Content (%)
0
50
100
150
200
0
5
10
15
20
25
30
35

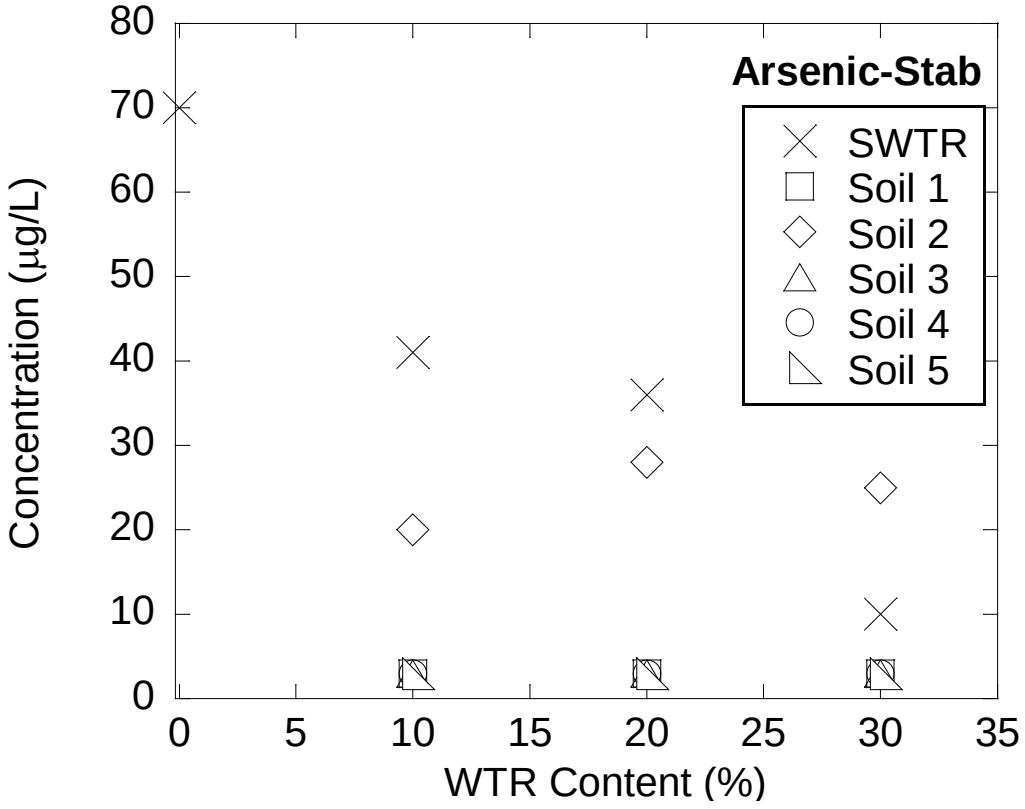
Arsenic-Stab
SWTR
Soil 1
Soil 2
Soil 3
Soil 4
Soil 5
Concentration (µg/L)
WTR Content (%)
0
10
20
30
40
50
60
70
80
0
5
10
15
20
25
30
35

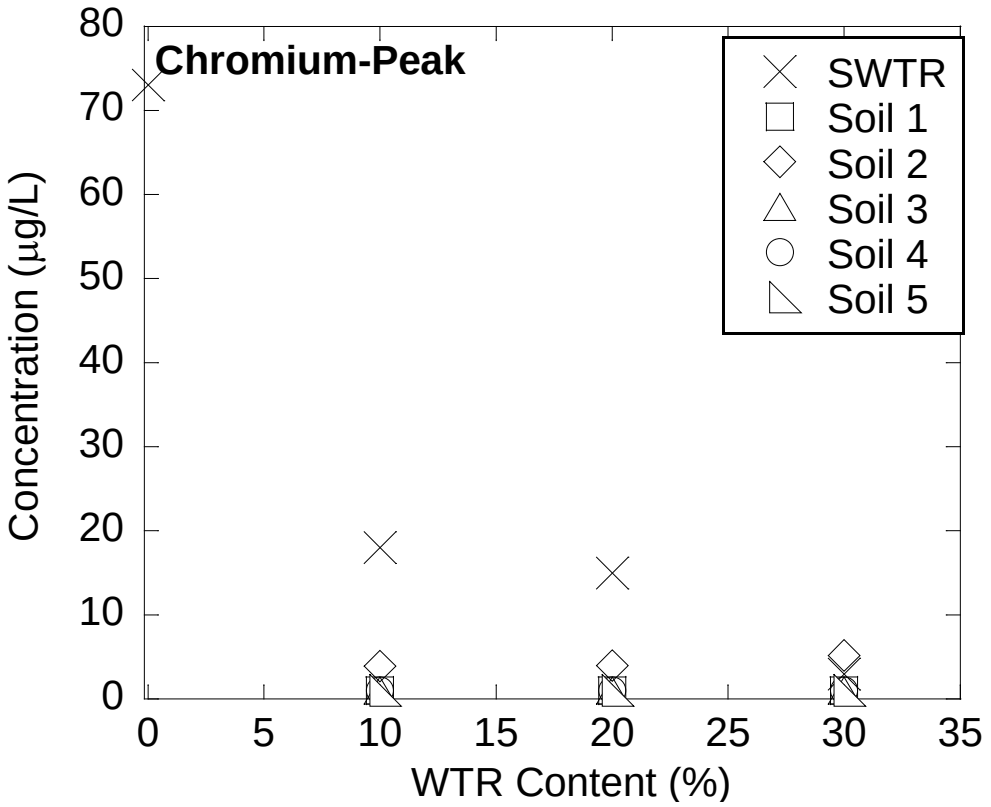
Chromium-Peak
SWTR
Soil 1
Soil 2
Soil 3
Soil 4
Soil 5
Concentration (µg/L)
WTR Content (%)
0
10
20
30
40
50
60
70
80
0
5
10
15
20
25
30
35

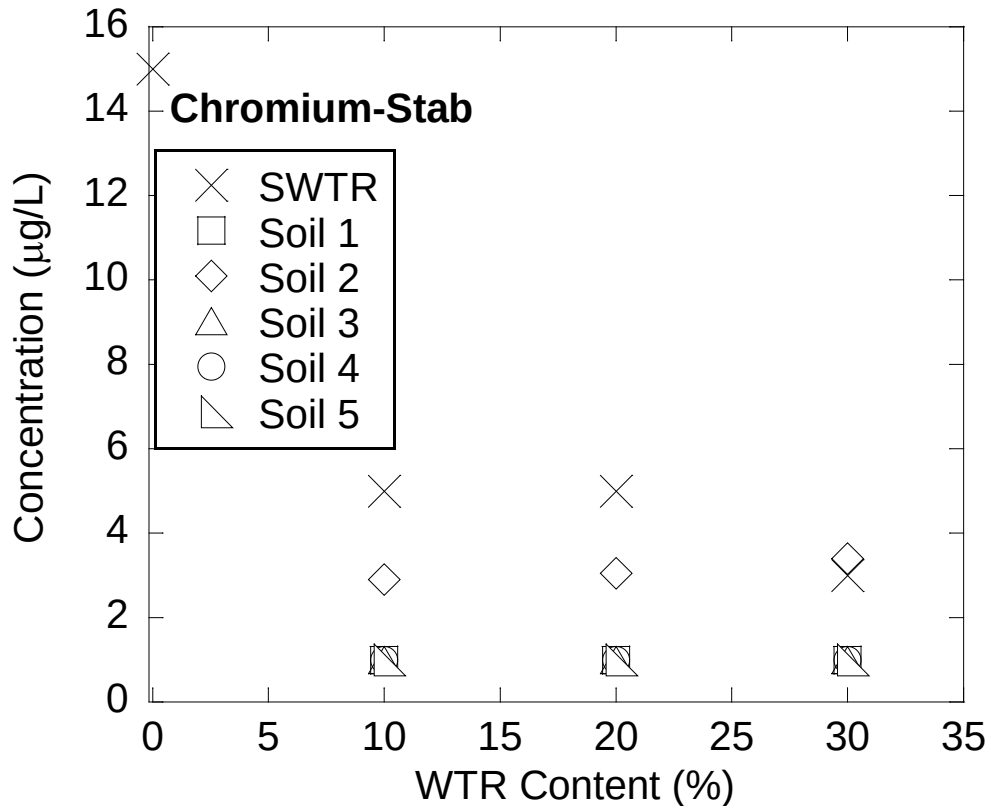
Chromium-Stab
SWTR
Soil 1
Soil 2
Soil 3
Soil 4
Soil 5
Concentration (µg/L)
WTR Content (%)
0
2
4
6
8
10
12
14
16
0
5
10
15
20
25
30
35

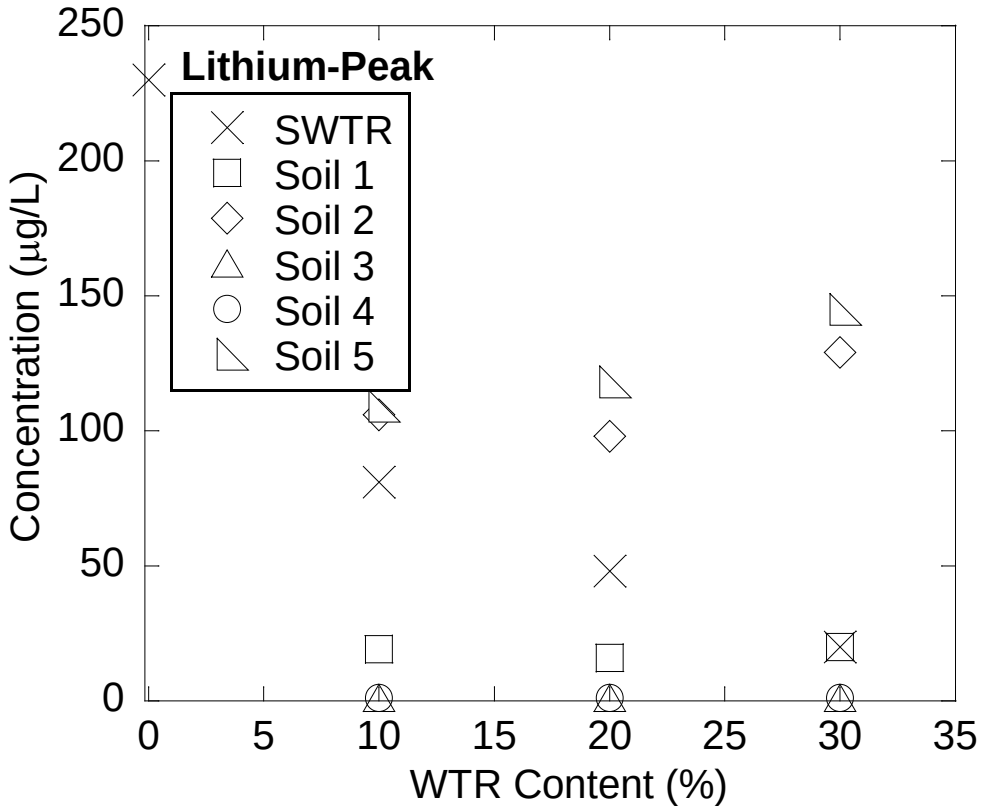
Lithium-Peak
SWTR
Soil 1
Soil 2
Soil 3
Soil 4
Soil 5
Concentration (µg/L)
WTR Content (%)
0
50
100
150
200
250
0
5
10
15
20
25
30
35

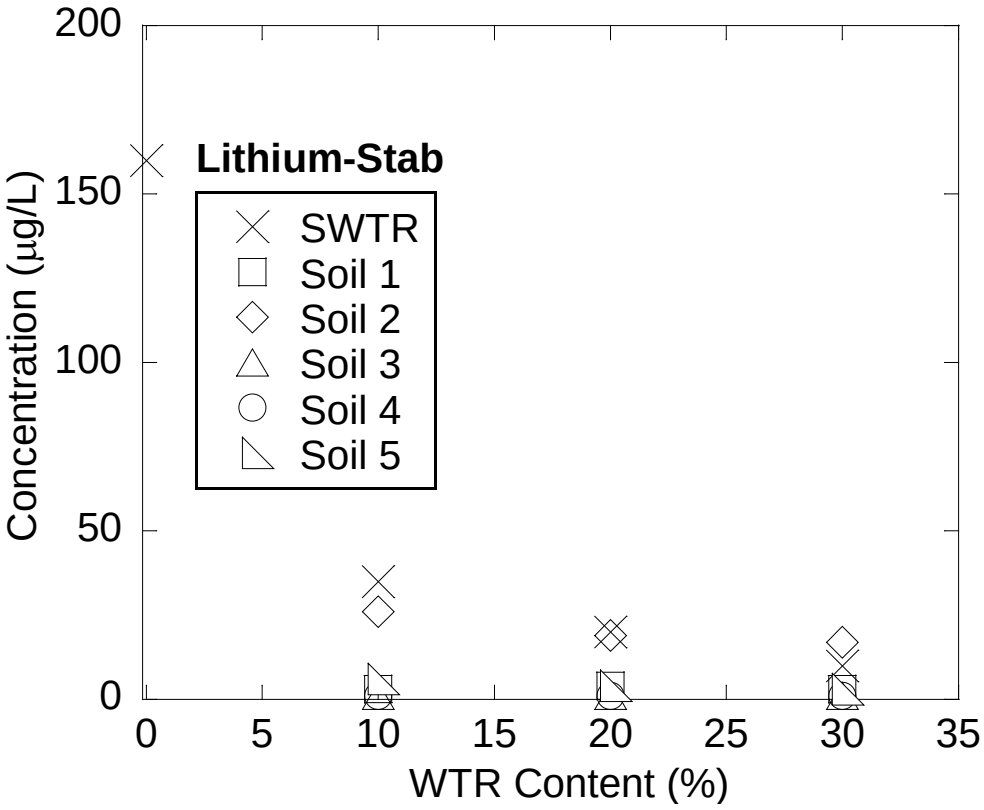
Lithium-Stab
SWTR
Soil 1
Soil 2
Soil 3
Soil 4
Soil 5
Concentration (µg/L)
WTR Content (%)
0
50
100
150
200
0
5
10
15
20
25
30
35

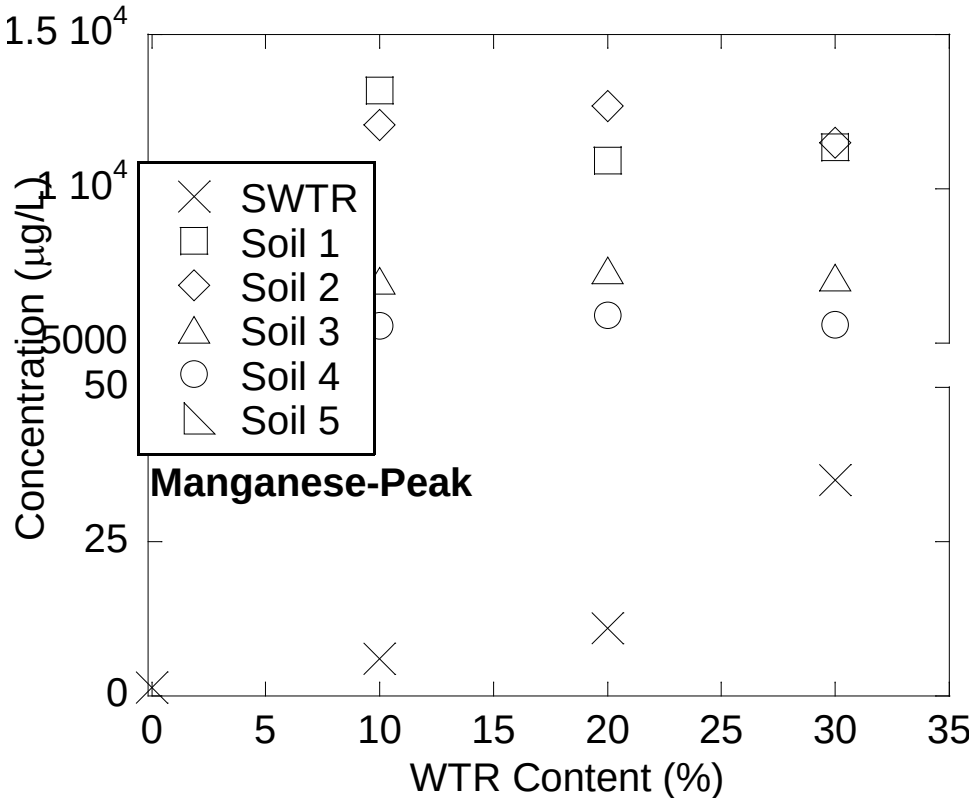
1.5 10^4
1 10^4
5000
50
25
0
Concentration (µg/L)
SWTR
Soil 1
Soil 2
Soil 3
Soil 4
Soil 5
Manganese-Peak
0
5
10
15
20
25
30
35
WTR Content (%)

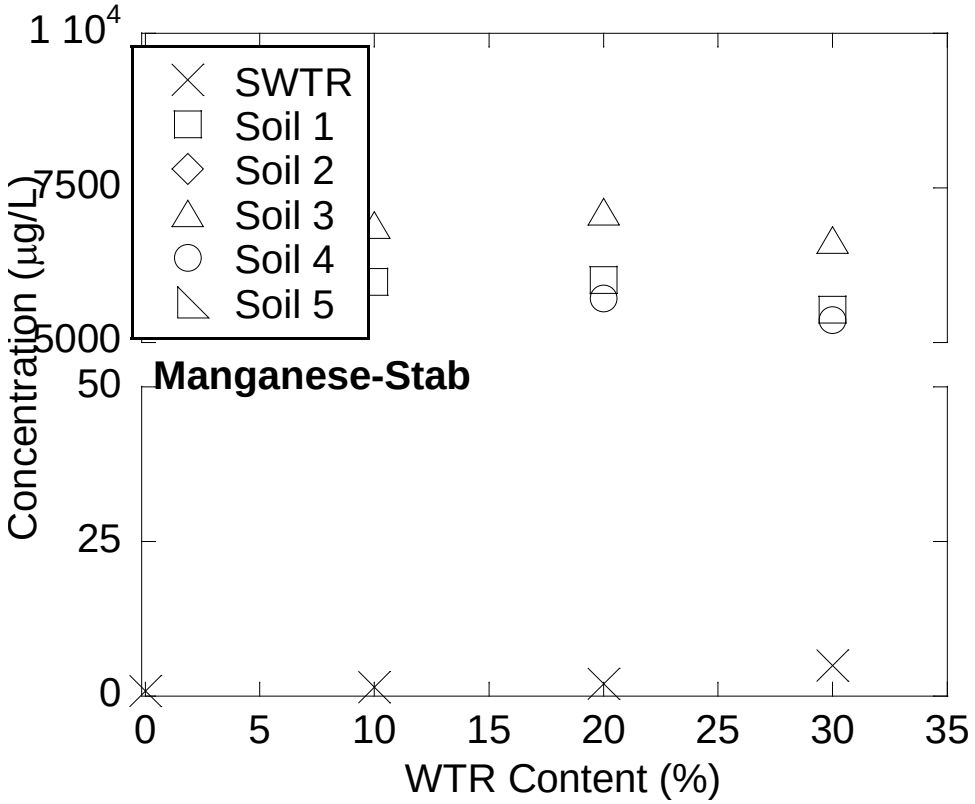
1 10^4
7500
5000
50
25
0
Concentration (µg/L)
SWTR
Soil 1
Soil 2
Soil 3
Soil 4
Soil 5
Manganese-Stab
0
5
10
15
20
25
30
35
WTR Content (%)

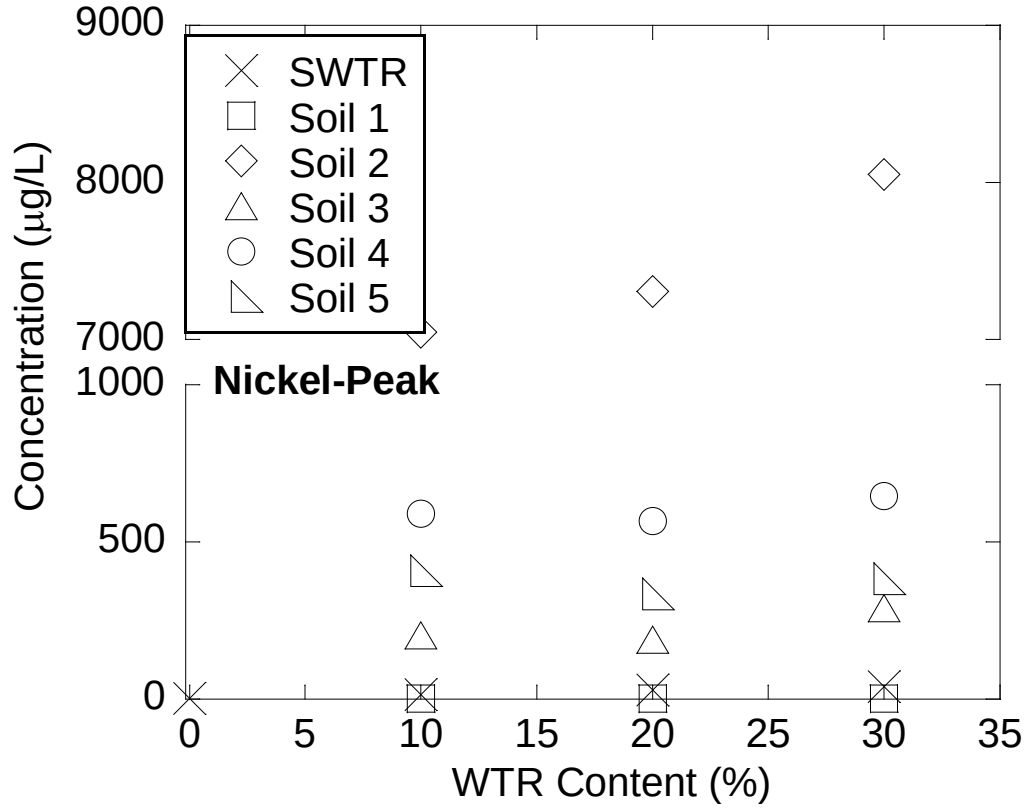
9000
8000
7000
1000
500
0
Concentration (µg/L)
SWTR
Soil 1
Soil 2
Soil 3
Soil 4
Soil 5
Nickel-Peak
0
5
10
15
20
25
30
35
WTR Content (%)

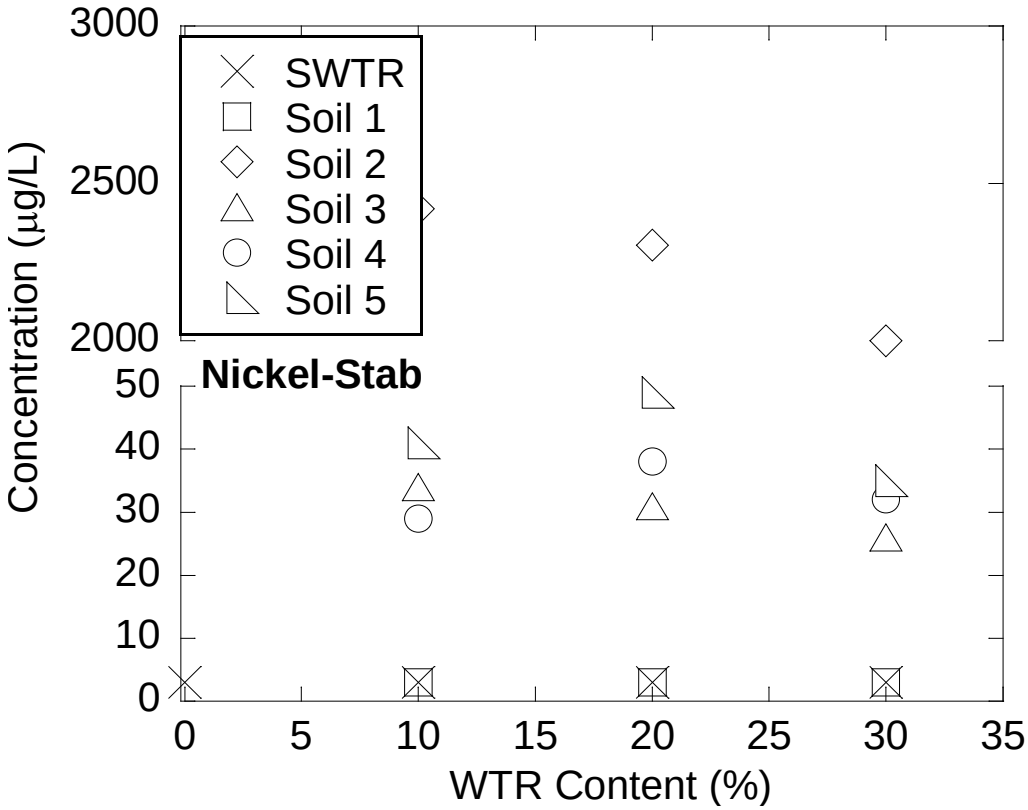
3000
2500
2000
50
40
30
20
10
0
Concentration (µg/L)
SWTR
Soil 1
Soil 2
Soil 3
Soil 4
Soil 5
Nickel-Stab
0
5
10
15
20
25
30
35
WTR Content (%)

APPENDIX B: WISCLEACH ANALYSIS RESULTS

Table B.1 Hydraulic and transport input parameters for pavement, embankment, subgrade and aquifer structures

Specimen	Hydraulic Conductivity K(m/year)	Effective Porosity, n_e	Hydraulic Gradient, i	Longitudinal Dispersivity, α_L (m)	Transverse Dispersivity, α_L (m)	Retardation Factor, R_d for Metals					
						Zn	Al	Pb	Cu	Ba	B
S	295	0.32	0.001	0.588	0.059	28	103.5	88	3.5	54	300
S30WTR	0.95	0.343	0.001	0.368	0.037	20.5	121.6	3.5	10.1	106	290
Subgrade 1	2.24	0.33	0.001	0.130	0.010	16	3.5	3.5	44.3	115	79
Subgrade 2	0.36	0.27	0.001	0.147	0.015	7.3	14.6	6.8	14.5	29	19.2
Encapsulation Layer	0.32	0.25	0.001	0.1	0.01	7.2	7.2	7.2	7.2	7.2	7.2
Pavement	18.29	0.35	0.001	0.1	0.01	1	1	1	1	1	1
Aquifer	3784	0.30	0.001	0.1	0.01	1	1	1	1	1	1

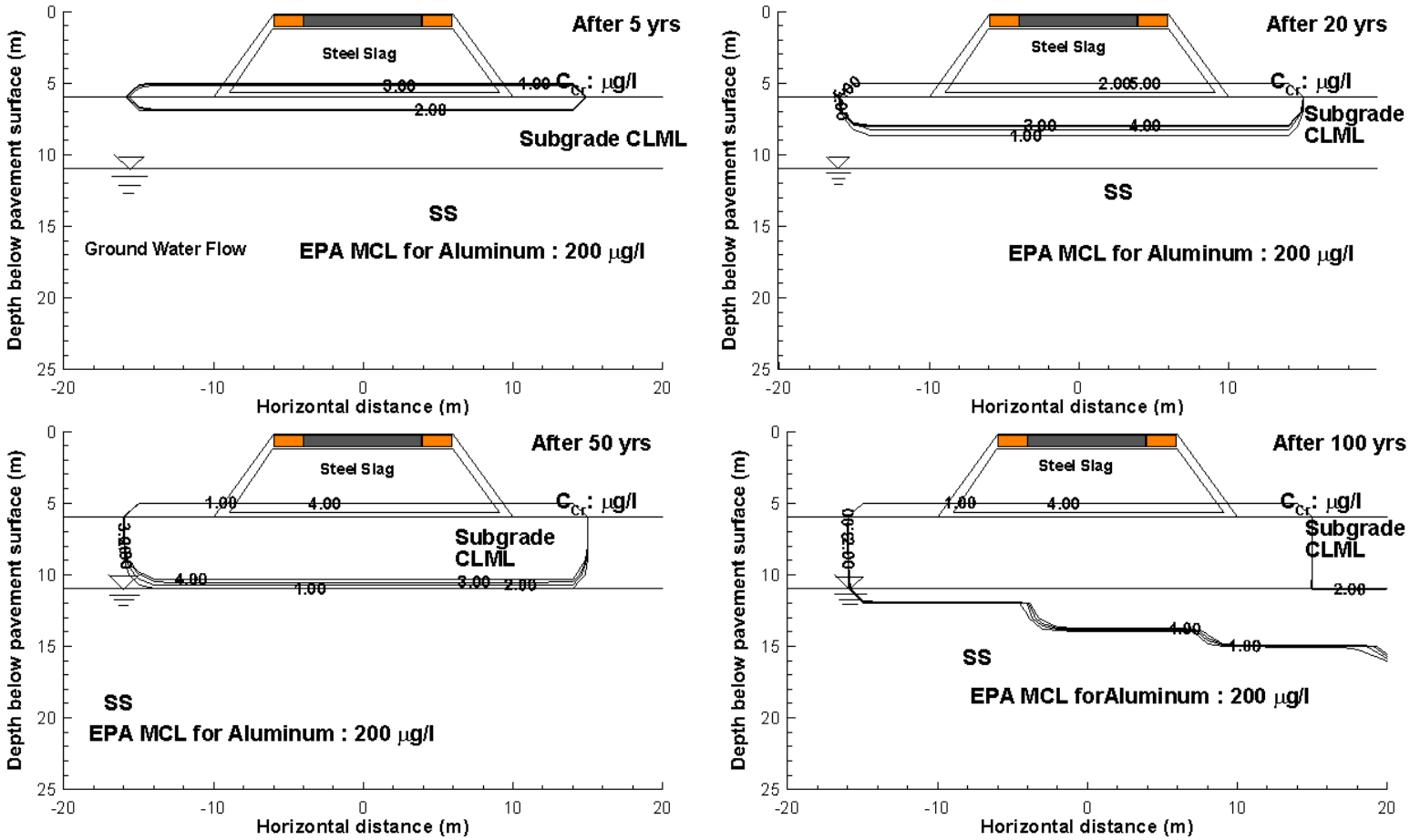
After 5 yrs
Steel Slag
3.00
1.00
2.00
C_{Cr}: µg/l
Subgrade CLML
SS
Ground Water Flow
EPA MCL for Aluminum : 200 µg/l
Depth below pavement surface (m)
Horizontal distance (m)
After 20 yrs
Steel Slag
2.00
5.00
3.00
1.00
4.00
C_{Cr}: µg/l
Subgrade CLML
SS
EPA MCL for Aluminum : 200 µg/l
Depth below pavement surface (m)
Horizontal distance (m)
After 50 yrs
Steel Slag
1.00
4.00
3.00
4.00
1.00
3.00
2.00
C_{Cr}: µg/l
Subgrade CLML
SS
EPA MCL for Aluminum : 200 µg/l
Depth below pavement surface (m)
Horizontal distance (m)
After 100 yrs
Steel Slag
1.00
4.00
3.00
2.00
4.00
1.00
C_{Cr}: µg/l
Subgrade CLML
SS
EPA MCL forAluminum : 200 µg/l
Depth below pavement surface (m)
Horizontal distance (m)

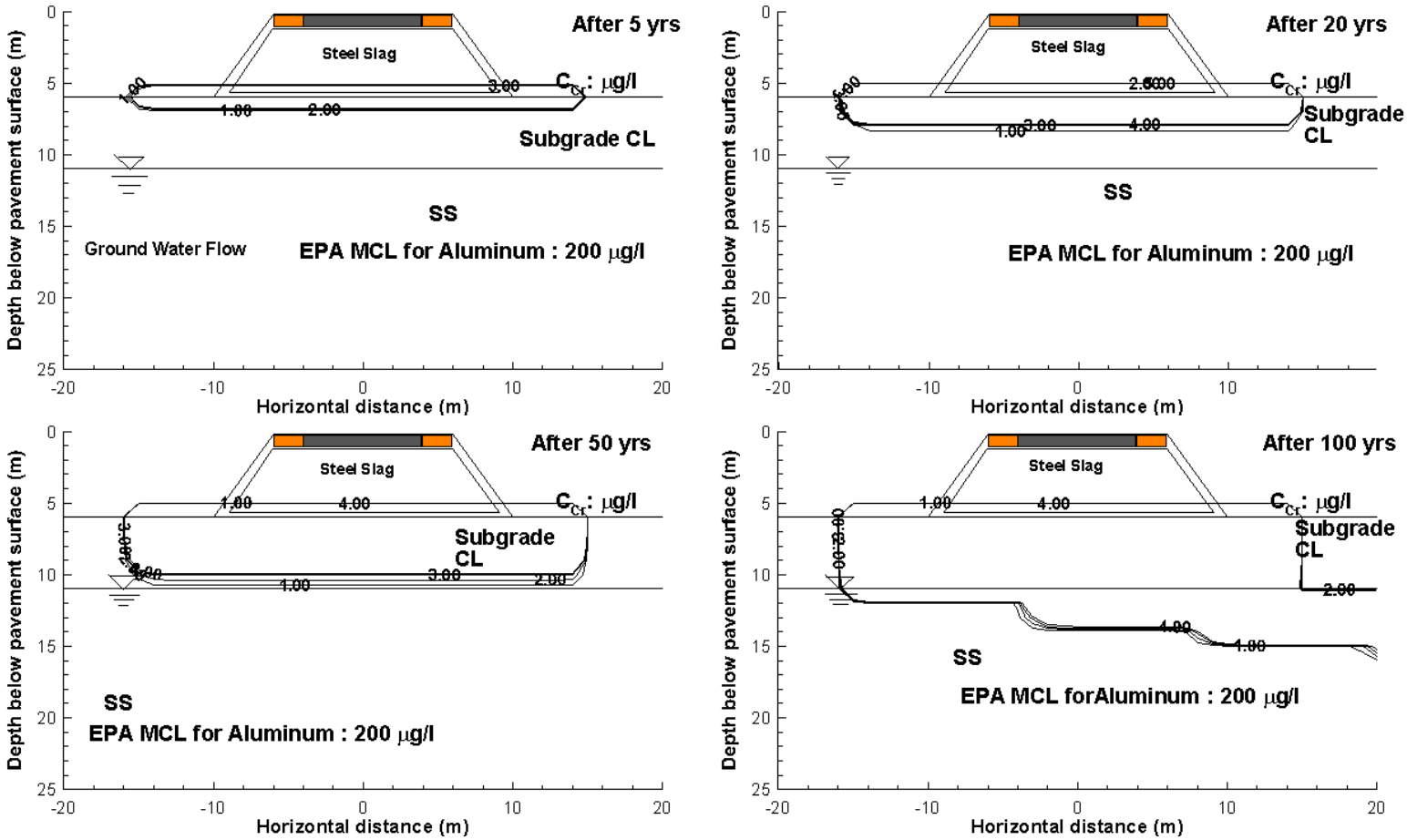
After 5 yrs
Steel Slag
C_{Cr}: µg/l
1.00
1.00
2.00
3.00
Subgrade CL
SS
Ground Water Flow
EPA MCL for Aluminum : 200 µg/l
Depth below pavement surface (m)
Horizontal distance (m)
After 20 yrs
Steel Slag
C_{Cr}: µg/l
1.00
3.00
4.00
Subgrade CL
SS
EPA MCL for Aluminum : 200 µg/l
Depth below pavement surface (m)
Horizontal distance (m)
After 50 yrs
Steel Slag
1.00
4.00
C_{Cr}: µg/l
Subgrade CL
1.00
3.00
2.00
SS
EPA MCL for Aluminum : 200 µg/l
Depth below pavement surface (m)
Horizontal distance (m)
After 100 yrs
Steel Slag
1.00
4.00
C_{Cr}: µg/l
Subgrade CL
2.00
1.00
1.00
SS
EPA MCL forAluminum : 200 µg/l
Depth below pavement surface (m)
Horizontal distance (m)

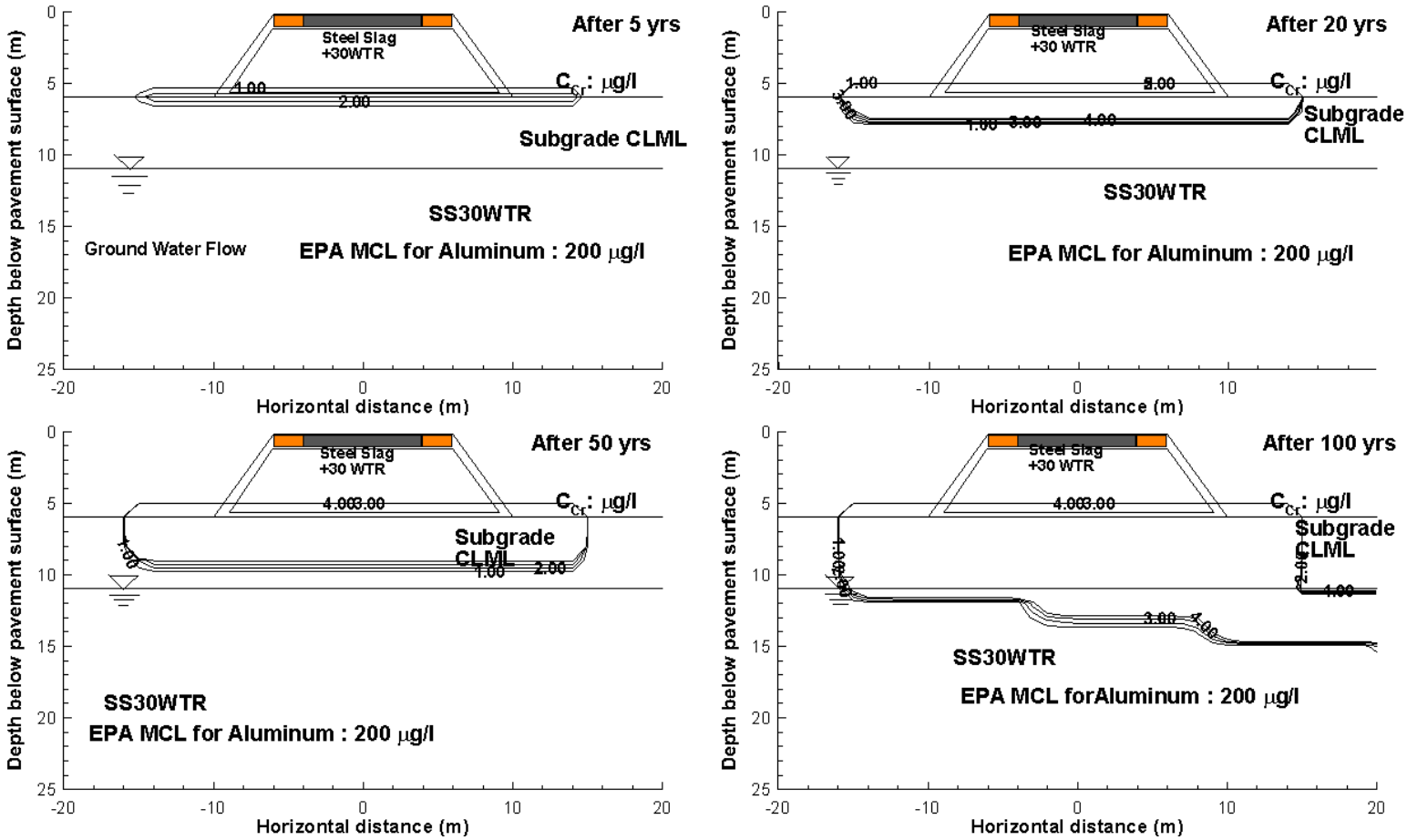
After 5 yrs
Steel Slag
+30WTR
C_{Cr}: µg/l
1.00
2.00
Subgrade CLML
SS30WTR
Ground Water Flow
EPA MCL for Aluminum : 200 µg/l
After 20 yrs
Steel Slag
+30 WTR
C_{Cr}: µg/l
1.00
5.00
1.00
3.00
4.00
Subgrade
CLML
SS30WTR
EPA MCL for Aluminum : 200 µg/l
After 50 yrs
Steel Slag
+30 WTR
4.00
3.00
C_{Cr}: µg/l
Subgrade
CLML
1.00
1.00
2.00
SS30WTR
EPA MCL for Aluminum : 200 µg/l
After 100 yrs
Steel Slag
+30 WTR
4.00
3.00
C_{Cr}: µg/l
Subgrade
CLML
2.00
4.00
3.00
4.00
SS30WTR
EPA MCL forAluminum : 200 µg/l
Depth below pavement surface (m)
Horizontal distance (m)
0
5
10
15
20
25
-20
-10
0
10
20

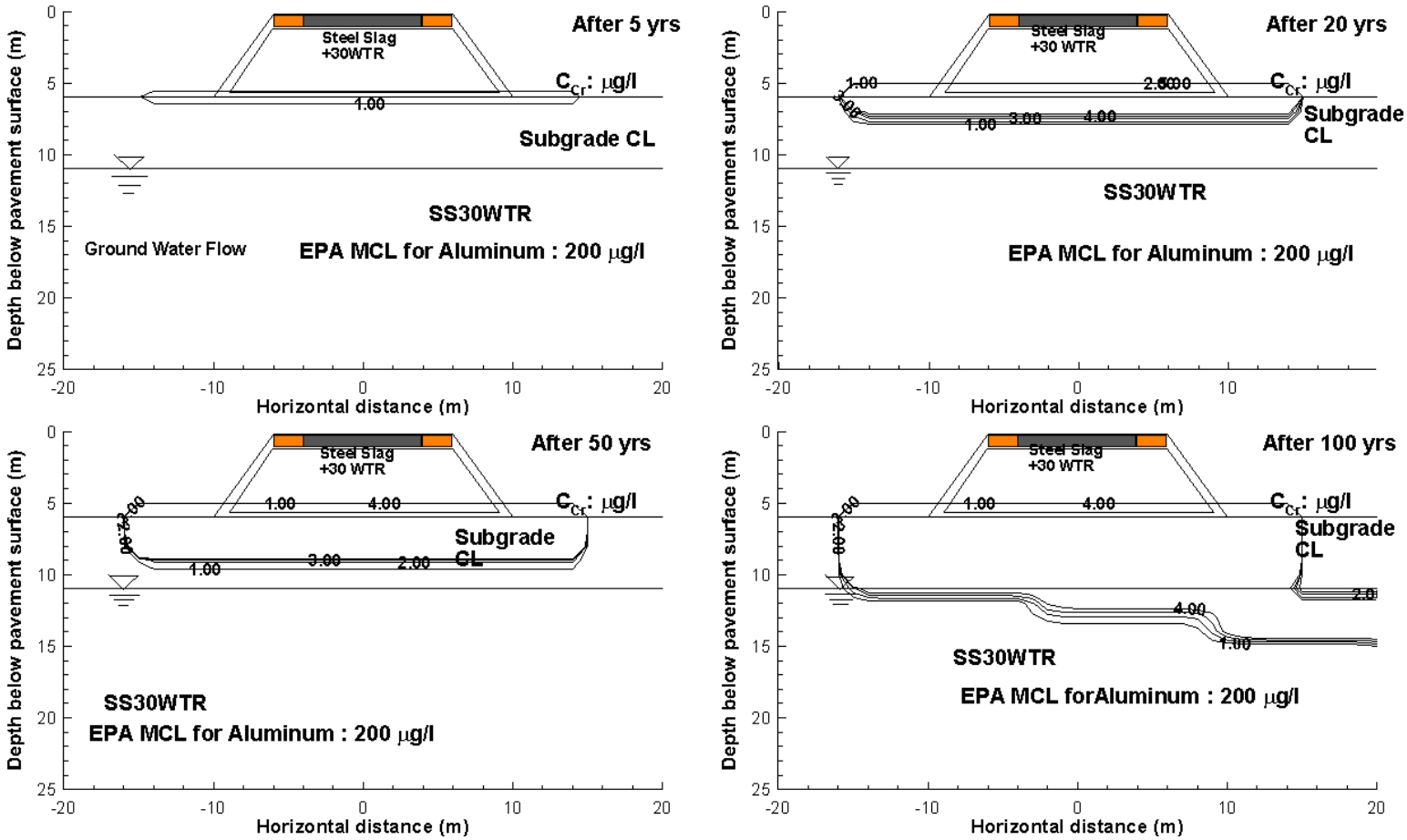
After 5 yrs
Steel Slag
+30WTR
C_{Cr}: µg/l
1.00
Subgrade CL
SS30WTR
Ground Water Flow
EPA MCL for Aluminum : 200 µg/l
After 20 yrs
Steel Slag
+30 WTR
1.00
2.00
3.00
4.00
Subgrade
CL
SS30WTR
EPA MCL for Aluminum : 200 µg/l
After 50 yrs
SS30WTR
EPA MCL for Aluminum : 200 µg/l
After 100 yrs
SS30WTR
EPA MCL forAluminum : 200 µg/l
Depth below pavement surface (m)
Horizontal distance (m)

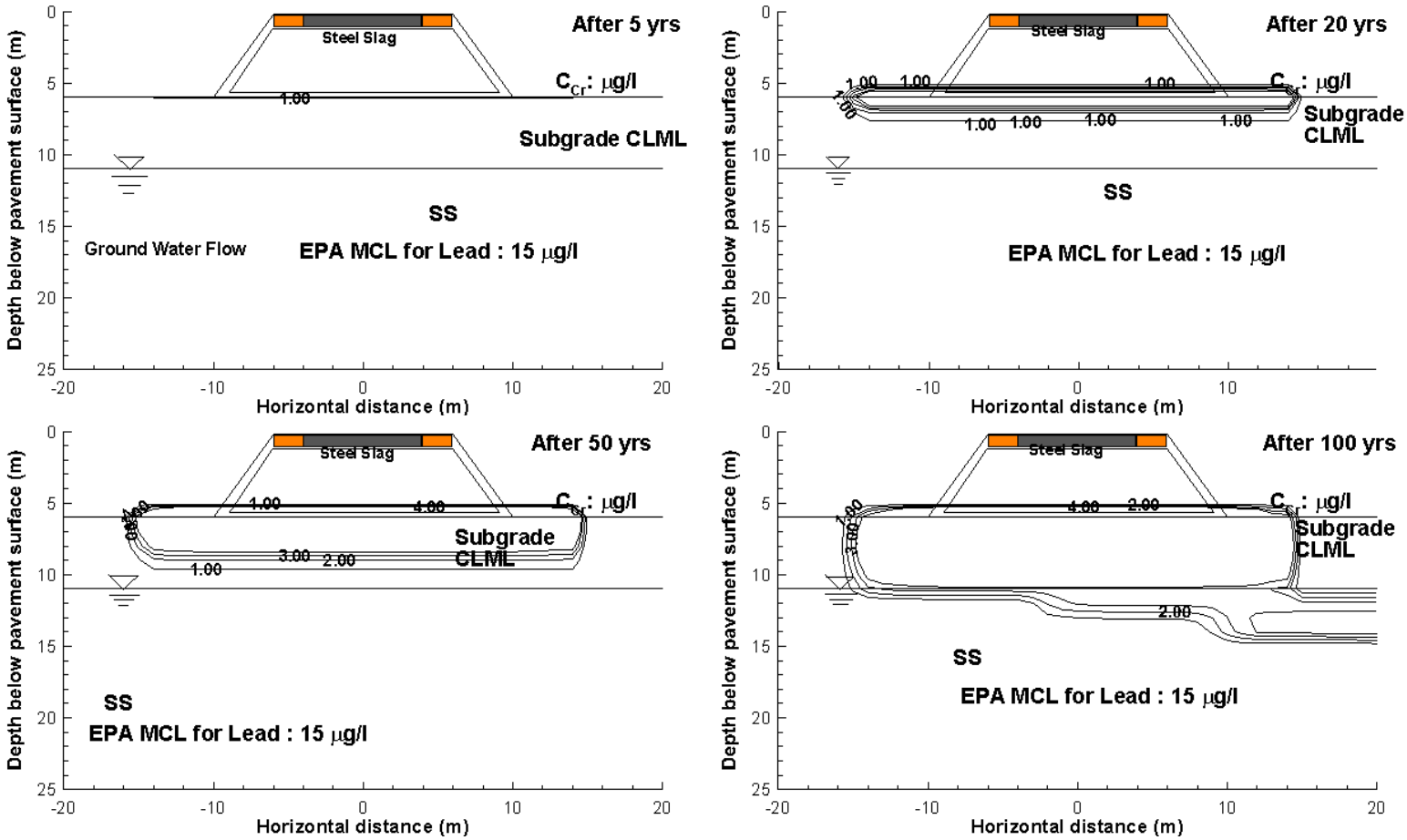
After 5 yrs
Steel Slag
C_{Cr}: µg/l
1.00
Subgrade CLML
SS
Ground Water Flow
EPA MCL for Lead : 15 µg/l
After 20 yrs
1.00
Subgrade CLML
After 50 yrs
4.00
3.00
2.00
After 100 yrs
Depth below pavement surface (m)
Horizontal distance (m)

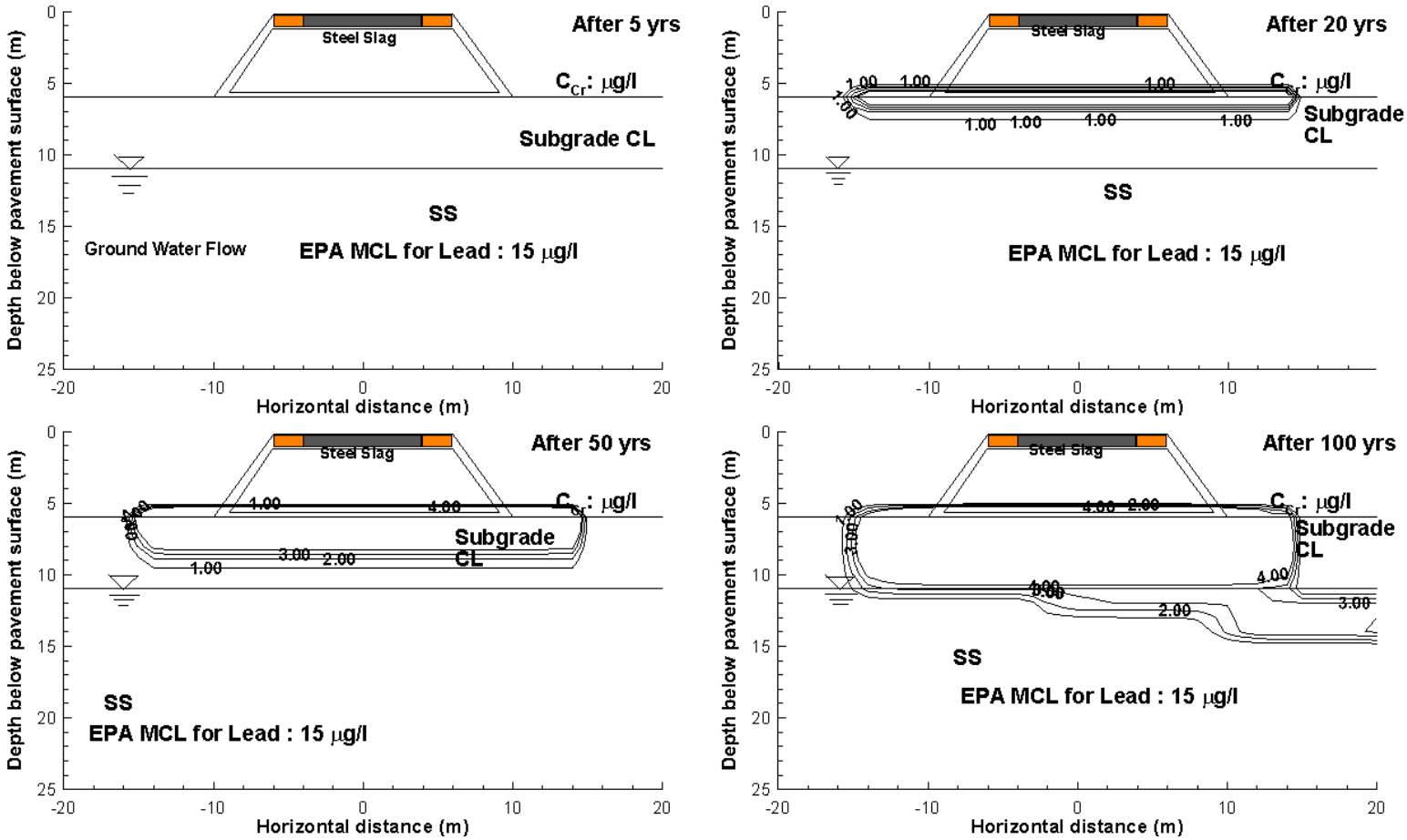
After 5 yrs
Steel Slag
C_{Cr}: µg/l
Subgrade CL
SS
Ground Water Flow
EPA MCL for Lead : 15 µg/l
After 20 yrs
Steel Slag
C_{Cr}: µg/l
1.00
Subgrade CL
SS
EPA MCL for Lead : 15 µg/l
After 50 yrs
Steel Slag
C_{Cr}: µg/l
1.00
4.00
3.00
2.00
Subgrade CL
SS
EPA MCL for Lead : 15 µg/l
After 100 yrs
Steel Slag
C_{Cr}: µg/l
4.00
2.00
Subgrade CL
3.00
SS
EPA MCL for Lead : 15 µg/l
Depth below pavement surface (m)
Horizontal distance (m)

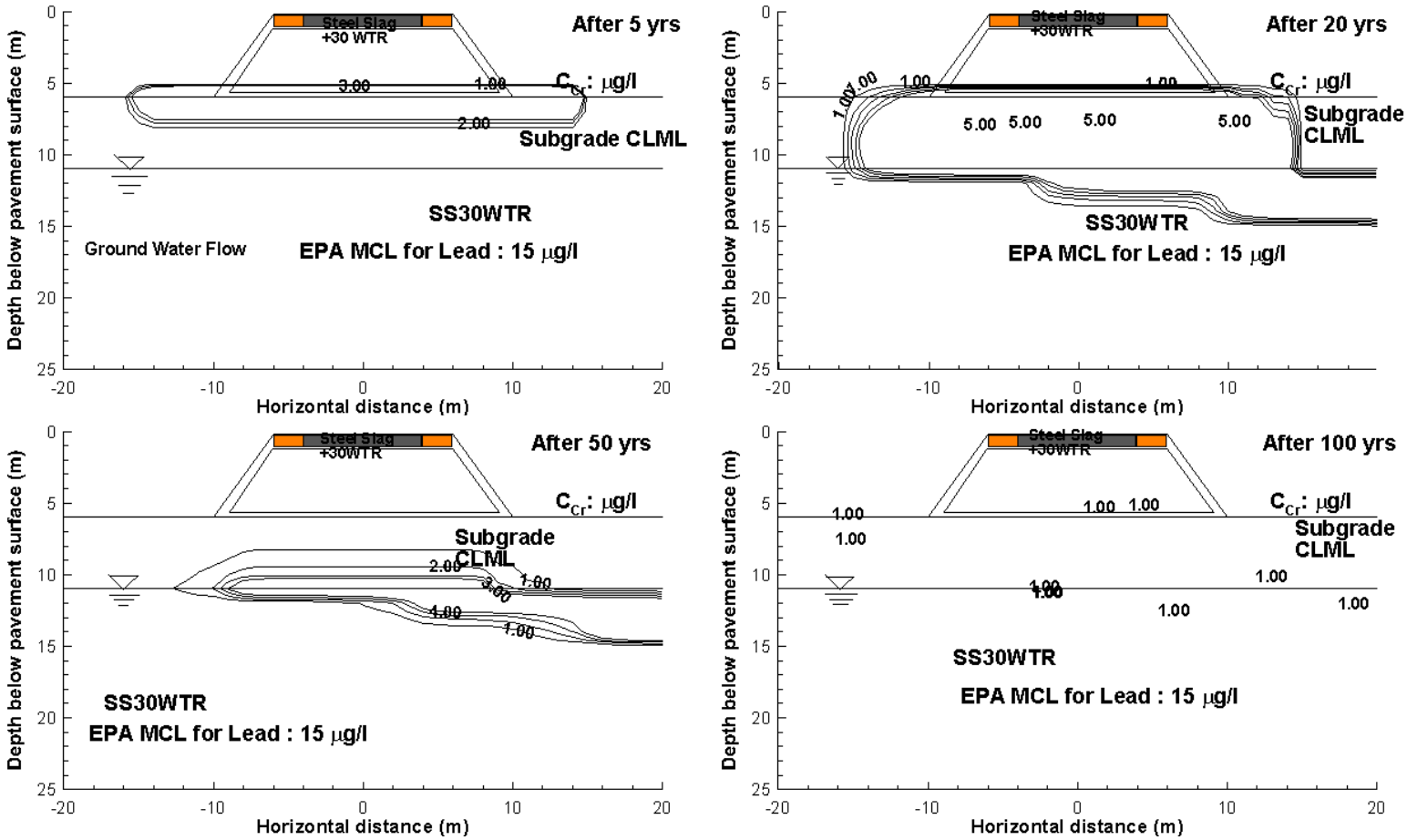
After 5 yrs
Steel Slag
+30 WTR
3.00
1.00
2.00
C_{Cr}: µg/l
Subgrade CLML
SS30WTR
Ground Water Flow
EPA MCL for Lead : 15 µg/l
After 20 yrs
Steel Slag
+30WTR
1.00
5.00
C_{Cr}: µg/l
Subgrade
CLML
SS30WTR
EPA MCL for Lead : 15 µg/l
After 50 yrs
Steel Slag
+30WTR
C_{Cr}: µg/l
Subgrade
CLML
2.00
1.00
SS30WTR
EPA MCL for Lead : 15 µg/l
After 100 yrs
Steel Slag
+30WTR
1.00
C_{Cr}: µg/l
Subgrade
CLML
SS30WTR
EPA MCL for Lead : 15 µg/l
Depth below pavement surface (m)
Horizontal distance (m)

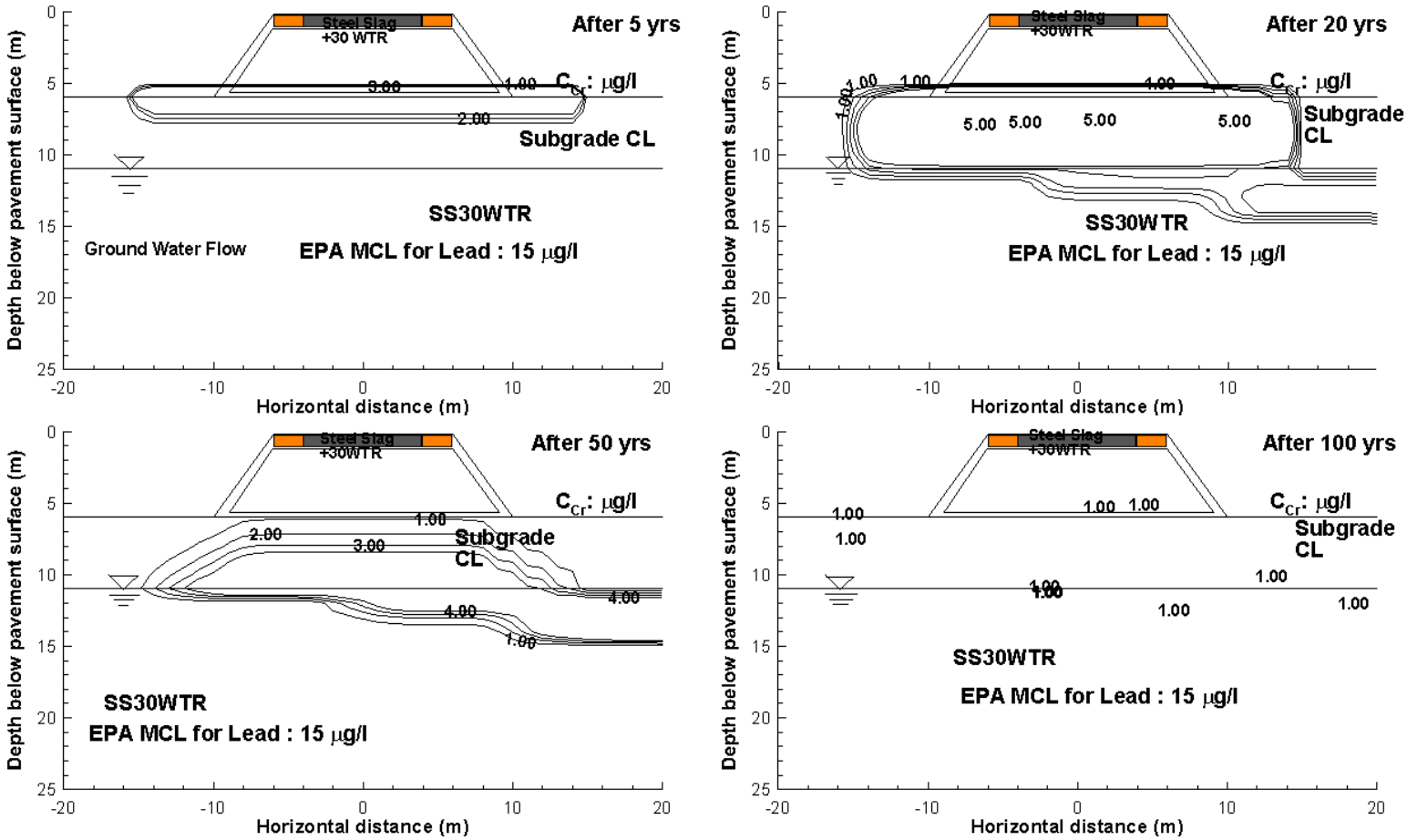
Steel Slag
+30 WTR
After 5 yrs
3.00
1.00
2.00
C_{Cr}: µg/l
Subgrade CL
SS30WTR
Ground Water Flow
EPA MCL for Lead : 15 µg/l
Depth below pavement surface (m)
Horizontal distance (m)
Steel Slag
+30WTR
After 20 yrs
1.00
1.00
1.00
1.00
5.00
5.00
5.00
5.00
C_{Cr}: µg/l
Subgrade CL
SS30WTR
EPA MCL for Lead : 15 µg/l
Depth below pavement surface (m)
Horizontal distance (m)
Steel Slag
+30WTR
After 50 yrs
1.00
2.00
3.00
4.00
4.00
1.00
C_{Cr}: µg/l
Subgrade CL
SS30WTR
EPA MCL for Lead : 15 µg/l
Depth below pavement surface (m)
Horizontal distance (m)
Steel Slag
+30WTR
After 100 yrs
1.00
1.00
1.00
1.00
1.00
1.00
1.00
1.00
C_{Cr}: µg/l
Subgrade CL
SS30WTR
EPA MCL for Lead : 15 µg/l
Depth below pavement surface (m)
Horizontal distance (m)

APPENDIX C: Preventing Swelling and Decreasing Alkalinity of Steel Slags Used in Highway Infrastructures

by Asli Y. Dayioglu, Ahmet H.. Aydilek and Bora Cetin

Preventing Swelling and Decreasing Alkalinity of Steel Slags Used in Highway Infrastructures

Asli Y. Dayioglu, Ahmet H. Aydilek, and Bora Cetin

Steel slag is a byproduct of iron and steel production by the metallurgical industries. Annually, 21 million tons of steel slags are produced in the United States, and most of this slag is landfilled. Landfilling represents significant economic loss and uses valuable land space. Although steel slag has great potential for use in highway applications, especially as a granular highway base or subbase material, it has not been used extensively because of its high swelling potential and alkalinity. Swelling potential deteriorates the structural stability of highways, and high alkalinity poses an environmental challenge. This study seeks a methodology that promotes the use of steel slags in highway base and subbase layers by minimizing these two main disadvantages. Two treatment methods were used. In the first method, steel slag material was coated with bituminous material. In the second method, the slag was mixed with water treatment residuals at various percentages by weight. The mixtures prepared in this study were subjected to accelerated swelling tests and batch water leach tests. Results of the swelling tests indicated that the addition of both water treatment residuals and bituminous material into steel slag decreased the swelling rate significantly. Furthermore, bituminous-coated mixtures did not exhibit any swelling. These two methods also decreased the effluent pH of steel slag from 12.3 to 11.65 (bitumen-coated slag) and 9.8 (slag mixed with water treatment residuals). The batch test results did not satisfy the pH 8.5 limit regulated by the Maryland Department of Environment for placement of industrial byproducts in highways.

Large quantities of byproducts result from steel and iron production. Steel slag is one of these byproducts. Approximately 21 million tons of steel slags are produced annually in the United States, and only 10% to 15% of these materials are recycled (*1*). Most slags are stockpiled or placed in landfills, which causes loss of valuable land space (*2*). Stockpiling of large amounts of steel slag creates an environmental challenge because of the potential for leaching of the large amounts of heavy metals in the steel slag (*1*). An innovative way to recycle these industrial byproducts is needed.

Steel slag has been used in a variety of applications in the construction industry. It has been used as a supplementary material in cement and concrete mixtures, as a granular material in highway base and subbase layers, and as an aggregate in asphalt mixes (usually hot-mix asphalt) (*3–6*). Rohde et al. studied electric arc furnace slag and recommended its use in the field (*3*). Suer et al. investigated the behavior of electric arc furnace slag on a section of a road where steel slag was used as base layer (*6*). Slags produced via blast furnace are used in a wide range of highway applications, such as granular bases, concrete and hot-mix-asphalt aggregate, and supplementary cementitious materials (*7*). However, slags obtained from basic oxygen furnaces and electric arc furnaces are less commonly used in highway applications because of their volumetric instability in the presence of moisture. This instability occurs because of the high free lime (CaO) and magnesia (MgO) contents, which can react with water in the presence of moisture and cause large expansion deformations (*8*). This behavior is not favorable, particularly when steel slag is to be used in rigid matrices. Therefore, reuse of slags (steel slag particularly) in highway layers is not preferred until their volumetric instability is tested (*9*).

Several efforts have been made to use steel slags in highway base and subbase, on low-volume roads, and for soil stabilization. Verhasselt and Choquet performed a series of accelerated bath tests on steel slag samples and claimed that the critical CaO content for the steel slags to be used in pavements was 4.5% and, according to the swelling tests, maximum permissible linear expansion is 1% (*10*). In addition, that study recommended placement of sand layers above and below the steel slag layer because voids inside the sand layer can tolerate the swelling of the steel slag. Geiseler stated that there is no need to restrict the volumetric expansion of steel slag in certain applications, such as construction of parking lots or landscaping works (*11*). That study proposed that free CaO content of nonaged steel slag should not exceed 7% and 4% for use in unbound layers and bituminous (asphalt) road layers, respectively. Deniz et al. conducted swelling tests on reclaimed asphalt pavement (RAP) samples, including surface binder RAP with 60% steel slag aggregates, surface RAP with 92% steel slag, steel slag RAP, and virgin steel slag, to compare expansion characteristics (*9*). Results showed that RAP materials with steel slag aggregates exhibited lower expansion behavior compared with virgin materials mixed with slags. It was stated that high absorption characteristics of bitumen of RAP materials and high alkalinity of steel slags might have yielded lower swelling potential. This phenomenon occurs because the surface texture of steel slags is rougher than other natural aggregates, their friction properties are superior, and they have a significantly improved adhesion ability with an asphalt binder.

In addition to its swelling potential, steel slags possess high alkalinity behavior and cause leaching of very alkaline effluent solutions to the surrounding environment. The Maryland Department of Environment (MDE) does not allow the use of waste materials with an effluent pH exceeding 8.5 (*12*). It is well known that steel slag materials contain significant amounts of CaO (40% to 60%) (*7*).

A. Y. Dayioglu and A. H. Aydilek, Department of Civil and Environmental Engineering, University of Maryland, College Park, 1173 Glenn L. Martin Hall, College Park, MD, 20742. B. Cetin, Department of Civil and Environmental Engineering, South Dakota School of Mines and Technology, 501 East Saint Joseph Street, Rapid City, SD 57701. Corresponding author: B. Cetin, bora.cetin@sdsmt.edu.

Transportation Research Record: Journal of the Transportation Research Board, No. 2401, Transportation Research Board of the National Academies, Washington, D.C., 2014, pp. 52–57.
DOI: 10.3141/2401-06

CaO reacts with water in the presence of moisture and produce a calcium hydroxide hydration reaction product, which causes an increase in pH of the equilibrium system caused by dissolution of OH^- ions (*13*). Previous studies focused extensively on improvement of the geomechanical behavior of the steel slags to be used in highway base and subbase layers (*3*, *7*, *9*). Few studies have focused on the environmental impact of the use of steel slags in highway engineering applications (*14–16*). However, none of these studies identified the concern about high effluent pH.

Previous research showed that steel slag can be a good alternative to natural aggregates that are conventionally used in highway base and subbase layers (*3*). However, most of these studies suggested that steel slags be aged and exposed to moisture conditions for a long time before their use. No method for suppressing the swelling potential and limiting the release of high-pH effluent solutions is provided. The present study tested the efficacy of an innovative methodology for decreasing the swelling potential of steel slags while controlling the effluent pH. In the study, steel slag materials were coated with bituminous asphalt material and mixed with water treatment residuals (WTR). These mixtures, along with the virgin steel slag material, were subjected to accelerated swelling tests and batch water leach tests.

Materials

The steel slag material used in this study was produced in a blast oxygen furnace. Aging has significant effects on swelling potential of any kind of slags, and the literature claims that aging decreases the swelling potential (*7*). In this research project, steel slag materials with three aging properties—6 months, 1 year, and 2 years—were used. As indicated by previous studies, increased aging is expected to decrease the amount of swelling in slags. However, in the present project, steel slag material aged 2 years exhibited the greatest swelling. The cause of this phenomenon could be the bonded calcium aluminosilicates in the steel slag, which may dissolve on long exposure to the atmosphere. Debris and foreign material in the steel slag were removed by hand before testing. The steel slag material is classified as well-graded sand with silt according to the Unified Soil Classification System and as A-1-b according to the AASHTO classification system. It exhibits no plasticity and contains 12% silty fines by weight. Table 1 summarizes the physical properties of the steel slag material. The natural water content and optimum compaction moisture content of steel slag material are 10% and 13.5%, respectively.

Bituminous coating and WTR amendment methodologies were applied to the steel slag material to prevent swelling and to decrease the effluent pHs. WTR, a byproduct of drinking water treatment, is an aluminum-based sludge and does not contain any surface or groundwater pollutants. WTR was collected from the drinking water treatment plant for the Rockville, Maryland, drainage area and was air dried and sieved through the No. 40 sieve before being mixed with steel slag. WTR contains 76% fines by weight and shows no plasticity. The bituminous coating was achieved with PG 64-22 asphalt binder (*17*). The specific gravity of the steel slag and asphalt binder is 3.45 and 1.02, respectively. The asphalt binder is solid at room temperature and is viscous fluid at 90°C. Measurements made according to U.S. Environmental Protection Agency SW-846 Method 9045 showed that the pH of steel slag and WTR materials was 12.4 and 6.9, respectively. Steel slag material was mixed with 2%, 3%, 4%, 5%, 7%, and 8% asphalt binder by weight, and WTR was added at 20%, 30%, and 40% by weight to the steel slag material. All mixtures prepared for the study were compacted at optimum moisture contents (W_{opt}) and maximum dry unit weights ($\gamma_{dry\text{-}max}$) with the standard Proctor effort (ASTM D 698). Steel slag and WTR materials were mixed thoroughly in the tray with additions of small amounts of water. Steel slag was sieved through the ⅜-in. (9.5 mm) sieve before it was mixed with asphalt binder; it was sieved through the ¾-in. (19-mm) sieve for preparation of the steel slag–WTR mixtures. Finer steel slag material was preferred in the mixtures of steel slag and bituminous coating to prevent coarser aggregates from adsorbing large portions of the asphalt binders added into the mixture. This procedure achieves a more uniform coating of the steel slag aggregates.

Method

Preparation of Bituminous Coating

Steel slag was oven dried for 24 h at 105°C and sieved through the ⅜-in. sieve. The oven-dried sample was weighed and placed in the oven. The required amount of asphalt binder grade (PG 64-22) was calculated, weighed, and put into the oven, along with all the metal equipment that was used during hot mixing (spoons, buckets, etc.). The binder, slag, and equipment were then heated to 170°C and kept in the oven for 3.5 h. Then, heated equipment was placed into the mixer, and slag samples were taken from the oven and thoroughly mixed for approximately 1 to 2 min (Figure 1*a*). Next, the heated binder was taken from the oven and poured into the bucket. Bitumen and steel slag were thoroughly mixed until all the particles were visibly coated and the mixture was warm. Finally, the bitumen-covered steel slag samples were spread on a flat surface and left overnight to cool completely (Figure 1*b*).

accelerated swelling tests

In accelerated swelling tests, compacted steel slag samples were exposed to hot water or steam to accelerate the swelling rate during the test. Swelling rates of the specimens were monitored for a shorter period than in long-term swelling tests (ASTM D-1883). For both

TABLE 1 Physical Properties of Steel Slag and WTR

Material	G_s	Gravel Content (%)	Sand Content (%)	Fines Content (%)	I_p (%)	W_n (%)	W_{opt} (%)	$\gamma_{dry\text{-}max}$ (kN/m^3)	pH
Steel slag	3.45	21	67	12	NP	10	13.5	22.2	12.4
Water treatment residual	na	0	24	76	NP	385	42	10.25	6.9

Note: G_s = specific gravity; I_p = plasticity index; W_n = natural water content; NP = non-plastic; na = not applicable.

(a)

(b)

FIGURE 1 Bitumen coating: (*a*) procedure and (*b*) coated samples.

tests, steel slag specimens were prepared for W_{opt} and $\gamma_{dry\text{-}max}$ in cylindrical molds; lateral movement was prevented, and one-dimensional swelling was measured.

Tests were performed according to the water-bath swelling test method described in ASTM D4792 (*Standard Test Method for Potential Expansion of Aggregates from Hydration Reactions*), and samples were compacted in standard California bearing ratio molds, which were equipped with dial gauges, according to the procedures described in ASTM 1883. Specimens were cured for 7 days at room temperature (22°C) at 100% relative humidity. Then, specimens were immersed in hot water (70°C ± 3°C) instead of room temperature to accelerate the procedure. A surcharge load of 2.5 kPa was applied to the specimens during the tests. The tests were continued until the measured swelling ratios were stabilized.

Batch Water leach tests

Duplicate batch water leach tests were conducted on the steel slag alone, WTR alone, and mixtures of steel slag and bituminous coating and steel slag and WTR in accordance with the test method for shake extraction of solid waste with water (ASTM D3987). Details of the test procedure and deviations from the ASTM D3987 test method are available elsewhere (*18*). The influent solutions were prepared with 0.02M sodium chloride solution to provide stable reaction conditions. Water leach tests were not conducted on bituminous coating alone because of the viscous nature of the bitumen material itself; it is difficult to maintain a 20:1 liquid-to-solid ratio in the water leach tests. In the literature, either the pH of bitumen material in water is given as neutral or pH is not available.

Results

sieve analysis and Compaction tests

Gradation of the steel slag material was altered during bituminous coating and WTR amendment. The original steel slag material consisted of 21%, 67%, and 12% gravel, sand, and fines content, respectively (Figure 2). Coating of the steel slag, and especially its fines portion (<0.075 mm), results in a relatively coarser aggregate material, which is likely to provide a stronger but more brittle highway base or subbase layer. Figure 2 shows that the gradation curves of steel slag–bituminous coating mixtures tend to be more uniform compared with the original grain size distribution of steel slag material. Furthermore, uniformity of the gradation curves for mixtures of steel slag and bituminous coating increases with an increase in bituminous coating content.

The W_{opt} and $\gamma_{dry\text{-}max}$ of the steel slag material used in this study are 13.5% and 22.2 kN/m^3, respectively (Table 1). These values are consistent with the compaction characteristics of the typical steel slag materials reported by others (*3, 9*). Figure 3 shows the moisture–dry density relationship of the steel slag–bituminous coating mixtures, steel slag–WTR mixtures, and steel slag and WTR alone. The figure shows that a 3% to 4% increase in bituminous coating content results in ~1.4 times decrease in W_{opt} of the steel slag–bituminous coating mixtures, as the W_{opt} of the coated granular steel slag material is influenced by the amount of fine material (*19*). Furthermore, $\gamma_{dry\text{-}max}$ of the steel slag alone and steel slag–bituminous coating mixtures decreased 1.1 times with a 3% to 4% increase in bituminous coating content. The literature indicates that coarser materials tend to provide higher dry densities (*20*). However, bituminous material

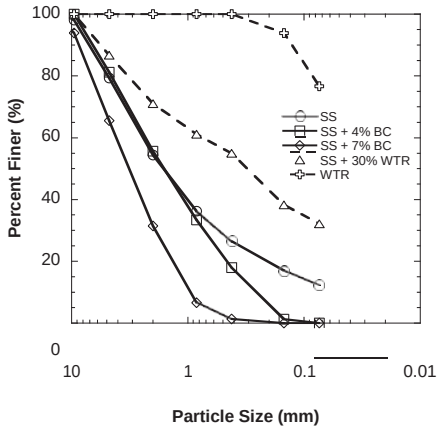

FIGURE 2 Grain-size distributions of steel slag, WTR, and steel slag–bituminous mixtures.

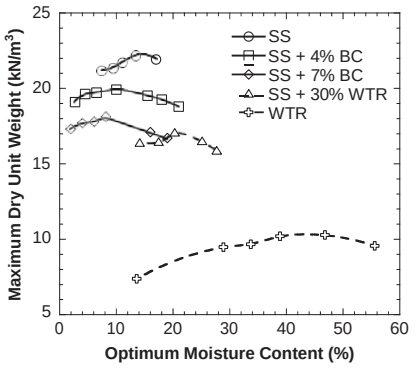

FIGURE 3 Moisture–density relationship of steel slag, WTR, steel slag–bituminous coating, and steel slag–WTR mixtures.

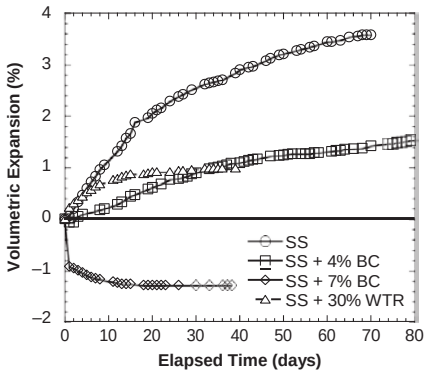

FIGURE 4 Volumetric expansion ratio curves for steel slag, steel slag 1 4% bituminous coating, steel slag 1 7% bituminous coating, and steel slag 1 30% WTR.

(asphalt binder PG 64-22) is a viscous and lightweight material, and addition of it may have caused a decrease in $\gamma_{dry\text{-}max}$ of the steel slag–bituminous coating mixtures. Similar trends are observed for steel slag–WTR samples. The steel slag specimens prepared with WTR material yield the lowest $\gamma_{dry\text{-}max}$ of all mixtures. Moreover, addition of WTR to the steel slag material increased the W_{opt} values from 13.5% to 21% (Figure 3). The WTR material contains 76% silty fines, which is probably the main reason for the lower $\gamma_{dry\text{-}max}$ and higher W_{opt} values for the steel slag–WTR mixtures.

Results of accelerated swelling test

ASTM D4792 suggests conducting swelling tests for at least 7 days to gather adequate data with which to evaluate the expansive behavior of the materials that are being tested. However, the swelling tests were generally continued beyond 7 days to ensure the swelling ratio was stabilized, that is, to fully assess both short- and long-term expansion behavior of the materials.

Figure 4 shows the variation of the volumetric expansion (percentage swelling) with time (days) for the steel slag alone and for treated steel slag specimens. Volumetric expansion of 100% steel slag increases with time, and the ratio of increase declines around Day 40. Hydration of the free CaO and MgO minerals is the main reaction that causes extensive swelling in the steel slag materials (*2*). A continuous increase in the swelling ratio for the steel slag observed after 40 days could be caused by hydration of the MgO minerals that are present in the steel slag. The hydration rate of CaO is relatively faster than the hydration rate of MgO. It takes only weeks for CaO minerals to complete their hydration process, but it takes years for MgO minerals. Therefore, it can be speculated that hydration of MgO minerals is the main cause of continuing expansion in the steel slag even after 40 days.

Amendment of 30% WTR by weight into steel slag material decreases the volumetric expansion ratio from 2.95% to 0.98% (Figure 4). This indicates that mixing steel slag with WTR may prevent swelling in highway base and subbase applications. According to Figure 4, the expansion rate of the 100% steel slag is lower than those measured for the steel slag plus 30% WTR mixture in the first 3 days. Wang claimed that the hydration rate of free CaO is initially slow because of the dense (high calcining) structure of free CaO in steel slag byproducts (*8*). Wang also stated that this phenomenon decreases the reaction rate that occurs between water and free CaO, which ultimately decreases the initial expansion rate.

The data in Figure 4 indicate that the bituminous-coated steel slag specimens exhibited initial settlements during the earlier stages of the accelerated swelling tests. Deniz et al. also found that the RAP that possessed steel slag aggregates exhibited initial settlements before onset of expansion and that the porous nature of the RAP materials with lower densities yielded a sudden settlement as soon as a surcharge load was placed (*9*). This caused a decrease in the volume of the RAP material instead of an expansion. Mixtures of steel slag and bituminous coating prepared in the present study have a more highly porous structure than the steel slag alone and the steel slag–WTR mixture because fines in the steel slag are replaced with bituminous material during the coating process. That the steel slag–bituminous coating mixtures are relatively highly porous and that the lubricant nature of the bitumen dominates the material behavior could be responsible for the observed instant high settlement rates.

Furthermore, steel slags coated with bituminous materials at 7% do not show any swelling potential (Figure 4). Bituminous coating decreases the infiltration rate of water into the steel slag aggregates, which prevents the hydrations of free CaO and magnesia MgO and thus the swelling of the granular steel slag material. This finding is consistent with previous research findings that the presence of bituminous material (e.g., RAP) significantly decreases hydration of free CaO and MgO (*9, 21*).

The expansive nature of the steel slag material is caused by hydration of calcium and magnesium oxides. Bitumen acts here as a coating mechanism to suppress the leaching of calcium from steel slag and thus to mitigate swelling and decrease pH. However, it is very difficult to achieve 100% coating of the particles, and absolute prevention of calcium leaching is almost impossible with a coating procedure.

As shown in Figure 4, the ultimate swelling ratio decreases with an increased amount of bitumen. However, one of the factors affecting the ultimate swelling ratio is the lubricant nature of bitumen. When the bitumen content is decreased to 4%, although the ultimate swelling

ratio is decreased by nearly 70%, swelling is still observed because the lubricant nature cannot dominate the material behavior and leaching of calcium cannot be totally prevented.

ph excursions

Water leach tests were conducted on steel slag alone, bituminous-coated steel slag, and steel slag–WTR mixtures. Water leach tests were conducted to monitor the variation of effluent pH of the steel slag materials with bituminous coating and amendment of WTR. MDE does not allow waste materials to be reused in construction applications unless the effluent pH is below 8.5. It is well known that CaO and MgO are the main minerals that increase the pH of the effluent solutions (*22*). The literature claims that steel slag contains significant amounts of CaO and MgO minerals, ranging from 30% to 55% and 5% to 15%, respectively (*23, 24*). This indicates that the steel slag material used in this study also poses great potential to leach out effluent solutions with alkaline properties (basic pH). Therefore, bituminous coating and amendment of WTR are applied to the steel slag material to lower to below 8.5 the pH of the effluent solutions that come out when the mixtures are exposed to moisture. Steel slag was coated with 2%, 4%, 5%, 7%, and 8% bituminous material by weight and were mixed with 20%, 30%, and 40% WTR material by weight.

The effluent pH of the tested specimens is summarized in Table 2. As expected, effluent pH of the 100% steel slag specimen is the highest in all mixtures (pH = 12.3) and exceeds the MDE limit for effluent pH of waste material (pH = 8.5). Figure 5 shows the effects of bituminous coating and amendment of WTR on the effluent pH of specimens prepared with steel slag. An increase in the amount of bituminous material from 2% to 8% by weight appears to decrease the effluent pH of the steel slag from 12.3 to 11.5. Bituminous material seals the surface of the particles and decreases the release of free CaO and MgO into the aqueous solution. However, this level of decrease in the effluent pH is not adequate to satisfy the MDE regulatory limits. Moreover, addition of bituminous material of more than 8% by weight will not be economically feasible and may influence the mechanical and physical properties of the steel slag granular materials by decreasing stiffness, strength, and hydraulic conductivity.

Figure 5 indicates that amendment of WTR into steel slag is more effective than bituminous coating of steel slag. The addition of WTR can lower the effluent pH of the steel slag to 9.8. The effluent pH of the WTR alone is neutral (pH = 7.24), likely the reason for the decrease in the effluent pH of the steel slag–WTR mixtures (Table 2). Although WTR amendment appears to be a better methodology for decreasing the pH of the effluent solution of steel slag, it does not satisfy the MDE effluent pH criteria (pH = 8.5). Furthermore, the amount of WTR added to steel slag–WTR mixtures is between 20% and 40% by weight and may significantly affect the geomechanical behavior of the steel slag granular material. Further testing is needed to evaluate the stiffness and strength behavior of these steel slag–WTR mixtures.

TABLE 2 Effluent pH of Specimens from Water Leach Tests

Specimen	Effluent pH	Specimen	Effluent pH
SS	12.3	SS + 8% BC	11.55
SS + 2% BC	12.25	SS + 20% WTR	10.5
SS + 4% BC	12.09	SS + 30% WTR	9.81
SS + 5% BC	11.95	SS + 40% WTR	9.7
SS + 7% BC	11.69	WTR	7.24

Note: SS = steel slag; BC = bituminous coating.

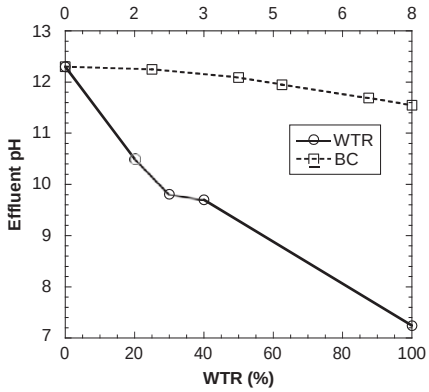

FIGURE 5 Effluent pH of specimens.

Conclusions

Recycling of steel slag material in highway construction could allow significant cost savings and meet the mechanical requirements for the design. A series of laboratory tests was conducted to investigate the swelling potential and effluent pH of steel slag material coated with bituminous material and mixed with WTR. The following conclusions can be drawn from the findings of this study:

1. An increase in the amount of bituminous material decreases $\gamma_{dry\text{-}max}$ and W_{opt} of the bitumen-coated steel slag. Addition of WTR to steel slag decreased $\gamma_{dry\text{-}max}$ and increased W_{opt} because of the high fines content of the WTR.
2. Swelling (volumetric expansion) tests were continued for a long period for a full assessment of the expansion trends of the specimens used in the current study. It was observed that bituminous coating and WTR amendment methodologies are very efficient in the prevention of significant expansion of the steel slag material. Mixing the steel slag material with 30% WTR material by weight decreased the swelling (expansion) rate from 2.95% to approximately 1%. The steel slag materials coated with bituminous material do not exhibit swelling, most likely because of the sealing off of the hydration of free CaO and MgO minerals by the bituminous material coating.
3. Steel slag–bituminous coating mixtures showed an initial settlement in the first day of the swell test. It was speculated that the porous nature and low $\gamma_{dry\text{-}max}$ values of these mixtures were the cause.
4. Effluent pH of the steel slag is a critical environmental challenge when the material is used as a granular aggregate in highway base or subbase layers. Increasing the amount of bituminous material and WTR in the mixtures decreases the pH of the effluent solutions. However, none of the mixtures resulted in leachate solutions that had a pH lower than 8.5, an MDE regulatory limit. This indicates that a further study is required on the specific pH issue.

1. Although the results of this study are promising and indicate that bituminous coating and WTR amendments are effective methodologies for preventing swelling, lowering the effluent pH of the steel slag materials and the influence of factors such as aging and curing period are yet to be investigated.

Acknowledgement

Funding for this project was provided by the Maryland State Highway Administration.

References

1. Proctor, D. M., K. A. Fehling, J. L. Wittenborn, J. J. Green, C. Avent, R. D. Bigham, M. Connolly, B. Lee, T. O. Shepker, and M. A. Zak. Physical and Chemical Characteristics of Blast Furnace, Basic Oxygen Furnace, and Electric Arc Furnace Steel Industry Slags. *Environmental Science and Technology*, Vol. 34, 2000, pp. 1576–1582.
2. Sorlini, S., A. Sanzeni, and R. Luca. Reuse of Steel Slag in Bituminous Paving Mixtures. *Journal of Hazardous Materials*, Vol. 209, No. 210, 2012, pp. 84–91.
3. Rohde, L., W. P. Nuñez, and J. A. P. Ceratti. Electric Arc Furnace Steel Slag: Base Material for Low-Volume Roads. In *Transportation Research Record: Journal of the Transportation Research Board, No. 1819*, Transportation Research Board of the National Academies, Washington, D.C., 2003, pp. 201–207.
4. Tsakiridis, E., G. D. Papadimitrious, and S. Tsivilis. Utilization of Steel Slag for Portland Cement Clinker Production. *Journal of Hazardous Materials*, Vol. 152, No. 2, 2008, pp. 805–811.
5. Shen, W., M. Zhou, and W. Ma. Investigation on the Application of Steel Slag–Fly Ash–Phosphogypsum Solidified Material as Road Base Material. *Journal of Hazardous Materials*, Vol. 164, No. 1, 2009, pp. 99–104.
6. Suer, P., J. Lindqvist, M. Arm, and P. Frogner-Kockum. Reproducing Ten Years of Road Ageing-Accelerated Carbonation and Leaching of EAF Steel Slag. *Science of Total Environment*, Vol. 407, 2009, pp. 511–518.
7. Wang, G., Y. Wang, and Z. Gao. Use of Steel Slag as a Granular Material: Volume Expansion Prediction and Usability Criteria. *Journal of Hazardous Materials*, Vol. 184, 2010, pp. 555–560.
8. Wang, G. Determination of the Expansion Force of Coarse Steel Slag Aggregate. *Construction and Building Materials*, Vol. 24, 2010, pp. 1961–1966.
9. Deniz, D., E. Tutumluer, and J. S. Popovics. Evaluation of Expansive Characteristics of Reclaimed Asphalt Pavement and Virgin Aggregate Used as Base Materials. In *Transportation Research Record: Journal of the Transportation Research Board, No. 2167*, Transportation Research Board of the National Academies, Washington, D.C., 2010, pp. 10–17.
10. Verhasselt, A., and F. Choquet. Steel Slags as Unbound Aggregate in Road Construction: Problems and Recommendations. *Proc., International Symposium on Unbound Aggregates in Roads*, London, 1989, pp. 204–211.
11. Geiseler, J. Use of Steel Works Slag in Europe. *Waste Management*, Vol. 16, Nos. 1–3, 1996, pp. 59–63.
12. *General Permit for Discharges from Mineral Mines, Quarries, Borrow Pits and Concrete and Asphalt Plants*. Maryland Department of the Environment. http://www.mde.state.md.us/assets/document/permit/minmine_per.pdf. Accessed Oct. 21, 2013.
13. Thomson, M. Why Is Type S Hydrated Lime Special? *Proc., International Building Lime Symposium*, Orlando, Fla., 2005.
14. Grubb, D. G., M. Wazne, and N. E. Malasavage. Characterization of Slag Fines for Use as a Dredged Material Amendment. *Proc., GeoFlorida: Advances in Analysis, Modeling and Design*, Orlando, Fla., 2010.
15. Grubb, D. G., M. Wazne, S. C. Jagupilla, and N. E. Malasavage. Beneficial Use of Steel Slag Fines to Immobilize Arsenite and Arsenate: Slag Characterization and Metal Thresholding Studies. *Journal of Hazardous, Toxic, and Radioactive Waste*, Vol. 15, No. 3, 2011, pp. 130–150.
16. Jagupilla, S. C., D. G. Grubb, and M. Wazne. Metals Immobilization and Removal Rates of Se(IV) and Se(VI) by Steel Slag Fines Media. *Proc., GeoCongress: State of the Art and Practice in Geotechnical Engineering*, Oakland, Calif., 2012.
17. *Material Safety Data Sheet. Asphalt PG-64-22*. Irving Oil Co. http://www.irvingoil.com/files/03310_ASPHALT_PG-64-22_MSDS_21.pdf. Accessed Oct. 31, 2013.
18. Cetin, B., A. H. Aydilek, and L. Li. Experimental and Numerical Analysis of Metal Leaching from Fly Ash Amended Highway Bases. *Waste Management*, Vol. 965, No. 5, 2012, pp. 965–978.
19. Uthus, L., Å. Hermansson, I. Horvli, and I. Hoff. A Study on the Influence of Water and Fines on the Deformation Properties and Frost Heave of Unbound Aggregates. *Proc., 13th International Conference on Cold Regions Engineering*, Orono, Maine, 2006, pp. 1–13.
20. Holtz, R. D., and W. D. Kovacs. *An Introduction to Geotechnical Engineering*. Prentice Hall, Englewood Cliffs, N.J., 1981.
21. Kandahl, P. S., and G. L. Hoffman. Evaluation of Steel Slag Fine Aggregate in Hot-Mix Asphalt Mixture. In *Transportation Research Record 1583*, TRB, National Research Council, Washington, D.C., 1997, pp. 18–36.
22. Johnson, C. A., M. Kaeppeli, S. Brandenberger, A. Ulrich, and W. Bauman. Hydrological and Geochemical Factors Affecting Leachate Composition in Municipal Solid Waste Incinerator Bottom Ash Part II. The Geochemistry of Leachate from Landfill Lostorf, Switzerland. *Journal of Contaminant Hydrology* Vol. 40, 1999, pp. 239–259.
23. Zhu, G., and S. Sun. Should Speed up the Utilization of Iron and Steel Slag. *China Steel*, Vol. 1, 2007, pp. 23–27.
24. Shi, C. Steel Slag—Its Production, Processing, Characteristics, and Cementitious Properties. *Journal of Materials in Civil Engineering*, Vol. 16, No. 3, 2004, pp. 230–236.

Any opinions, findings, and conclusions or recommendations expressed in this paper are those of the authors and do not necessarily reflect the views of the Maryland State Highway Administration.

The Physicochemical and Biological Processes in Soils Committee peer-reviewed this paper.

REFERENCES

Ahmedzade, P. and Sengoz, B. (2009). Evaluation of steel slag coarse aggregate in hot mix asphalt concrete. Journal of Hazardous Materials 165-(1-3), 300-305.

Andreas, L., Herrmann, I., Lidstrom-Larrsson, M., and Lagerkvist, A. (2005). Physical properties of steel slag to be reused in a landfill cover. Proceedings of Sardinia, Tenth International Waste Management and Landfill Symposium, Environmental Sanitary Engineering Centre, Cagliari, Italy, Oct. 3-7.

Apul, D. S., Gardner, K. H., Eighmy, T. T., Fällman, A.-M., and Comans, R. N. J. (2005). Simultaneous application of dissolution/precipitation and surface complexation/surface precipitation modeling to contaminant leaching. Environmental Science and Technology, 39-15, 5736 - 5741.

Astrup, T., Dijkstra, J. J., Comans, R. N. J., Van der Sloot, H. A., and Christensen, T. H. (2006). Geochemical modeling of leaching from MSWI air-pollution-control residues. Environmental Science & Technology, 40-11, 3551-3557.

ATSDR (2008). Toxicological profile for aluminum. Agency for toxic substances and disease registry,Atlanta,GA, p. 357, http://www.atsdr.cdc.gov/toxprofiles/tp.asp?id=191&tid=34, Last Updated December 4 2014, Accessed on December 4 2014.

Banks, M. K., Schwab, A. P., Alleman, J. E., Hunter, J. G., and Hickey, J. C. (2006). Constructed wetlands for the remediation of blast furnace slag leachates. FHWA/IN/JTRP-2006/03. Joint Transportation Research Program, Indiana Department of Transportation and Purdue University, West Lafayette, Indiana, US.

Bankowski, P., Zou, L., and Hodges, R.H. (2004). Reduction of metal leaching in Brown coal fly ash using geopolymers. Journal of Hazardous Materials 14, 59 - 67.

Barabasz, W., Albinska, D., Jaskowska, M., and Lipiec, J. (2002). Ecotoxicology of aluminium. Polish Journal of Environmental Studies 11, 199-203.

Barra, M., Ramonich, E.V., and Munoz, M.A. (2001). Stabilization of soils with steel slag and cement for application in rural and low traffic roads. Proceedings of the Beneficial Use of Recycled Materials in Transportation Application, 423-432.

Bin-Shafique, S., Benson, C., Edil, T., and Hwang, K. (2006). Leachate concentrations from water leach and column leach tests on fly–ash stabilized soil. Environmental Engineering Science 23-1, 51-65.

Boyer, B. (1994). Alkaline leachate and calcareous tufa originating from slag in a highway embankment near Baltimore, Maryland. Transportation Research Record 1434. pp. 3-7.

Camacho, L. M. and Munson-McGee, S. H. (2006). Anomalous transient leaching behavior of metals solidified/stabilized by pozzolanic fly ash. Journal of Hazardous Materials, 137-1, 144-151.

Cetin, B., Aydilek, A.H., and Guney, Y. (2012a). Leaching of four trace metals from high carbon fly ash stabilized highway base layers, Resources, Conservation and Recycling, 58, 8-17.

Cetin, B., Aydilek, A.H., and Li, L. (2012b). Experimental and numerical study of metal leaching from fly ash amended highway bases, Waste Management, 32-5, 965-978.

Cetin, B., Aydilek, A.H., and Li, L. (2013). Leaching Behavior of Al, As and Cr from High Carbon Fly Ash Amended Highway Structural Fills, Journal of the Transportation Research Board, 2349, 72-80.

Cetin, B., Aydilek, A.H., and Li, L. (2014). Trace metal leaching from embankment soils amended with high carbon fly ash, Journal of Geotechnical and Geoenvironmental Engineering, ASCE, 140- 1, 1-13.

Chaurand, P., Rose, J., Briois, V., Olivi, L., Hazemann, J. L., Proux, O., Domas, J., and Bottero, J.Y. (2007). Environmental impacts of steel slag reused in road construction: A crystallographic and molecular (XANES) approach. Journal of Hazardous Materials, 139-3, 537-542.

Chavez, M. L., de Pablo, L., and Garcia, T.A. (2010). Adsorption of Ba2+ by Ca-exchange clinoplite tuff and montmorollinite clay. Journal of Hazardous Materials, 175, 216- 223.

Cohen, S. M., Arnold, L. L., Eldan, M., Lewis, A. S., and Beck, B. D. (2006). Methylated arsenicals: the implications of metabolism and carcinogenicity studies in rodents to human risk assessment. Critical Reviews in Toxicology. 36, 99-133.

Cornelis, G., Johnson, C.H., Van Gerven, T., and Vandecasteele, C. (2008). Leaching mechanisms of oxyanionic metalloid and metal species in alkaline solid wastes, Applied Geochemistry, 23, 955-976.

Cornelis, G., Van Gerven, T., Vandecasteele, C., Kirb, J. K., and Mclaughlin, M. J. (2011). Geochemical constraints in slag valorisation: the case of oxyanions and nanoparticles, Proceedings of the Second International Slag Valorization Symposium, April 18-20, Leuven, Belgium.

Cotton, A.F. and Wilkinson, G. (1999). Advanced Inorganic Chemistry, 5th ed. John Wiley & Sons, Inc., New York.

Das, B., Prakash, S., Reddy, P. S. R., and Misra, V.N. (2007). An overview of utilization of slag and sludge from steel industries. Resources Conservation and Recycling, 50- 1, 40-57.

De Smedt, F., Brevis, W., and Debels, P. (2005). Analytical solution for solute transport resulting from instantaneous injection in streams with transient storage. Journal of Hydrology, 315, 25–39.

De Windt, L., Chaurand, P., and Rose, J. (2011). Kinetics of steel slag leaching: Batch tests and modeling, Waste Management, 31, 225-235.

Deniz, D., Tutumluer, E., and Popovics, J. (2009). Expansive characteristics of reclaimed asphalt pavement (RAP) used as base materials. Research Report ICT-09-055, Illinois Center for Transportation.

Deniz, D., Tutumluer, E., and Popovics, J. (2010). Evaluation of expansive characteristics of reclaimed asphalt pavement and virgin aggregate used as base materials. Transportation Research Record 2167, 10-17.

Dijkstra, J. J., Meeussen, J. C. L., and Comans, R. N. J. (2004). Leaching of heavy metals from contaminated soils: An experimental and modeling study. Environmental Science and Technology, 38-16, 4390-4395.

Eighmy, T. T., Eusden, J. D., Krzanowski, J. E., Domingo, D. S., Stampfli, D., Martin, J. R., and Erickson, P. M. (1995). Comprehensive approach toward understanding element speciation and leaching behavior in municipal solid-waste incineration electrostatic precipitator ash. Environmental Science & Technology, 29(3), 629- 646.

Elsayed-Ali, O. H., Abdel-Fattah, T., and Elsayed-Ali, H. E. (2011). Copper cation removal in an electrokinetic cell containing zeolite, Journal of Hazardous Materials, 185, 1550-1557.

Elseewi, A. A., Page, A. L., and Grimm, S. R. (1980). Chemical characterization of fly ash aqueous systems. Journal of Environmental Quality 9, 424 - 428.

Emery, J. J. (1974). A simple test procedure for evaluating the potential expansion of steel slag. Proc. of the 1974 Annual Conference, Roads and Transportation Association of Canada, Toronto, Ontario, 90-103.

Ettler, V., Mihaljevic, M., and Sebek, O. (2010). Antimony and arsenic leaching from secondary lead smelter air-pollution-control residues. Waste Management & Research 28, 587-595.

Evans, A.C. (2006). Compaction control of large-sized granular solis/aggregates: the vibrating hammer method of compaction and time domain reflectometry, M.Sc. Thesis, Purdue University, West Lafayette, Indiana.

Fällman, A. M. (2000). Leaching of chromium and barium from steel slag in laboratory and field tests-a solubility controlled process? Waste Management, 20, 149-154.

Fällman, A. M. and Aurell, B. (1996). Leaching tests for environmental assessment of inorganic substances in wastes, Science of the Total Environment. 178, 71-84.

Fällman. A.M. and Hartlèn, J. (1994). Leaching of slags and ashes - controlling factors in field experiments versus in laboratory tests. In: Goumans, J.J.J.M., van de Sloot, H.A., Aalbers Th.G., editors. Environmental aspects of construction with waste materials: Studies in Environmental Science 60. Amsterdam: Elsevier, 39-54.

Fedje, K.K. (2010). Metals in MSWI fly ash - problems or opportunities? PhD Thesis, Chalmers University of Technology, Göteborg, Sweden

Fernandez-Olmo, I., Lasa, C., and Irabien, A. (2007). Modeling of zinc solubility in stabilized/solidified electric arc furnace dust. Journal of Hazardous Materials, 144-3, 720-724.

Fernandez-Olmo, I., Lasa, C., Lavin, M. A., and Irabien, A. (2009). Modeling of amphoteric heavy metals solubility in stabilized/solidified steel foundry dust. Environmental Engineering Science, 26-2, 251-261.

Fruchter, J. S., Ral, D., and Zachara, J. M. (1990). Identification of solubility-controlling solid phases in a large fly ash field lysimeter. Environmental Science and Technology, 24-8, 1173 - 1179.

Garrabrants, A. C., Sanchez, F., and Kosson, D. S. (2004). Changes in constituent equilibrium leaching and pore water characteristics of a Portland cement mortar as a result of carbonation. Waste Management, 24-1, 19-36.

Geiseler, J. (1994). Steel slag-generation, processing and utilization. Proceedings of the International Symposium on Resource Conservation and Environmental

Technologies in Metallurgical Industry, pp. 87–97, Toronto, Canada, August 1994.

Geiseler, J. (1996). Use of steel works slag in Europe. Waste Management 16(1-3), 59-63.

Ghionna, V., Pedroni, S., Tenani, P., and Veggi, S. (1996). Geotechnical investigation on steel slags mixtures for landfills embankments construction. Proceedings of the Second International Conference on Environmental Geotechnics, Osaka, Japan, November 5-8, Balkema , Rotterdam, 709-714.

Gitari, W. M., Fatoba, O. O., Petrik, L. F., and Vadapalli, W. R. K. (2009). Leaching characteristics of selected South African fly ashes: Effect of pH on the release of major and trace species. Journal of Environmental Science and Health Part A, 44, 206-220.

Gomes, J. F. P. and Pinto, C. G. (2006). Leaching of heavy metals from steelmaking slags, Revista del Metalurgia 42-6, 409-416.

Goswami, R. K. and Mahanta, C. (2007). Leaching characteristics of residual lateric soils stabilized with fly ash and lime for geotechnical applications, Waste Management 27, 466– 481.

Grubb, D., Wazne, M., Jagupilla, S., and Malasavage, N. (2011). Beneficial use of steel slag fines to immobilize arsenite and arsenate: slag characterization and metal thresholding studies. Journal of Hazardous, Toxic, and Radioactive Waste 15, Special Issue: Contaminant Mixtures: Fate, Transport, and Remediation, 130–150.

Grubb, D., Wazne, M., Jagupilla, S., Malasavage, N., and Bradfield, W. (2013). Aging effects in field-compacted dredged material: steel slag fines blends. Journal of Hazardous Toxic and Radioactive Waste, 17-2, 107–119.

Halim, C. E., Short, S., Amal, R., Scott, J. A., Beydoun, D., and Low, G. (2005). Modelling the leaching of Pb, Cd, As, and Cr from cementitious waste using PHREEQC, Journal of Hazardous Materials, 125, 45-61.

Havanagi, V. G., Sinha, A. K., Arora, V. K., and Mathur, S. (2012). Waste materials for construction of road embankment and pavement layers. International Journal of Environment Engineering Research, 1-2, 51-59.

Healy, J., Bradley, S.D., Northage, C., and Scobbie, E. (2001). Inhalation exposure in secondary aluminum smelting. The Annals of Occupational Hygiene. 45, 217–225.

Holtz, R. D. and Kovacs, W. D. (1981). An Introduction to Geotechnical Engineering, Prentice Hall, Englewood Cliffs, N.J.

Hughes, M. F. (2002), Arsenic toxicity and potential mechanisms of action, Toxicology Letters, 133 (1), 1-16.

Huijgen, W. J. J. and Comans, R. N. J. (2006). Carbonation of steel slag for CO2 sequestration: Leaching of products and reaction mechanisms, Environmental Science and Technology, 40, 2790-2796.

Irving Oil Co. (2013) Material Safety Data Sheet. Asphalt PG-64-22. http://www.irvingoil.com/files/03310_ASPHALT_PG-64-22_MSDS_21.pdf. Accessed Oct. 31, 2013.

Ischii, Y., Fujizuka, N., and Takahashi, T. (1993). A fatal case of acute boric acid poisoning. Clinical Toxicology, 31-2, 345-352.

Iwashita, A., Sakaguchi, Y., Nakajima, T., Takanashi, H., Ohki, A., and Kambara, S. (2005). Leaching characteristics of boron and selenium for various coal fly ashes. Fuel, 84, 479–485.

Izquierdo, M. and Querol, X. (2012). Leaching behaviour of elements from coal combustion fly ash: An overview. International Journal of Coal Geology, 94, 54-66.

Jankowski J., Colin, R. W., French, D., and Groves, S. (2006). Mobility of trace elements from selected Australian fly ashes and its potential impact on aquatic ecosystems. Fuel 85, 243 – 256.

Jegadeesan, G., Al-Abed, S. R., and Pinto, P. (2008). Influence of trace metal distribution on its leachability from coal fly ash. Fuel, 87, 1887-1893.

Johnson, C. A., Kaeppeli, M., Brandenberger, S., Ulrich, A., and Bauman, W. (1999). Hydrological and geochemical factors affecting leachate composition in municipal solid waste incinerator bottom ash Part II. The geochemistry of leachate from Landfill Lostorf, Switzerland. Journal of Contaminant Hydrology 40, 239-259.

Johnson, G. V. and Zhang, H. (2004). Cause and Effects of Soil Acidity, Oklahoma Cooperative Extension Fact Sheet, PSS-2239, Oklahoma State University, Stillwater, Oklahoma.

Jomova, K., Jenisova, Z., Feszterova, M., Baros, S., Liska, J., Hudecova, D., Rhodesd, C. J., Valkoc, M. (2011). Arsenic: toxicity, oxidative stress and human disease. Journal of AppliedToxicology, 31, 95-107.

Juckes, L. M. (2003). The volume stability of modern steelmaking slags. Mineral Processing and Extractive Metallurgy 112-3, 177-197.

Juenger, M. C., Monteiro, P. M., and Gartner, E. M. (2006). In situ imaging of ground granulated blast furnace slag hydration. Journal of Materials Science, 41-21, 7074-7081.

Kandahl, P. S. and Hoffman, G. L. (1997). Evaluation of steel slag fine aggregate in hot-mix asphalt mixture. Transportation Research Record 1583, 18–36.

Kenkel, J. (2003). Analytical chemistry for technicians. 3rd Edition, Boca Raton - Florida: Lewis Publishers.

Kim, A.G. (2006). The effect of alkalinity of class F PC fly ash on metal release. Fuel 85, 1403 – 1413.

Kim, K., Park, S. M., Kim, J., Kim, S. H., Kim, Y., Moon, J. T., Hwang, G. S., and Cha, W.S. (2009). Arsenic concentration in pore water of an alkaline coal ash disposal site: Roles of siderite precipitation/dissolution and soil cover. Chemosphere, 77, 222 - 227.

Komonweeraket, K., Benson, C. H., Edil, T. B., and Bleam, W. F. (2010). Mechanisms controlling leaching of heavy metals from soil stabilized with fly ash, GeoEngineering Report No. 02-14, 2, Geo Engineering Program, University of Wisconsin-Madison, Madison, WI.

Kosson, D.S., Van Der Sloot, H.A., Sanchez, F., and Garrabrants, A. C. (2002). An integrated framework for evaluating leaching in waste management and utilization of secondary materials, Environmental Engineering Science, 19(3), 159-204.

Krewski, D., Yokel, R. A., Nieboer, E., Borchelt, D., Cohen, J., Harry, J., and Rondeau, V. (2007). Human health risk assessment for aluminium, aluminium oxide, and aluminium hydroxide. Journal of Toxicology and Environmental Health, Part B: Critical Reviews, 10(Supp. 1), 1-269.

Langmuir, D. (1997). Aqueous environmental geochemistry. 1st edition, New Jersey: Prentice – Hall, Inc..

Lee, A.R. (1974). Blastfurnace and steel slag: production, properties and uses. Edward Arnold Ltd,. London.

Lee, P.Y. (1976). Study of irregular compaction curves. Soil Specimen Preparation for Laboratory Testing, ASTM STP 599, American Society of Testing Materials, 278-288.

Lee, P.Y. and Suedkamp, R.J. (1972). Characteristics of irregularly shaped compaction curves. Highway Research Record 381, 1-9.

Li, L., Benson, C. H., Edil, T. B., and Hatipoglu, B. (2007). Groundwater impacts from coal ash in highways. Waste and Resource Management 159, 151 – 163.

Lim, T. T., Tay, J. H., Tan, L. C., and Choa, V. (2004). The changes in mobility and speciation of heavy metals in clay-amended incinerator fly ash, Environmental Geology, 47, 1-10.

Liu, Y., Li, Y., Li, X., and Jiang, Y. (2008a). Leaching behavior of heavy metals and PAHs from MSWI bottom ash in long – term static immersing experiment. Waste Management 28, 1126 - 1136.

Liu, Y. Y., Zhao, Y. S., Dong, J., Liu, P., Zhu, Z. G., and Sun, Y. (2008b) pH buffering capacity of geological media on landfill leachate, Huan Jing Ke Xue, 29-7, 1948-1954.

Malviya, R. and Chaudhary, R. (2006). Leaching behavior and immobilization of heavy metals in solidified/stabilized products. Journal of Hazardous Materials, 137-1, 207-217.

Manna, G. K. and Parida, B. B. (1965). Aluminum chloride induced meiotic chromosome aberrations in the grasshopper. Phloeoba antennata Naturwissenschaften. 52, 647–648.

Maryland Department of State Planning. (1973). Natural soil groups of Maryland. Technical Series Publication Number 199, December 1973.

Material Safety Data Sheet (2013). Asphalt PG-64-22. Irving Oil Co. http://www.irvingoil.com/files/03310_ASPHALT_PG-64-22_MSDS_21.pdf., Accessed Oct. 31, 2013.

Mayes, W. M, Younger, P. L., and Aumonier, J. (2008). Hydrogeochemistry of alkaline steel slag leachates in the UK, Water, Air and Soil Pollution, 195(1-4), 35-50.

MD-SHA, (2004). Roadway design manual. Maryland State Highway Administration.

Meima, J. A. and Comans, R. N. J. (1998). Application of surface complexation/precipitation modeling to contaminant leaching from weathered

municipal solid waste incinerator bottom ash. Environmental Science and Technology, 32-5, 688-693.

Meima, J. A. and Comans, R. N. J. (1999). Leaching of trace elements from municipal solid waste incinerator bottom ash at different stages of weathering. Applied Geochemistry, 14-2, 159-171.

Morar, D., Aydilek, A. H., Seagren, E. A., and Demirkan, M. M. (2012). Metal Leaching from Fly Ash- Sand Reactive Barriers, Journal of Environmental Engineering, 138-8, 815-825.

Morar, D. L. (2008). Leaching of metals from fly ash – amended permeable reactive barriers, M.Sc. Thesis, University of Maryland – College Park.

Motz, H. and Geiseler, J. (2001). Products of steel slags an opportunity to save natural resources. Waste Management 21-3, 285-293.

Myeni, S. C. B., Traina, S. J., Logan, T. J., and Waychunas, G. A. (1998). Oxyanion behavior in alkaline environments: Sorption and desorption of arsenate in ettringite. Environmental Science & Technology, 31-6, 1761-1768.

Narukawa, T., Takatsu, A., Chiba, K., Riley, K. W., and French, D. H. (2005). Investigation on chemical species of arsenic, selenium and antimony in fly ash from coal fuel thermal power stations. Journal of Environmental Monitoring, 7-12, 1342-1348.

Noureldin, A. S. and McDaniel, R. S. (1990). Evaluation of surface mixtures of steel slag and asphalt. Transportation Research Record 1269, 133-149.

Ogata, A. and Banks, R. B. (1961). A solution of the differential equation of longitudinal dispersion in porous media. Professional. Paper No. 411-A, U.S. Geological Survey, Washington, D.C.

Ozkok, E., Davis, A. P., and Aydilek, A. H. (2015). Treatment methods for mitigation of high alkalinity in leachates of aged steel slag, Journal of Environmental Engineering, ASCE, 141-9, 1-9.

Pandey, V. C., Singh, J. S., Singh, R. P., Singh, N., and Yunus, M. (2011). Arsenic hazard in coal fly ash and its fate in Indian scenario. Resource, Conservation and Recycling. 55, 819-835.

Patrick, L. (2012). Lead toxicity, a review of the literature. Part I: exposure, evaluation, and treatment. Alternative Medicine Review 11-1, 1-22.

Perry, H. M, Jr., Kopp, S. J., and Perry, E. F. (1989). Hypertension and associated cardiovascular abnormalities induced by chronic Barium feeding. Journal of Toxicol Environ. Health. 28-3, 373-388.

Praharaj, T., Powell, M. A., Hart, B. R., and Tripathy, S. (2002). Leachability of elements from sub-bituminous coal fly ash from India. Environment International 27, 609 - 615.

Proctor, D. M., Fehling, K. A., Shay, E. C., Wittenborn, J. L., Green, J. J., Avent, C., Bigham, R. D., Connolly, M., Lee, B., Shepker, T. O., and Zak, M. A. (2000). Physical and chemical characteristics of blast furnace, basic oxygen furnace, and electric arc furnace steel industry slags. Environmental Science & Technology, 34-8, 1576-1582.

Quina M. J., Bordado, J. C. M., and Quinta-Ferreira R. M. (2009). The influence of pH on the leaching behavior of inorganic components from municipal solid waste APC residues. Waste Management, 29, 2483-2493.

Rohde, L., Nunez, W. P., and Ceratti, J. A. P. (2003). Electric arc furnace steel slag base material for low-volume roads. Transportation Research Record 1819, 201-207.

Rojas, M. F. and M. I. S. Rojas. (2004). The chemical assessment of the electric arc furnace slag as construction material: expansive compounds. Cement and Concrete Research 34-10, 1881-1888.

Sabbas, T., Polettini, A., Pomi, R., Astrup, T., Hjelmar, O., Mostbauer, P., Cappai, G., Magel, G., Salhofer, S., Speiser, C., Heuss-Assbichler, S., Klein, R., and Lechber, P. (2003). Management of municipal solid waste incineration residues. Waste Managementgmt. 23, 61–88.

Sadiq, M., Locke, A., Spiers, G., and Pearson, D. A. B. (2002). Geochemical behavior of arsenic in Kelly Lake Ontario. Water, Air, and Soil Pollution, 141, 299-312.

Sauer, J. J., Benson, C. H., Aydilek, A. H., and Edil. T. B. (2012). Trace elements leaching from organic soils stabilized with high carbon fly ash, Journal of Geotechnical and Geoenvironmental Engineering, ASCE, 138- 8, 968-980.

Shaw, C. A. and Tomljenovic, L. (2013). Aluminum in the central nervous system (CNS): toxicity in humans and animals, vaccine adjuvants, and autoimmunity, Immunologic Research, 56 (2-3), 304-316.

Shen, W., Zhou, M., and Ma, W. (2009). Investigation on the application of steel slag–fly ash–phosphogypsum solidified material as road base material. Journal of Hazardous Materials, 164-1, 99–104.

Solem-Tishmack, J. K. and McCarthy, G. J. (1995). High-calcium combustion by-products: engineering properties, ettringite formation, and potential application in solidification and stabilization of selenium and boron. Cement and Concrete Research, 25, 658-670.

Sorlini, S., Sanzeni, A., and Luca, R. (2012). Reuse of steel slag in bituminous paving mixtures. Journal of Hazardous Materials, 209- 210, 84–91.

Sparks, D. L. (2003). Environmental Soil Chemistry, second edition, Academic Press, California.

Stumm, W. and Morgan, J. J. (1996). Aquatic Chemistry, Chemical Equilibria and Rates in Natural Waters, 3rd ed. John Wiley & Sons, Inc., New York, 1022 p.

Suer, P., Lindqvist, J., Arm, M., and Frogner-Kockum, P. (2009). Reproducing ten years of road ageing-accelerated carbonation and leaching of EAF steel slag. Science of Total Environment, 407, 511–518.

Svilovic, S., Rusic, D., and Stipisic, R. (2009). Modeling batch kinetics of copper ions sorption using synthetic zeolite NaX, Journal of Hazardous Materials 170, 941-947.

Tossavainen, M., Engstrom, F., Yang, Q., Menad, N., Larsson, M. L., and Bjorkman, B. (2007). Characteristics of steel slag under different cooling conditions. Waste Management, 27-10, 1335-1344.

Tsakiridis, E., Papadimitrious, G. D.,and Tsivilis, S. (2008). Utilization of steel slag for portland cement clinker production. Journal of Hazardous Materials, 152- 2, 805–811.

U.S. Environmental Protection Agency. (1990). Drinking water criteria document on barium., NTIS PB91-142869, Washington D.C.

U.S. Environmental Protection Agency. (2006). Air quality criteria for lead final report. (http://www.epa.gov/ttn/naaqs/standards/pb/s_pb_cr_cd.html), EPA/600/R-05/144aF-bF. Washington,DC,

U.S. Environmental Protection Agency. (2008). Health Effects Support Document for Boron, EPA-822-R-08-002.

U.S. Food and Drug Administration. (2000). Regulations on aluminum in large and small volume parenterals used in total parenteral nutrition, Fed. Regist. 2000;65:4103–4111

U.S. Geological Survey (2014). *Slag-Iron and Steel, Annual Review*, Mineral Industry Surveys, U.S. Geological Survey, Minerals Yearbook, Reston, VA.

Uthus, L., Hermansson, Å., Horvli, I., and Hoff, I. (2006). A study on the influence of water and fines on the deformation properties and frost heave of unbound aggregates. Proc., 13th International Conference on Cold Regions Engineering, Orono, Maine, 2006, 1–13.

van der Hoek, E. E., van Elteren, J. T., and Comans, R. N. J. (1996). Determination of As, Sb, and Se speciation in fly ash leachates. International Environment, 63, 67-79.

van Der Sloot, H. A., Hoede, D., and Bonouvrie, P. (1991). Comparison of different regulatory leaching test procedure for waste materials and construction materials. ECN-C--91-082, Netherlands Energy Research Foundation (ECN), Petten.

van Genuchten, M. Th., Leij, F. J., Skaggs, T. H., Toride, N., Bradford, S. A., Pontedeiro, E. M. (2013a). Exact analytical solutions for contaminant transport in rivers.1.The equilibrium advection-dispersion equation, Journal of Hydrology and Hydromechanics, 61-2, 146–160.

van Genuchten, M. Th., Leij, F. J., Skaggs, T. H., Toride, N., Bradford, S. A., Pontedeiro, E. M. (2013b). Exact analytical solutions for contaminant transport in rivers.2. Transient storage and decay chain solutions. Journal of Hydrology and Hydromechanics, 61-3, 250–259.

Verhasselt, A. and Choquet, F. (1989). Steel slags as unbound aggregate in road construction: problems and recommendations. Proceedings of International Symposium on Unbound Aggregates in Roads, London, 204–211.

Vitkova, M., Ettler, V., Sebek, O., and Mihaljevic, M. (2008). Metal – contaminant leaching from lead smelter fly ash using pH – Stat Experiments, Mineralogical Magazine, 72, 521 – 524.

Voglar, G. E. and Lestan, D. (2010). Solidification/stabilisation of metals contaminated industrial soil from former Zn smelter in Celje, Slovenia, using cement as a hydraulic binder. Journal of Hazardous Materials, 178, 926-933.

Wan Zuhairi, W. Y., Samsudin, A. R., and Ridwan, N. (2008). The retention characteristics of heavy metals in natural soils using soil column experiment,

Proceedings of the 12th International Conference of International Association for Computer Methods and Advances in Geomechanics (IACMAG) 1-6 October, 2008 Goa, India

Wang, G. (1992). Properties and utilization of steel slag in engineering applications, PhD Thesis, University of Wollongong, New South Wales, Australia.

Wang, G. (2010). Determination of the expansion force of coarse steel slag aggregate. Construction and Building Materials, 24, 1961–1966.

Wang, G., Wang, Y., and Gao, Z. (2010). Use of steel slag as a granular material: volume expansion prediction and usability criteria. Journal of Hazardous Materials, 184, 555-560.

Wegman, D. H., Eise, E. A., and Hu, X. (1994). Acute and chronic respiratory effects of sodium borate particulate exposures. Environmental Health Perspective. 100-7, 119-128.

Wehrer, M. and Totsche, K.U. (2008). Effective rates of heavy metal release from alkaline wastes – quantified by column outflow experiments and inverse simulations. Journal of Contaminant Hydrology 101, 53 – 66.

Whalley, C., Hursthouse, A., Rowlat, S., Iqbal-Zahid, P., Vaughan, H., and Durant, R. (1999). Chromium speciation in natural waters draining contaminated land, Glasgow, UK. Water, Air and Soil Pollution, 112, 389– 405.

Wones, R .G., Stadler, B. L., and Frohman, L. A. (1990). Lack of effect of drinking water barium on cardiovascular risk factor. Environmental Health Perspective. 85, 355-359.

Xiong, J. B., He, Z. L., Mahmood, Q., Liu, D., Yang, X., and Islam, E. (2008). Phosphate removal from solution using steel slag through magnetic separation. Journal of Hazardous Materials, 152, 211–215.

Yildirim, I. Z. and Prezzi, M. (2009). Use of steel slag in subgrade applications. FHWA/IN/JTRP-2009/32 Final Report, West Lafayette, Indiana.

Yzenas, J. J. (2008). Utilization of Steel Furnace Slag in Asphalt, Presentation in ADC60 Waste Management and Resource Efficiency in Transportation Summer Conference, July 13-15, Broadway, NY